THE UNIVERSITY OF MICHIGAN

INDUSTRY PROGRAM OF THE COLLEGE OF ENGINEERING

MACROSCOPIC YIELDING BEHAVIOR OF POLYMERIC MATERIALS

Ram Singh Raghava

A dissertation submitted in partial fulfillment
of the requirements for the degree of
Doctor of Philosophy in the
University of Michigan
Department of Civil Engineering
1972

November 1972

IP-847

ACKNOWLEDGEMENTS

The author wishes to express his gratitude to the individuals and organizations that are mentioned below.

To Professor Robert M. Caddell, who has been a most stimulating co-chairman and an outstanding advisor. It was a rich and memorable experience to work under him. His assistance during the program and the care he took in correcting the manuscript of this thesis are very much appreciated.

The author is indebted to Professor Gregory S. Y. Yeh, Co-Chairman, for introducing me to the field of polymeric materials and for the valuable advice he provided.

It is a pleasure to express my appreciation for the help rendered by Professor Anthony G. Atkins during the whole program.

The author also expresses his gratitude to Professor William F. Hosford for his help at various stages and for many stimulating (and some time heated) discussions.

It is indeed a pleasure to acknowledge the help of Professor Kenneth C. Ludema for his advice in regard to some of the instrumentation used in this work and for his constant encouragement during my four years of study at The University of Michigan.

The author expresses his thanks to Professor John A. Clark, Chairman, Department of Mechanical Engineering, for providing a Teaching Fellowship and to the Whirlpool and Union Carbide Corporations for providing financial help during part of his doctoral program.

Mr. Clarence Johnson must be mentioned for his outstanding job of machining the tube specimens; despite almost daily crises of overload in the machine shop, he never compromised on the accuracy of the work.

I wish to thank Mr. Clyde Schoenhals for his excellent job of machining the pressure chamber and Mr. Wally Koebnick for the help rendered during parts of the experimentation.

I would like to thank Mrs. Mary Anne Brocious and Mrs. Marisa Helfen for all their help in typing the various drafts of this thesis.

Finally, to my parents for their constant encouragement, love and innumerable sacrifices during my absence from home, I give my deepest thanks.

TABLE OF CONTENTS

LIST OF TABLES

LIST OF ILLUSTRATIONS

LIST OF SYMBOLS

A	Material constant.
a	Material constant.
B	Ratio of hydrostatic pressure and tensile yield strength measured at ambient conditions. (P/T)
b	Material constant.
C	Yield stress in direct compression at ambient conditions.
D	Mean normal stress normalized with respect to tensile yield stress. (σ_m/T)
$d, d_i \ldots$	Initial and instantaneous values of diameter for thin wall tube tests.
E	Young's modulus.
e_1, e_2, e_3	Nominal strains in principal directions.
f	Loading function.
G	Shear modulus.
h,w	Widths of tool and specimen in plane strain compression test.
I_1	First invariant of stress tensor.
I_2	Second invariant of stress tensor.
I_3	Third invariant of stress tensor.
J_1	First invariant of stress deviatoric tensor.
J_2	Second invariant of stress deviatoric tensor.
J_3	Third invariant of stress deviatoric tensor.
K	Yield function.
k	Yield stress in pure shear.

L	Applied load.
P	Hydrostatic pressure.
p	Internal pressure in thin wall tube.
R	Yield stress (tension as well as compression) under hydrostatic pressure normalized with respect to tensile yield stress at ambient conditions.
R_1	Axial stress normalized with respect to tensile yield stress.
R_2	Circumferential stress normalized with respect to tensile yield stress.
R_C	Yield stress (compressive) under hydrostatic pressure normalized with respect to tensile yield stress at ambient conditions.
R_T	Yield stress (tensile) under hydrostatic pressure normalized with respect to tensile yield stress at ambient conditions.
t, t_i	Initial and instantaneous thickness of thin wall tubes.
t_o, t_a	Initial and instantaneous thickness of strip specimen.
T	Tensile yield stress at ambient conditions.
V	Material constant.
X	Ratio of yield stress in compression to tension at ambient conditions. (C/T)
α	Constant.
β	Nonnegative scalar.
$d\epsilon_1, d\epsilon_2, d\epsilon_3$	Plastic strain increments in the principal directions.
ϵ_1, ϵ_2	True strains in two principal directions.
$\bar{\epsilon}$	Effective strain under multiaxial stress states.
λ	Lame's constant.
μ	Material constant.
μ_1, μ_2, μ_3	Material constants.

ν	Poisson's ratio.
σ	Yield stress under hydrostatic pressure.
$\sigma_1, \sigma_2, \sigma_3$	Principal stresses.
σ_d	Direct stress in plane strain compression.
σ_m	Mean normal stress.
τ_{oct}	Octahedral shear stress.
τ_s	Shear stress in torsion.
$\tan \theta$	Material constant.
$\tan \phi$	Function defined by Normality Rule.
F,H,M,N,Q,S	Constants in suggested anisotropic yield criterion.

CHAPTER I. INTRODUCTION

"In discussion with sensible professional men, I have not infrequently encountered the opinion expressed that it would be wasting vain efforts to develop a theory on which the strength of materials could be based scientifically. Homogeneous bodies of materials, I was told, do not exist; homogeneous states of stress are not encountered. It seems, therefore utterly impossible to deduce a law of nature from experience. Since the existing irregularities furthermore are of such a nature that they nearly completely obscure any orderly behavior it has little interest to track down the half blurred traces of such laws. Under these circumstances nothing else remains than to make special tests in every important case and to pay no heed to a physical interpretation of the results. I had to admit in each case that nothing could be said against this reasoning and yet for more than one hundred years, there have been attempts again and again to establish order within the confusing abundance of the experiences. If one should succeed in finding a few rules under which many experiences could be subordinated - of course rules in which some confidence can be placed - no law of nature would have been derived, but some means found for judging the probability of new results of experience." (Mohr, Otto, Z. Ver. deut. Ing., p. 740, 1901).

In order to achieve the desired satisfactory operation of any machine and/or part thereof, it is necessary to know the properties of the material from which the structure is to be made. Mechanical

properties of materials are dependent upon temperature, time, environment and type and rate of external loading. A particular material could be capable of withstanding one loading while it may not sustain a different loading configuration. It is virtually impossible to specify the properties of materials for all possible types of loading. The most widely used "strength" properties are those determined from tests conducted under uniaxial tension and/or uniaxial compression. In order to predict the behavior of a material other than for specified loading states, it is advantageous to establish a law or rule which incorporates the applied stress state and certain basic properties obtained from simple tests.

As is well known, no material is truly perfect in structure. There may be defects on the microscopic level yet it is still reasonable and possible to develop macroscopic relationships that prove very useful in an engineering sense. Even here, certain idealizations are assumed. For instance, in the macroscopic theory of plasticity, it is common to invoke the following assumptions in terms of material behavior and structure:

1. Macroscopic homogeneity,
2. Isotropy,
3. No time effects,
4. Hydrostatic pressure does not influence yielding and
5. Size effects are not present.

The first assumption dictates that a given property of the material must be the same at each point. Isotropic behavior indicates that properties in different directions are identical at any point. With

most metals, the third assumption is quite reasonable as long as temperatures are relatively low (say below the recrystallization range or below half melting point on the absolute scale). Regarding the fourth assumption, Bridgman [1] has shown this to be quite reasonable where metals are involved, but it may not be true for other solids (which is part of the background of this dissertation).

I.1 Macroscopic Yielding of Metals

Yielding behavior of metals has been investigated extensively and numerous theories of yielding have been proposed. The most widely accepted are those of Tresca [2] and von Mises [3].* In 1864 Tresca [2] published his maximum shear stress theory which states that the shear resistance of a material determines the onset of plastic flow or "yielding."

The validity of the Tresca yield criterion, which assumes that plastic flow is only dependent upon the maximum and minimum principal stresses, was investigated thoroughly by Guest [4]-[6] in experiments with thin wall tubes. He found that the intermediate principal stress had only a slight influence on yielding.

von Mises [3] proposed a criterion which assumes that the weighted average of all three principal stresses influences plastic flow (in contrast with Tresca). This criterion [3] was later interpreted by Nadai [7] to be based upon a critical octahedral "shear stress," while Hencky [8] interpreted it in terms of distortion energy.

---

* Although this criterion was first introduced indirectly by J. Clerk Maxwell (see for example Fracture, Vol. II, p. 492, published by Academic Press, 1968) it will be referred to herein by the more widely used name of von Mises.

In 1926 Lode [9] reported extensive tests in which thin walled tubes of iron, copper and nickel were subjected to combined axial tension and internal pressure; these were conducted to compare the Tresca and von Mises hypotheses and his results favored the latter. In 1931, Taylor and Quinney [10] tested nearly isotropic copper and steel tubing in combined tension and torsion and found that the deviation from the Mises criterion (though small) was real and could not be explained on the basis of experimental inaccuracy and anisotropy. Their findings led Stockton and Drucker [11] to modify the von Mises criterion by including the so-called third invariant of the stress tensor (see Chapter II).

Lessells and MacGregor [12] tested thin walled tubes of an alloy steel under axial tension and internal pressure; their experimental results agreed reasonably well with the von Mises criterion.

I.2 Yielding of Polymeric Materials

Since the dawn of civilization man has used natural polymers as materials from which weapons, tools, clothing and shelter could be produced. Today, the naturally occurring polymers which include such materials as wood, rubber, wool, cotton, silk, leather and paper have been augmented by hundreds of synthetic polymers, commonly known as plastics.

Polymers, in recent years, have found use in a wide variety of applications. Some are being used in dental and medical applications. Their excellent insulation properties make them well suited for electrical application. Additionally, they have found extensive use as packaging materials. In terms of mechanical applications, certain gears,

bearings, and seals are made of plastic. As a replacement for metals, they now find wide acceptance as pipes for transporting fluids.

Since plastics are now being considered for more extensive use as structural materials, their mechanical properties are of extreme interest to designers. The use of different polymers is often dictated as much by their mechanical properties as by their chemical behavior. In the design of many parts, it is necessary to know the magnitudes of mechanical properties such as yield strength, ductility and impact strength. An understanding of the yielding of polymers is of considerable interest not only for design considerations but also because of the potential use of traditional forming processes for producing differently shaped parts made from these solids.

Polymeric materials, unlike metals, show a pressure dependency on yielding (as discussed later). Additionally, they are more sensitive to temperature and strain rate effects than are metals. The phenomenon of stress relaxation is also quite pronounced. Because of these varying effects, studies devoted to the yielding behavior of polymeric materials have been conducted on the microscopic as well as the macroscopic level.

I.2.1 Macroscopic Yielding. Recognizing the fact that the yielding of polymeric materials is pressure dependent, several authors [13]-[18] have, in recent years investigated the yield behavior of glassy polymers. All of the criteria they propose are either a pressure-dependent Tresca or a modified von Mises criterion. Whitney [13] investigated the yielding behavior of polystyrene (PS) under biaxial stress states. He proposed that the experimental results (tension, compression, pure shear and plane strain compression) fit a pressure-dependent Tresca criterion.

Sternstein [14],[15] studied the yielding and crazing behavior of polymethylmethacrylate (PMMA) and proposed that shear yielding is governed by a pressure modified von Mises criterion written in terms of octahedral shearing stresses and other material parameters.

Bowden and Jukes [16] studied the yielding behavior of PMMA under plane strain with axial pull. They proposed a pressure modified Tresca criterion as being acceptable. In a recent publication Bowden and Jukes [17] conducted tests on a variety of polymers and have suggested three criteria for different situations. One is a modified von Mises (as suggested by Sternstein et al.). Another is a pressure modified Tresca and the third criterion (as suggested by Whitney) is yet a different version of a modified Tresca where they use shear stress as a function of the mean of all three principal stresses instead of the mean of maximum and minimum principal stresses. (The mathematical forms of these various theories are discussed in Chapter II). They [17] contend that the polymers when deforming homogeneously without shear bands (such as high density polyethylene (HDPE), polyvinychloride (PVC), and PMMA), should obey a modified von Mises criterion while those that deform inhomogeneously by the formation of shear bands (such as polyethylene terephthalate (PETP) and PS) should obey a modified Tresca criterion where shear stress is a linear function of the mean of the three principal stresses. They have, however, developed experimental yield loci only for PMMA and PS.

Bauwens [18] has proposed a relationship similar to that of Sternstein et al. based on tension and torsion tests using hollow

cylindrical specimens of PVC. The criterion used by Sternstein et al. and Bauwens was proposed by Drucker and Prager [19] in studies of soil mechanics problems, and it has also been discussed by Nadai [7].

Most work has been performed on the yielding behavior of glassy polymers. Far less study has been devoted to the yielding behavior of crystalline polymers. (In Section I.2.2, these different structures are discussed in detail.) In the present investigation, one crystalline (HDPE) and two amorphous (polycarbonate (PC) and PVC) polymers were subjected to studies involving macroscopic yielding. This was done to determine if the suitability of any phenomenological theory of yielding was dependent upon the structure and morphology of such materials.

I.2.2 Microscopic Aspects of Polymer Deformation. A polymer is a large molecule built up by the repetition of small, simple chemical units. Most of the commercial plastics exhibit either of the two common morphologies, the "crystalline" morphology or the "amorphous" morphology. Typical of those exhibiting the crystalline morphology are PE and Nylons. Exhibiting the amorphous morphology are, for example, PS, PC and PMMA. Although slightly crystalline, PVC is predominantly amorphous. For the purposes of this thesis, all polymers that vitrify and have disordered structures will be called glassy amorphous polymers. At sufficiently high temperatures, a linear polymer is rubbery amorphous but not glassy. At sufficiently low temperatures, the same polymer is a hard, rigid solid. There are two completely distinct mechanisms by which a polymer can solidify upon cooling: it can crystallize, or it can vitrify (form a glass). When a liquid above its melting point is cooled, it may undergo discontinuous change in the primary thermodynamic quantities such as volume or heat content or the secondary thermodynamic

quantities such as expansion coefficient or heat capacity (derivatives of the primary thermodynamic quantities). The temperatures at which these changes take place are called primary order and secondary order transitions.

A noncrystalline polymer below the temperature at which such a second-order transition occurs is said to be in the glassy state. The material is called a glass, and the temperature of the change is called the glass-transition temperature. This temperature is frequently denoted by T_g. There is actually no sharply defined glass transformation temperature, but rather a range of temperature over which changes occur. Crystalline (usually semicrystalline) as well as amorphous polymers are found to have the T_g at low temperatures.

The mechanical properties of glassy polymers are dependent upon the glass transition (T_g). It is generally observed that if the material is above T_g it is ductile and tough while it tends toward brittleness below T_g. However, there are materials which are still tough even below their T_g (e.g., PC and PVC). It has also been observed that the yielding behavior of polymers depends very much upon the ambient temperature.

I.2.2.1 Yielding of Glassy Amorphous Polymers. In the last ten years or so various theories have been proposed to explain the yield behavior of glassy amorphous polymers. Upon yielding and after reaching a total tensile strain of about 10 percent, these materials often develop a "neck" within which the material undergoes a severe deformation. This phenomenon has been called cold drawing in the literature. As opposed to this ductile behavior, brittle behavior may

be manifest in some glassy polymers appearing as tiny cracks; these are not true cracks and are called crazes. If the specimen were transparent before deformation, it generally becomes whitened due to the development of crazes.

Different mechanisms have been proposed to explain the phenomenon of yielding. Müller [20] and Jackel [21] described yielding as resulting from an increase in local temperature above ambient due to adiabatic heating. However, Robertson [22] points out that the temperature rise results from yielding rather than yielding occurring from a temperature rise.

Another explanation [22] considers that due to the applied shear stress, the viscosity of the polymeric material is lowered and yielding then takes place. The effect of shear stress on the rate of flow is described by the Ree-Eyring [23] type equation. The experimental data obtained by Lazurkin [24], Bauwens et al., [25]-[28], Roetling [29]-[31] and Brady and Yeh [32] fit the Eyring equation quite well if appropriate factors are employed. Robertson [33],[34] has suggested still another explanation in this regard; he proposes that the applied stresses induce a liquid-like structure in an "ordered state" which leads to yielding.

Litt et al., [35],[36], Rusch et al., [37],[38], Ender [39] and Dibenedetto et al., [40],[41] have used the free volume theory, first proposed by Doolittle [42], to explain the yielding of glassy amorphous polymers. It says that when deformed polymers attain sufficient free volume (at least equal to volume at T_g), certain degrees of freedom are released.

In summary, there is as yet no single, generally accepted mechanism that satisfactorily explains the yielding behavior of amorphous polymers at the microscopic level.

I.2.2.2 Yielding of Crystalline Polymers. The yielding and flow of "crystalline" polymers generally involves deformations in both crystalline and amorphous regions of the structure. The lamellar crystals are essentially embedded in an amorphous matrix, although they are often connected together by intercrystalline links. The molecular weight and the crystallization conditions affect both the amount of amorphous material and the number of intercrystalline links.

The mechanism of deformation of crystalline plastics is very complicated. Most of the work in this area has been done on single crystals. In bulk materials, where crystalline as well as amorphous phases exist, the deformation takes place in both phases. First there is elongation of "spherulites" in the direction of loading. As the spherulites elongate there is interlamellar slip, this causes deformation in the noncrystalline layers as well as in the crystalline lamella.

Except for the presence of the intercrystalline links, the yielding and flow characteristics of the noncrystalline layers are generally expected to be much like those of completely amorphous polymers. At temperatures above T_g the deformation of the noncrystalline layers should be easy. At temperatures below T_g, the yielding and flow stresses continually increase, because of the increasing rigidity of the amorphous phase.

Superimposed upon the behavior of the noncrystalline layers, however, is the restraint to deformation from the intercrystalline links.

The restraint derives from the links, which transmit directly to the crystal, part of the applied stress and the fact that due to virtually any deformation of the noncrystalline matrix the links must lengthen. The links probably lengthen by pulling material out of the crystals. This is the suggestion of the experiments of Vadimsky et al. [43].

Other crystallographic deformations observed have been twinning, glide along the molecular axis coupled with a crystal rotation, and phase transformation. No attempt shall be made to discuss them here. Geil [44] and Peterlin [45] have described these deformation mechanisms in some detail.

I.3 Influence of External Hydrostatic Pressure on the Yield Strength of Polymeric Material

The mechanical properties of glassy amorphous as well as crystalline polymers have been investigated under direct hydrostatic pressure in tension and compression. Holliday et al. [46] and Biglione et al. [47] investigated the effect of pressure on the tensile strength of PS and report that it increases. Ainbinder et al. [48] have examined the behavior of several glassy and crystalline polymers at moderate pressures in tension and compression. Pae et al. [49]-[51] have tested (PE), polytetrafluoroethylene (PTFE), and polypropylene, (PP). They reported that yield strength goes up with the pressure. Sardar et al. [52] have examined the properties of PP under tension up to 110 Kbar, and reported that Young's modulus increases linearly with pressure while the rate of increase of tensile yield strength decreases at high pressures.

Vroom and Westover [53] and Laka and Dzenis [54] have used a number of polymers (PS, PTFE, PMMA, and acrylonitrile-butadiene-styrene (ABS)) in this regard. Mercury served as the pressure medium, since they [53] contend that oil may act as a plasticizer which could increase the ductility of the polymer being studied. Some of their findings were that the yield strength increases for ABS and PTFE, while pressure has no effect on PS. They report that ultimate elongation increases with pressure for ABS but for PS, PTFE and PMMA it decreases. Young's modulus increases for all. This information has been presented in more concise form in Table III.1.

Recently Rabinowitz et al. [55] studied the torsional stress-strain response of isotropic PMMA, PETP, and PE under hydrostatic pressure up to 7 Kbar; an increase in both Young's modulus, and yield strength was observed for all three polymers. They also observed a ductile-brittle transition, at 3.2 Kbar, for PET while PE is reported to remain ductile through the whole pressure range; this is contrary to the findings of Pae et al. [52].

Recently the results of Davis and Pampillo [56], who studied PE at high pressure, have been used to explain the pressure dependence of yield strength by a theory of rate process. They observed that as the pressure increased, yield strength increased, however, the total elongation decreased as pressure increased. Pressures up to 8.3 Kbar were used and they evaluated the effect on what they call the pressure activation volume. As the pressure increases, this activation volume decreased.

It seems reasonable to conclude that hydrostatic pressure does indeed increase the yield strength of almost all polymers irrespective of the structure. Indirectly this shows that a yield criterion for polymeric materials should be pressure dependent.

CHAPTER II. THEORETICAL CONSIDERATIONS

II.1 Yield Surface

In the most general case a yield criterion will depend upon the complete state of stress at the point under consideration and will, therefore, be a function of the nine components of stress at that point. For a material loaded to the initial onset of yield, this can be expressed by the relationship

$$f(\sigma_{ij}) = K \quad , \tag{2.1}$$

where i and j vary from 1 to 3 and K is a constant.

If the assumptions given in Chapter I are made, and the yield surface is represented in principal stress space, the above relationship could be simplified to

$$f(\sigma_1,\sigma_2,\sigma_3) = K \quad , \tag{2.2}$$

where σ_1, σ_2 and σ_3 are principal stresses.

The yield criterion could also be expressed as a function of the stress invariants I_1, I_2 and I_3 as:

$$f(I_1,I_2,I_3) = K \quad , \tag{2.3}$$

where

$$I_1 = \sigma_1 + \sigma_2 + \sigma_3 \quad , \tag{2.4a}$$

$$I_2 = -(\sigma_1\sigma_2 + \sigma_2\sigma_3 + \sigma_3\sigma_1) \tag{2.4b}$$

and

$$I_3 = \sigma_1\sigma_2\sigma_3 \quad . \tag{2.4c}$$

The state of stress can be split into two parts; one is called the mean normal stress and the other the stress deviator or reduced stress. The mean normal stress is the arithmetic mean of the three principal stresses and is defined as follows:

$$\sigma_m = \frac{\sigma_1 + \sigma_2 + \sigma_3}{3} = I_1/3 \quad , \tag{2.5}$$

where σ_m can be considered as a hydrostatic stress. It has been mentioned in Chapter I that the influence of hydrostatic pressure does not affect yielding of metals. (Some exceptions have been reported [57]-[59].) If one assumes that yielding is unaffected by hydrostatic pressure, it is then possible to work with the reduced stress form rather than actual stress form. If J_1, J_2 and J_3 are the three stress invariants in reduced form, they can be expressed as:

$$J_1 = 0 \quad , \tag{2.6a}$$

$$J_2 = \frac{1}{3}(I_1^2 + 3I_2) = \frac{1}{6}[(\sigma_1 - \sigma_2)^2 + (\sigma_2 - \sigma_3)^2 + (\sigma_3 - \sigma_1)^2], \tag{2.6b}$$

$$J_3 = \frac{1}{27}(2I_1^3 + 9I_1 I_2 + 27I_3)$$

$$= \frac{1}{27}(2\sigma_1 - \sigma_2 - \sigma_3)(2\sigma_2 - \sigma_1 - \sigma_3)(2\sigma_3 - \sigma_1 - \sigma_2) \quad . \tag{2.6c}$$

The yield criterion in the reduced stress form can be expressed as a function of J_2 and J_3 as follows:

$$f(J_2, J_3) = K \quad . \tag{2.7}$$

If the yield criterion is independent of J_3 and only depends upon J_2, it reduces to the well known von Mises criterion. If plotted in principal stress space J_2 describes a circular cylinder whose generator has the direction <1,1,1> .

If the yield criterion is a function of only two principal stresses (maximum and minimum) and independent of I_1, it expresses the Tresca criterion. In three-dimensional principal stress space, this describes a regular hexagonal prism, whose generator also has the direction <1,1,1>. Although the Tresca criterion can be written in terms of J_2 and J_3, the resulting expression becomes very cumbersome and has found little acceptance in such a form.

Drucker [60] has used the criterion dependent upon J_2 and J_3 in the following form:

$$f = f(J_2, J_3) = J_2^3 - \alpha J_3^2 \quad . \tag{2.8}$$

This criterion plotted in the (σ_1, σ_2) plane lies between the von Mises and Tresca criteria (Fig. 1). By a suitable choice of α it allows a good correlation with experimental results. In the analysis of Osgood's data, Drucker [60] has used $\alpha = 2.25$.

Very recently Hosford [61] has proposed a criterion in the following form:

$$f = \left[\frac{(\sigma_1 - \sigma_2)^n + (\sigma_2 - \sigma_3)^n + (\sigma_1 - \sigma_3)^n}{2} \right]^{1/n} \quad \text{where } \sigma_1 > \sigma_2 > \sigma_3 \tag{2.9}$$

when n = 2, it represents von Mises criterion while the Tresca criterion is obtained for n = 1. By suitable choice of n a good correlation can be obtained with experimental results.

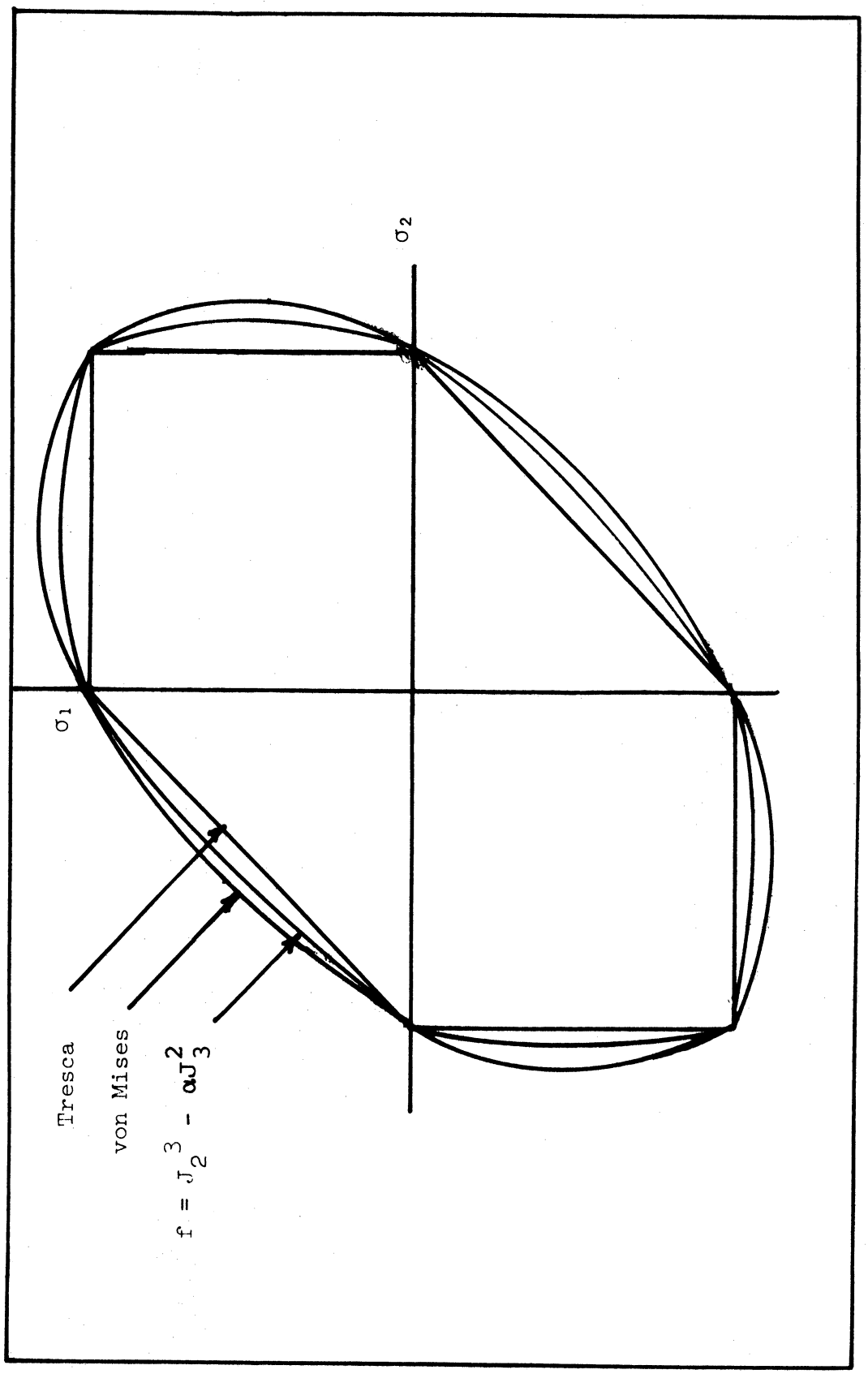

FIG. 1 COMPARISON OF DIFFERENT YIELD CRITERIA.

II.2 Previous Studies Involving the Yielding of Polymers

Since the yielding of polymers is influenced by the hydrostatic component of stress, it is necessary to include the first invariant, I_1, in a yield criterion for such materials. Thus, a yield criterion which includes the first and second invariants of stress will satisfy all the minimum requirements demanded by polymeric materials. Drucker [19] had proposed earlier such a yield criterion for soils as follows:

$$J_2^{1/2} + aI_1 = b \quad . \tag{2.10}$$

This criterion has also been discussed by Nadai [7] who proposed that the octahedral shear stresses are functions of the mean normal stress. If plotted in principal stress space equation (2.10) describes a cone whose axis is in <1,1,1> direction.

Both Sternstein [14],[15] and Bauwens [18] have used the criterion described by (2.10) in their yield studies. Bowden and Jukes [17] later suggested that this was also applicable for materials which deform homogeneously. Although these people [14]-[18] have used different constants in defining this criterion, the concept is the same.

Sternstein [15] expresses the criterion for shear yielding of PMMA as follows:

$$\tau_{oct} = \tau_s - \mu\sigma_m \quad , \tag{2.11}$$

where τ_{oct} is the octahedral shear stress, τ_s is the yield stress in pure shear, and σ_m and μ are the mean normal stress and a "friction" coefficient, respectively. According to his experimental results,

Sternstein [15] contends that μ is independent of temperature but is strain-rate dependent. τ_s is temperature as well as strain-rate dependent.

Bauwens [18] has used the following form:

$$\tau_{oct} + A\sigma_m = V \quad , \tag{2.12}$$

where A and V are constants and σ_m is the mean normal stress. If this criterion is expressed in terms of the three principal stresses it appears as follows:

$$\sqrt{(\sigma_1 - \sigma_2)^2 + (\sigma_2 - \sigma_3)^2 + (\sigma_3 - \sigma_1)^2} + A(\sigma_1 + \sigma_2 + \sigma_3) = 3V \quad . \tag{2.13}$$

For the plane stress state ($\sigma_3 = 0$) this reduces to:

$$\sqrt{2(\sigma_1^2 + \sigma_2^2 - \sigma_1 \sigma_2)} + A(\sigma_1 + \sigma_2) = 3V \tag{2.14}$$

or

$$\sqrt{\sigma_1^2 + \sigma_2^2 - \sigma_1 \sigma_2} + \frac{A}{\sqrt{2}}(\sigma_1 + \sigma_2) = \frac{3}{\sqrt{2}} V \quad . \tag{2.15}$$

A and V can be evaluated in terms of the yield strengths in tension, T,* and compression, C,* and will be given by two roots expressed in terms of either σ_1 or σ_2. Consider the case where $\sigma_2 = 0$ (i.e., uniaxial tension or compression in the σ_1 direction), then

---

* Wherever T and C appear throughout this thesis, they refer to the absolute values of tensile and compressive yield stress at ambient conditions.

$$\pm\sigma_1 + \frac{A}{\sqrt{2}}\sigma_1 = \frac{3}{\sqrt{2}}V \quad . \tag{2.16}$$

If C and T are <u>absolute</u> values

$$T + \frac{A}{\sqrt{2}}T = \frac{3}{\sqrt{2}}V \tag{2.17}$$

and

$$C - \frac{A}{\sqrt{2}}C = \frac{3}{\sqrt{2}}V \quad , \tag{2.18}$$

subtracting equation (2.18) from equation (2.17) gives:

$$(T - C) + \frac{A}{\sqrt{2}}(T + C) = 0$$

or

$$A = \frac{\sqrt{2}\,(C - T)}{(C + T)} \quad . \tag{2.19}$$

Substituting this expression for A into equation (2.17) there results:

$$T + \frac{T(C - T)}{(C + T)} = \frac{3}{\sqrt{2}}V$$

or

$$V = \frac{2\sqrt{2}\,(CT)}{3(C + T)} \quad . \tag{2.20}$$

On substituting the values of constants A and V from equations (2.19) and (2.20) into equation (2.13), one obtains

$$\sqrt{(\sigma_1 - \sigma_2)^2 + (\sigma_2 - \sigma_3)^2 + (\sigma_3 - \sigma_1)^2} + \sqrt{2}\,\frac{(C - T)}{(C + T)}\,(\sigma_1 + \sigma_2 + \sigma_3) = \frac{2\sqrt{2}\,(CT)}{(C + T)} \quad . \tag{2.21}$$

Equations (2.21) is also the same as equation (2.11) except that the constants are expressed in terms of <u>absolute</u> values of the yield strengths in tension and compression.

Whitney [13] has assumed that yielding is dependent upon the maximum and minimum principal stresses and expresses this criterion as follows:

$$\frac{\sigma_1 - \sigma_3}{2} = \frac{T}{2} + \frac{(\sigma_1 + \sigma_2 + \sigma_3)}{3} \tan \theta \ , \qquad (2.22)$$

where T is the yield stress in direct tension, $\tan \theta$ is a material constant, and σ_1 and σ_3 are the maximum and minimum principal stresses respectively. He incorrectly calls it a Mohr or Coulomb-Navier criterion.

Bowden and Jukes [17] proposed the following three criteria:

a. $$\sqrt{(\sigma_1 - \sigma_2)^2 + (\sigma_2 - \sigma_3)^2 + (\sigma_3 - \sigma_1)^2}$$

$$= \sqrt{6} \left[k + \mu_1 \frac{(\sigma_1 + \sigma_2 + \sigma_3)}{3} \right] . \qquad (2.23)$$

b. $$\frac{\sigma_1 - \sigma_3}{2} = k + \mu_2 \frac{(\sigma_1 + \sigma_3)}{2} \ . \qquad (2.24)$$

c. $$\frac{\sigma_1 - \sigma_3}{2} = k + \mu_3 \frac{(\sigma_1 + \sigma_2 + \sigma_3)}{3} \ . \qquad (2.25)$$

The criterion expressed by equation (2.23) is equivalent to (2.21) as proposed by Nadai [7], Sternstein [15], Bauwens [18], and Drucker [19]. Equation (2.24) is widely called the "Mohr-Coulomb" criterion; however, in soil mechanics, the term "Coulomb criterion" is widely used; in applied mechanics, the term "Mohr's criterion" has been widely used, and in geology and rock mechanics, the appellation "Coulomb-Navier criterion" is sometimes used. For a historical review see reference [62].

The criterion expressed by equation (2.25) assumes that although yielding is dependent upon the difference of maximum and minimum principal stresses, it is influenced by the mean of the three principal stresses rather than the normal stress, $(\sigma_1 + \sigma_3)/2$, acting on the plane of maximum shear. The criterion described by equation (2.25) has also been recently suggested by Schofield and Wroth [63] whose book is devoted to soil mechanics. The criterion of equation (2.22) suggested by Whitney [13] is identical to that of equation (2.25).

II.3 Suggested Yield Criterion

The criterion suggested here is essentially a pressure-dependent von Mises yield criterion.

This criterion in principal stress space is expressed as follows:

$$(\sigma_1 - \sigma_2)^2 + (\sigma_2 - \sigma_3)^2 + (\sigma_3 - \sigma_1)^2 + 2(C - T)(\sigma_1 + \sigma_2 + \sigma_3) = 2CT \quad . \tag{2.26}$$

The first three terms of the above equation are the same as those of von Mises' criterion while the term $(\sigma_1 + \sigma_2 + \sigma_3)$ includes hydrostatic stress. When C = T (i.e., if the yield strengths in tension and compression are equal), equation (2.26) reduces to the von Mises criterion. The author arrived at this criterion independently, recognizing that the criterion proposed by Whitney did not pass through the experimental points in second and fourth quadrants of his yield locus. This is shown in Fig. 2. The author drew an ellipse through Whitney's experimental points and obtained an equation from the obtained curve. Later the author learned that Stassi D'Alia [64] had proposed this earlier as a type of universal yield criterion. Although Stassi D'Alia [64] has

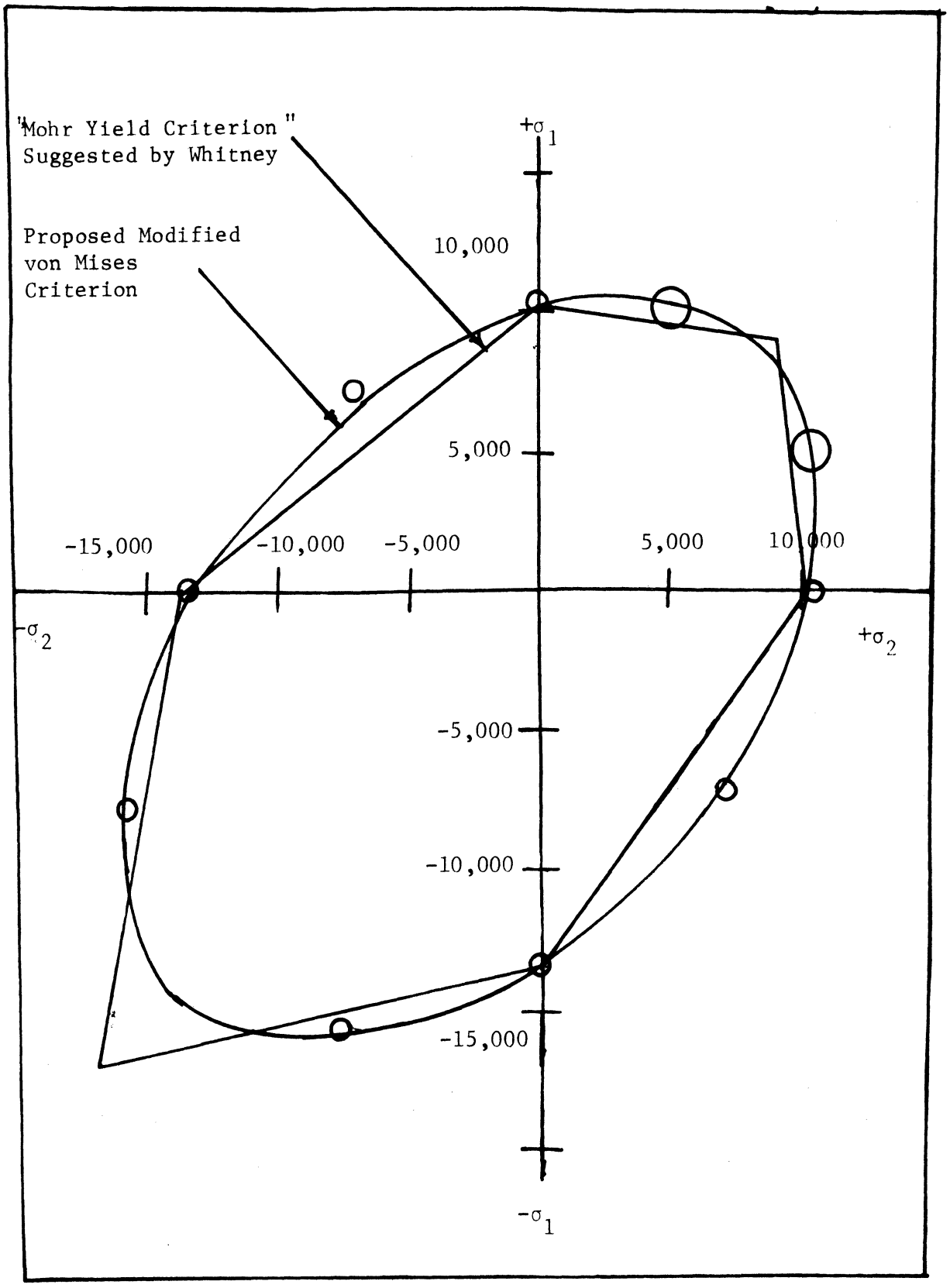

FIG. 2 TEST RESULTS OBTAINED BY WHITNEY [13] SHOWING THE FIT WITH THE "MOHR-COULOMB" YIELD CRITERION [13] AS COMPARED WITH THE MODIFIED VON MISES CRITERION EXPRESSED BY EQUATION (2.26).

made extensive use of this criterion for a number of materials, it had not, until now, been employed where polymers were involved. It must be noted that Meldahl [65] presented this criterion in the form of a three-dimensional model of a yield surface; he attributed the concept to Schleicher [66]. Tschoegl [67] has recently discussed this as one of several possible "failure" surfaces for honeycomb materials; e.g., polyurethane foam. As pointed out by Stassi D'Alia, this criterion fits such experimental results as those of Coffin [68] who conducted tests with thin wall tubes of gray cast iron. One of the reasons that drew this criterion to the author's attention was that under external hydrostatic pressure, a parabolic relationship between the yield strength and hydrostatic pressure is predicted; this agrees with observed experimental findings. In comparison equation (2.12) or (2.21) predicts a linear relationship between yield strength and hydrostatic pressure and in three-dimensional stress space it plots as a cone whose axis coincides with <1,1,1> direction. The various forms of these yield criteria are summarized in Appendix C.

II.4 Normalized Forms of Yield Criteria

Since the properties of a given polymer may differ from one batch to another, experimental problems could arise. Tests conducted by this author on different batches of PVC and PE indicated that for both of these materials, pertinent property values did indeed vary between batches. As it is desirable to plot the experimental results on a common curve, it was decided to normalize the yield criterion with respect to yield strength in tension. This bypasses the problem of using absolute values which could differ from batch-to-batch.

As the intended yield studies were to construct biaxial plots (i.e., σ_1, σ_2 space), equations (2.21) and (2.26) were reduced by setting $\sigma_3 = 0$. By defining the normalizing factors:

$$R_1 = \frac{\sigma_1}{T} \quad \text{and} \quad R_2 = \frac{\sigma_2}{T}$$

(2.21) and (2.26) can, in sequence, be expressed as:

$$\sqrt{R_1^2 + R_2^2 - R_1 R_1} + \frac{(C - T)}{(C + T)}(R_1 + R_2) = \frac{2\, C/T}{(C/T + 1)} \quad , \tag{2.27}$$

$$R_1^2 + R_2^2 - R_1 R_2 + (C/T - 1)(R_1 + R_2) = C/T \quad . \tag{2.28}$$

Equations (2.27) and (2.28) are functions of the ratio of yield strength in compression and tension under ambient conditions, C/T, only. To plot a "predicted" yield locus for a particular material, it is only necessary to determine these two property values. Figure 3 illustrates such a comparison for a C/T ratio of 2.0.

II.5 Plane Strain Flow

Imposing the condition of plane strain upon equations (2.21) and (2.26), two important results may be noted.

Assuming that the yield criterion and "plastic potential" are similar in shape, the plastic stress-strain relations (or flow rules) can be written as follows: (see e.g., [69])

$$d\varepsilon_{ij} = \beta \frac{\partial f}{\partial \sigma_{ij}} df \quad , \tag{2.29}$$

where the yield function can be chosen as f(ij).

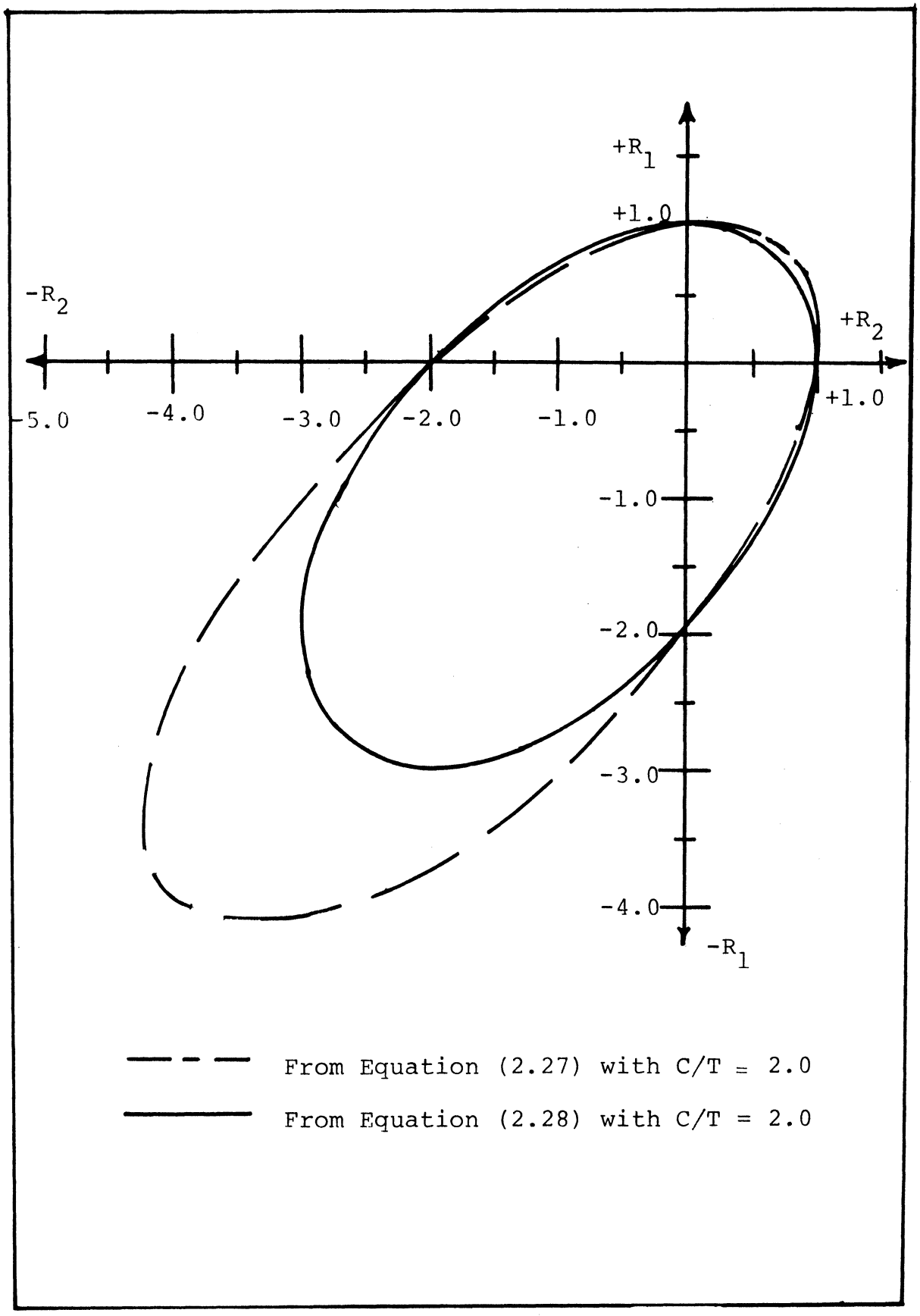

FIG. 3 COMPARISON OF TWO YIELD CRITERIA (AS EXPRESSED BY EQUATIONS (2.27) AND (2.28))FOR A C/T RATIO OF 2.0.

If equation (2.10) is introduced as f in (2.29) and considering the condition of plane strain such that $d\varepsilon_2 = 0$, it can be shown that:

$$\frac{\sigma_1 - \sigma_3}{2} = \frac{-3a}{(1 - 3a^2)^{1/2}} \left[\frac{\sigma_1 + \sigma_3}{2} \right] + \frac{b}{(1 - 3a^2)^{1/2}} \quad . \qquad (2.30)$$

The full development leading to (2.30) may be found in Appendix A.

Now equation (2.10) is the form of the yield criterion suggested by Sternstein [15] and Bauwens [18], and (2.30) is simply (2.10) for plane strain conditions. It can be seen that the left-hand side of equation (2.30) is the maximum shear stress and is a function of the normal stress acting on the plane of maximum shear. As can be seen by comparison with (2.24), this is the Mohr-Coulomb criterion used by Bowden and Jukes [16]. In essence then, (2.24) is really a specialized form of (2.10) and since the multi-axial stress case is certainly not restricted to plane strain deformation, the Mohr-Coulomb criterion does not possess the general applicability that one seeks in a yield criterion. It is worth observing that the Tresca criterion is a special form of the Mohr-Coulomb hypothesis; this suggests that Tresca criterion itself is strictly a plane strain criterion.

If the plane strain condition is applied to Eq. (2.26) and taking $d\varepsilon_2 = 0$, there results:

$$\left[\frac{\sigma_1 - \sigma_3}{2} \right]^2 = \frac{(C + T)^2}{12} - (C - T) \frac{(\sigma_1 + \sigma_3)}{2} \quad . \qquad (2.31)$$

Again, Appendix A may be consulted for the complete algebraic development. Equation (2.31) predicts a parabolic relationship between the maximum shear stress and the normal stress acting on the maximum shear plane. This type of relationship had been proposed by Leon, as noted in [7], for predicting cleavage fractures.

II.6 Dilatation

Whitney [13] was the first worker to make dilatometric measurements on PS under direct compression and found that the plastic volume at first increases then remains constant. Coffin [68] tested thin-walled tubes of gray cast iron under various biaxial stress states and along with yield measurements, he also measured the three principal strains. From these he computed the volume change and found that the plastic volume does indeed increase under compressive as well as tensile loading. He observed an increase in the yield stress of gray cast iron with the superposition of hydrostatic pressure. Based upon theoretical considerations, Drucker [70] has argued that if the strength of a homogeneous and isotropic material is influenced by hydrostatic pressure then it is essential that the plastic volume should change during subsequent deformation in order not to violate the First Law of Thermodynamics. Although in this present work no attempt was made to make dilatometric measurements, dilatation expressions have been derived using both equations (2.21) and (2.26).

Invoking the flow rules and applying (2.29) to equation (2.21), leads to

$$d\varepsilon_1 + d\varepsilon_2 + d\varepsilon_3 = 3\beta \frac{(C - T)}{(C + T)} \quad , \tag{2.32}$$

while the use of equation (2.26) gives

$$d\varepsilon_1 + d\varepsilon_2 + d\varepsilon_3 = 6\beta(C - T) \quad . \tag{2.33}$$

As discussed by Hill [69], it is unlikely that β remains constant during deformation; what is most significant is that β is a positive quantity. Thus any change in plastic volume is dependent upon the differences in the absolute values of the compressive and tensile yield strengths. No real material is known to the author whose tensile yield exceeds the compressive yield; in essence therefore, one other requirement of a realistic yield criterion is that it should lead to predictions of dilatation that are not negative. Both of the criteria under discussion (i.e., equation (2.21)) and (2.26) satisfy this requirement.

In this regard, the recent work reported by Davis and Pampillo [71] contains some puzzling results. Under the superposition of hydrostatic pressure, they made dilatometric measurements on PMMA and PC and reported that the volume of PMMA did not change while the volume of PC decreased during yielding. This anomalous behavior is explained [71] using arguments based upon a theory of rate processes, but there is not as yet universal agreement in regard to this behavior. They did, however, indicate that the yield strength of PC increases with pressure, a fact that is fairly well supported in the literature.

II.7 Effect of Hydrostatic Pressure on Yield Stress

Many workers have shown that the yield strength in tension as well as in compression goes up with the application of hydrostatic pressure. Variation of yield stress can be expressed either as a function of hydrostatic pressure or as a function of mean normal stress. Yield stress variation from equations (2.21) and (2.26) is shown as a function of hydrostatic pressure as well as mean normal stress. Consider that a hydrostatic pressure, P, is applied to a specimen which is then subjected to a tensile test. The stress state may be expressed as

$$\sigma_2 = \sigma_3 = -P \quad ; \quad \sigma_1 = \sigma - P \quad ,$$

and interest centers around the value of the apparent stress σ needed to cause tensile yielding. Substitution of the above results into equation (2.26) gives:

$$\sigma^2 + (C - T)(\sigma - 3P) = CT \quad . \tag{2.34}$$

Equation (2.34) can be rewritten in different forms. If expressed in terms of the mean normal stress, it becomes:

$$\sigma^2 + 3(C - T)\sigma_m = CT \quad . \tag{2.35}$$

If normalized with respect to T, one gets:

$$\left[\frac{\sigma}{T}\right]^2 + 3\left[\frac{C}{T} - 1\right]\left[\frac{\sigma_m}{T}\right] = \frac{C}{T} \tag{2.36}$$

or

$$R^2 + 3(X - 1)D = X \quad , \tag{2.37}$$

which gives two equal and opposite roots of R, R_T and R_C and can be expressed as

$$R_T = -R_C = \sqrt{X - 3D(X - 1)} \quad , \tag{2.38}$$

where

$$\frac{\sigma_1 + \sigma_2 + \sigma_3}{3} = \frac{\sigma - 3P}{3} = \sigma_m$$

and

$$R = \sigma/T \quad , \quad X = C/T \quad , \quad D = \sigma_m/T \quad .$$

Equation (2.34), if written in the following normalized form

$$R = -\frac{(X - 1)}{2} \pm \frac{1}{2}\left[(X + 1)^2 + 12B(X - 1)\right]^{1/2} \tag{2.39}$$

predicts parabolic relationship between hydrostatic pressure and yield stress. Here B = P/T. Either of the equations (2.38) or (2.39) may be used to predict the effect of pressure on yielding.

Following a similar procedure, equation (2.21) can be expressed as:

$$\pm\sigma + \frac{(C - T)}{(C + T)}(\sigma - 3P) = \frac{2CT}{(C + T)} \tag{2.40}$$

or

$$\pm\sigma + \frac{3(C - T)}{(C + T)}\sigma_m = \frac{2CT}{(C + T)} \quad . \tag{2.41}$$

If normalized with respect to T, (2.41) simplifies to:

$$\pm(\sigma/T) + \frac{3(C/T - 1)}{(C/T + 1)} \left[\frac{\sigma_m}{T}\right] = \frac{2\ C/T}{(C/T + 1)} \quad . \tag{2.42}$$

If written in the notations of equation (2.38) it appears as

$$R_T = -R_C = \frac{2X}{1 + X} - \frac{3(X - 1)}{1 + X} D \quad . \tag{2.43}$$

Similarly, equation (2.40) can be written in the normalized form as follows:

$$\frac{\sigma}{T} = \frac{3P}{T} \frac{(C/T - 1)}{2\ C/T} + 1 \tag{2.44a}$$

and

$$\frac{\sigma}{T} = -\frac{3P}{T} \frac{(C/T - 1)}{2} - C/T \quad . \tag{2.44b}$$

If expressed in terms of variables of equation (2.39) the two roots appear

$$R_T = \frac{3B(X - 1)}{2X} + 1 \tag{2.45a}$$

and

$$R_C = -\frac{3B(X - 1)}{2} - X \quad . \tag{2.45b}$$

In the ensuing chapters of this work equations (2.38), (2.39), (2.43) and (2.45a and b) will find major application.

CHAPTER III. PREVIOUS EXPERIMENTAL STUDIES

During the past decade, studies involving the macroscopic yielding of polymers have been reported by several authors [13]-[18]. One might categorize the work conducted to date as being related to the influence of pressure as it affects the yield locus or as it affects the tensile and/or compressive yield strength. A brief summary of the major works is now presented.

III.1 Yield Loci Studies

Whitney and Andrews [13] were the first to investigate the yield behavior of PS under biaxial stress state. They proposed a yield criterion for PS based upon their findings and labeled it as Mohr or Coulomb-Navier criterion. However, it can be seen from Fig. 2 that the yield criterion suggested by them [13] does not pass through the test points obtained in pure shear.

Bowden and Jukes [16] constructed a yield locus for PMMA based upon results obtained with a Ford-type test [72]. Because of the relative "brittleness" of this polymer, they could not obtain experimental points when the magnitude of tensile stress was higher than the compressive stress. They also proposed a Mohr or Coulomb-Navier criterion for PMMA. In a recent publication [17] they have tested PS, PMMA, PVC and PE and have concluded that different yield criteria should be used depending upon the homogeneity of deformation of the particular polymer.

Based upon studies which utilized thin-wall tubes, both Sternstein et al. [14],[15] and Bauwens [18] proposed a criterion involving the octahedral shear stress and the mean normal stress as being most appropriate for their findings. This has been described previously as a pressure-dependent von Mises criterion. All of these studies have been confined to glassy amorphous polymers.

III.2 Yielding Studies Under Hydrostatic Pressure

The effect of hydrostatic pressure on yield stress has been studied by a number of workers [46]-[56]. Glassy amorphous, semi-crystalline and crystalline polymers have been included in those investigations. The apparatus used for generating the pressure and conducting the testing is essentially like that used by Bridgman [73] or Pugh [74]. In the main, the influence of pressure on tensile or compressive behavior has been investigated although Rabinowitz et al. [55] have tested PMMA, PET and PE under torsion. Table III.1 summarizes the principle findings of these workers. All of them agree that the Young's modulus increases with pressure regardless of the polymer or pressure medium. Laka and Dzenis [54] have attributed this to compaction of the material under high hydrostatic pressure. As seen in Table III.1, contradictory results do exist in a number of instances and a reasonable explanation for this is certainly lacking at the present time. In order to settle these discrepancies it is essential that the tests should be conducted at high hydrostatic pressures with different fluid media. No such attempt is made in this work.

Table III.1

* Summary of Work Involving the Influence of Pressure on Mechanical Properties of Various Polymers

Polymer	Test Type	Mechanical Properties: Young's Modulus	Yield Strength	Ultimate Elongation	Ultimate Strength	Remarks
PS	Compression	Increases	Increases then levels off	Very slight increase	Increase	Maximum hydrostatic pressure 2.0 Kbar. Oil pressure medium. [48]
	Tension	Increases		Decreases	Decreases	Mercury pressure medium. Maximum hydrostatic pressure used was 2.0 Kbar. [53]
	Tension	Increases	Increases	Increases	Increases	Pressure medium not specified. Brittle to ductile transition was observed between hydrostatic pressure of 2 to 3 Kbar. Maximum hydrostatic pressure used was 6.0 Kbar. [47]
	Tension		Increases	Increases		Test was conducted only for one hydrostatic pressure. Maximum hydrostatic pressure used was 7.5 Kbar. [46]
PMMA	Tension and Compression	Increases	Increases	Increases	Increases	Maximum fluid pressure used was 2.0 Kbar. [48]

* Any blank spaces mean no information reported.

Polymer	Test Type	Mechanical Properties: Young's Modulus	Yield Strength	Ultimate Elongation	Ultimate Strength	Remarks
Teflon PTFE	Tension	Increases	Increases	Decreases		A gradual transition from ductile to brittle occurred. The morphology of the fracture surfaces changed from rough texture to cleavage type. Maximum hydrostatic pressure used was 7 Kbar. [50]
	Tension	Increases	Increases	Decreases		Maximum hydrostatic pressure used was 2 Kbar. [54]
PC	Tension		Increases			Maximum hydrostatic pressure used was 2 Kbar. Pressure medium oil. [78]
PE	Compression	Increases				[48]
	Tension	Increases	Increases	Decreases		[49]
	Tension	Increases	Increases	Decreases		The increase in strength is explained by a theory of rate processes. Pressure medium n-pentane and water. [56]
PMMA	Tension	Increases	Decreases	Decreases	Decreases	[53]
	Tension	Increases	Increases		Increases	Necking was observed when the surface was protected from the oil pressure medium. [54]

		Mechanical Properties				
Polymer	Test Type	Young's Modulus	Yield Strength	Ultimate Elongation	Ultimate Strength	Remarks
	Torsion	Increases	Increases	Increases	Increases	Pressure medium 50/50 mixture of castor oil and brake fluid. Ductile-brittle transition at 3.2 Kbar. [55]
PET	Torsion	Increases	Increases	Increases		[55]
	Tension	Increases	Increases			[55]
POM	Tension	Increases	Increases then levels off			[52]
PP	Tension	Increases	Increases	Decreases		At high pressure the neck forms but does not propagate. Sharp crack develops and fracture takes place. [50]
Teflon (PTFE)	Tension	Increases		Decreases	Increases	[53]
PE	Tension	Increases	Increases	No change		Under high pressure whitening disappears and the specimen becomes transparent. [54]

CHAPTER IV. PRESENT EXPERIMENTAL INVESTIGATION

The principal purpose behind the work conducted in this study was to subject several yield criteria, including one not previously used, to a comparison with experimental results and to determine if one criterion was most acceptable. A second intent of this work was to conduct enough exploratory tests to compare the tensile and compressive yield strengths of the test polymers as a function of hydrostatic pressure. The upper limit of pressure to be used was based upon the maximum differences between the mean stress experienced in uniaxial tension and compression for the test polymers. Since the "strongest" polymer was PC, whose tensile yield was about 10,000 psi and compressive yield about 12,000 psi, the range of mean normal stress was of the order of 7000 psi. This led to an arbitrary choice of 10,000 psi as an upper limit of the pressure medium.

IV.1 Materials

Two glassy amorphous polymers (PC and PVC) and one crystalline type (HDPE) were chosen for this study. All materials were obtained from a commercial source as round cross-sectional bar stock of 1 1/2 inch diameter. During this study, specimens were taken from two bars of PVC (referred to as PVC-A and PVC-B in the results), and three bars of PE (specified as PE-A, -B, or -C). Such distinctions were essential since the properties of interest varied from bar to bar for these two polymers. No such coding was needed with PC since the properties did not vary from

one bar to another. No special treatments were given to the bars. They were used in the "as received" condition which was referred to as "standard" by the commercial company.

IV.2 Uniaxial Tension Test

From each bar, tensile specimens were produced with the longitudinal axis of the specimen being parallel to the axis of the original bar. Specimens had a uniform gage section of 4-inch length with a cross section that was 0.300 inch by 0.300 inch square. The overall length was 6 inches with the ends of the specimens being threaded for adaptation to grips on a 500 kg Instron Machine (Model TM-SM). Every test was conducted at a crosshead speed of 0.02 inch/min, the specimen elongation being measured with an Instron Strain Gage Extensometer (Type G51-11M). This had a 1 inch gage length and an allowable uniform extension of 10 percent. The load was sensed by a standard Instron load cell whose calibration was checked periodically with dead weights. A record of load-elongation was obtained on the Instron chart recorder, with the output of the extensometer used to drive the chart. Contraction in the lateral directions during a test was, in general, measured simultaneously using flat micrometers. Comparative contraction measurements were also obtained using two Instron Transverse Strain Sensors (Type G57-12M). Agreement with micrometer values was so close that most of these data were obtained with micrometers because of simplicity. These measurements were used to evaluate true stress and also to check on possible anisotropic behavior of the material. By converting the longitudinal and lateral measurements to axial and lateral

strains, Poisson's ratio was calculated. These values of Poisson's ratio were used in certain analyses of experimental results as will be shown. Calibration of the extensometer and transverse sensors were performed with the aid of the table actuating mechanism from a tool-maker's microscope. This calibrating device was accurate to the order of 10^{-4} inches.

IV.3 Compression Tests

Direct compression tests were conducted on specimens machined in both the axial and radial directions from the bar stock. The specimens were of 1/2 inch x 1/2 inch square cross section and 3/4 inch high. A square cross section was chosen because it was expedient to mount a transverse strain sensor that indicated the change in one of the lateral dimensions.

Specimens were compressed between two hardened and ground platens. To minimize frictional effects, molybdenum disulphide grease was used as a lubricant. All such specimens were deformed at an Instron cross-head speed of 0.02 inch/min. The Instron load was recorded on a gear-driven chart. The change in the height of specimens was deduced by knowing chart speed and the Instron cross-head speed. Because it was necessary to make corrections for the machine stiffness during the change of specimen height, the combined stiffness of the compression load cell and the Instron was determined by compressing the cross-head against the load cell.

Lateral dimensional changes were found with the aid of an Instron Transverse Strain Sensor. This was mounted across two parallel faces,

and it was assumed that changes in each lateral dimension were reasonably similar. Spot checks with micrometers indicated this to be a good assumption. Calibration of the sensor was discussed previously and during an actual test, the output of the sensor was recorded on a two-channel Sanborn Recorder (Model 152-100A).

IV.4 Thin-Wall Tube Tests

IV.4.1 Manufacture of Tubes. Thin-wall tubes having an external diameter of 0.890 inch and wall thickness of 0.040 inch were machined from the bar stock. The overall length of the tubes was 6 inches with the test section length being 2 1/2 inch. To ensure concentricity and to hold close tolerances on the wall thickness, care had to be exerted during machining. The sequence of machining was as follows: (a) first, a 3/4 inch diameter hole was drilled; (b) this was then enlarged to 25/32 inch diameter; (c) subsequently, two reamers of 51/64 inch and 13/16 inch diameter were used to finish the hole to the required dimensions. The tube was then mounted on a mandrel for the finish machining of the outer diameter. In this way, excessive twisting of or distortion of the tube was avoided. The cutting fluid used was hydraulic oil which was also eventually used as the fluid for providing internal pressure with the tubes; it also served as the pressure medium in the pressure chamber used for hydrostatic experiments. The particular cross section of the tube was chosen so that the load capacity of the Instron machine was not exceeded during any of these tests.

IV.4.2 Constant Stress Ratio Loading. The tubes were loaded under either tension or compression by Instron crosshead movement and the

internal pressure was supplied by a hydraulic pump. In order to achieve radial loading (the ratio of axial stress to tangential stress being constant), the ratio of load to pressure was predetermined for a particular value of the stress ratio. As the axial load increased, the pressure was also increased by continued actuation of a hand pump. As shown in Fig. 4, the radial loading along OA was achieved using small discrete steps of axial load and internal pressure. Since the Instron cross-head speed was quite low, sufficient time was available for increasing the pressure to a predetermined value, thereby closely approaching a true radial loading path. The state of stress of point A in Fig. 4 could also have been reached via a number of different paths; these would require varying the stress ratio instead of keeping it constant. An alternate path such as OCA could have led to the stress state at A. A few tests were tried with this type of loading path but this approach was abandoned as it proved difficult to use. Since there is no well-defined boundary between the elastic and the plastic region, it was virtually impossible to find the limit to which the load in first one direction, and then in the other direction, could be applied without crossing the yield boundary.

Various constant stress ratio tests in the tension-tension and tension-compression quadrants of the yield locus were conducted with thin-wall tubes. Figure 5 is a line drawing showing how a tube was subjected to circumferential or "hoop" stress only; in effect this is an open-ended tube. The end adapter contains a passage through which the pressurized oil enters the tube and produces the internal pressure.

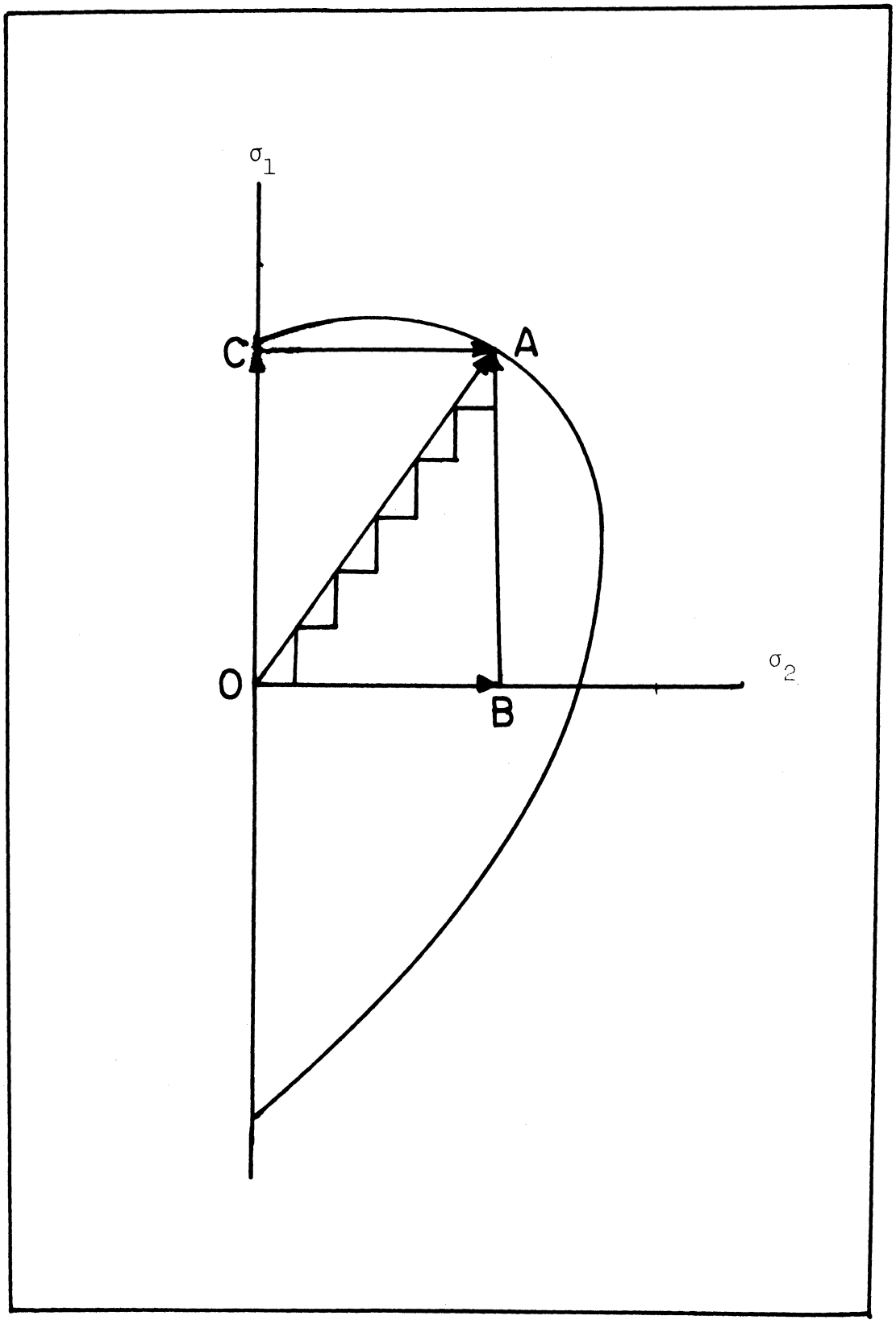

FIG. 4 ILLUSTRATION SHOWING ALTERNATE LOADING PATHS TO REACH A COMMON POINT ON A YIELD LOCUS.

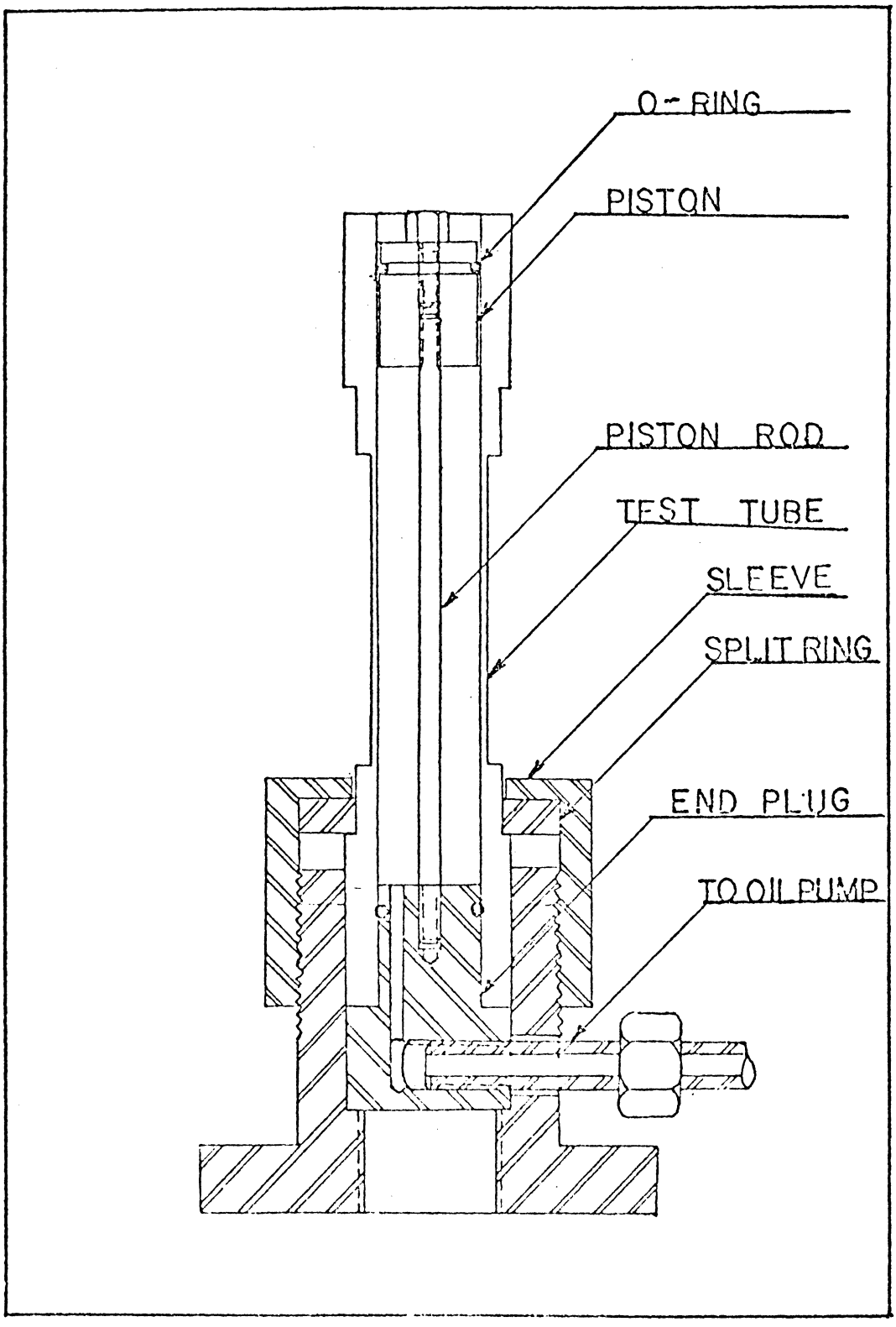

FIG. 5 SCHEMATIC OF THE TEST SETUP USED TO CONDUCT AN "OPEN-ENDED" TUBE TEST FOR DETERMINING THE "HOOP" YIELD STRESS.

An aluminum piston, having an O-ring seal, was connected to the lower end plug by means of the piston rod. This prevented the piston from moving out of the test tube as pressure was increased and any axial forces created by the O-ring would be negligible. Thus, such a test produced a stress state that was, for practical purposes, free from any axial stress.

In the general case, where internal pressure was to be accompanied by axial tension or compression, identical adapters were fitted to both ends of the test tube. Each adapter was connected to special grips on the Instron through the outer sleeve. As the machine applied tensile load, it was transmitted to the tube through the split rings. For compressive loading, the bottom adapter rested on the Instron load cell while force was transmitted by the Instron cross-head which contacted the top end adapter. Figures 6 and 7 are two views of the test setup; axial loads were recorded on the Instron recorder with the chart being driven by the output from the extensometer. Internal pressure was indicated by a bourdon tube-type pressure gage which was calibrated with a dead weight tester.

Axial deformation (either extension or contraction) was measured with the same extensometer used for tension testing. Tangential strains were evaluated by measuring the external diameter of the tube with micrometers. Some effort was expended to measure the actual thickness of the polyethylene tubes during loading by using an inductance pickup as discussed in reference [75]. However it was found that the changes in tube thickness were only a few thousandths of an inch. Such small

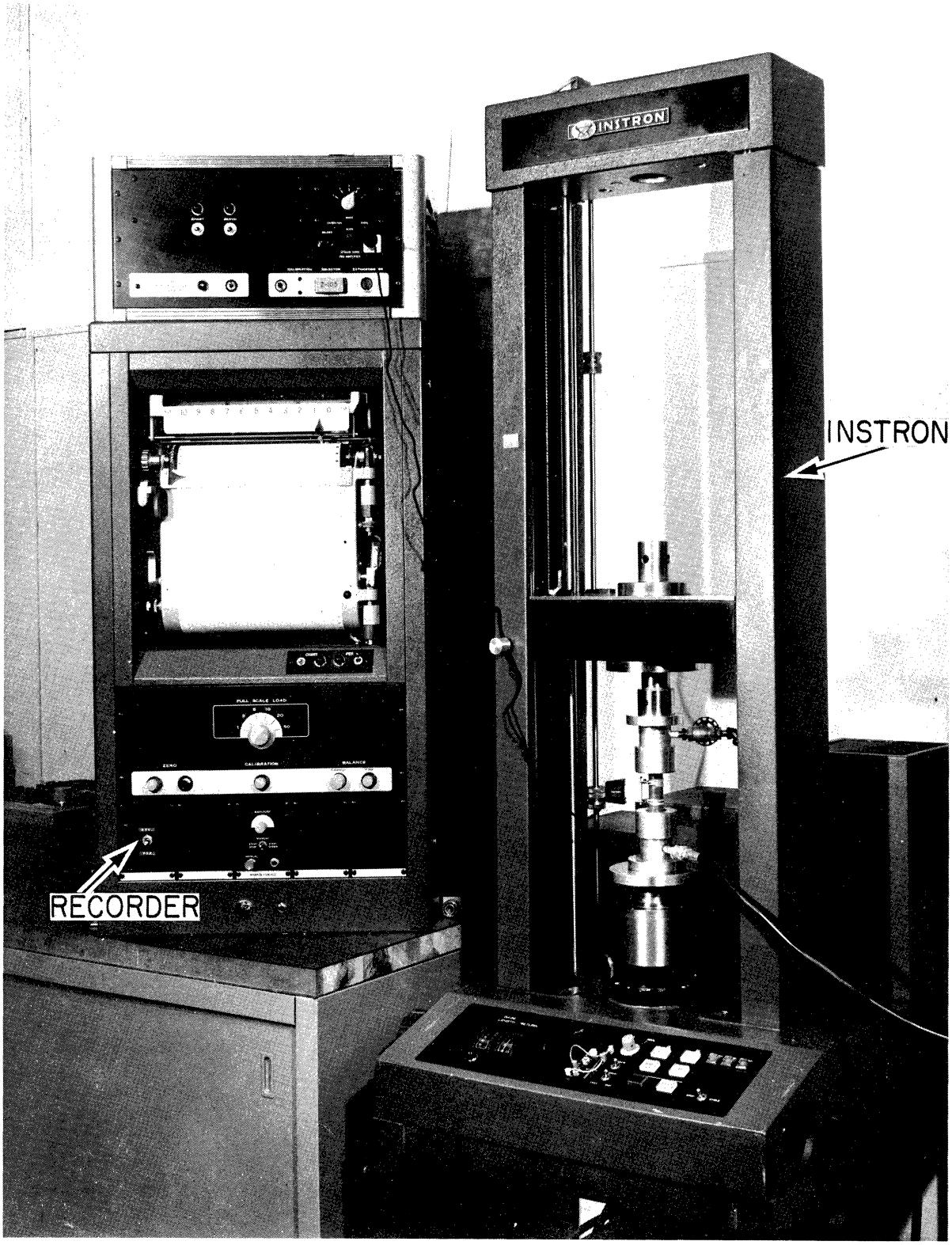

FIG. 6 GENERAL VIEW OF INTERNAL PRESSURE AND AXIAL COMPRESSIVE LOADING.

FIG. 7 DETAIL VIEW OF INTERNAL PRESSURE AND AXIAL COMPRESSIVE LOADING.

changes could not have been used in the computation of stresses and strain with sufficient reliability. Instead it was found expedient to use the principle of volume constancy to determine both the thickness strain and the instantaneous thickness. In order to check the validity of this assumption tension tests were conducted on PC tubes (without using internal pressure) and true stress values were found by using areas based upon constancy of volume. The true stress-strain curve obtained in this way was identical within experimental error to the true stress-strain curve determined with a standard tensile specimen as described in Section IV.2.

IV.4.3 Computation of True Stresses and Strains. Nominal axial and lateral strains were calculated from the measured data. True strains were calculated using the following relations:

$$\epsilon_1 = \log_e (1 + e_1) \tag{4.1}$$

and

$$\epsilon_2 = \log_e (1 + e_2) \ , \tag{4.2}$$

where e_1 is nominal axial strain,

e_2 is nominal tangential strain and

ϵ_1 and ϵ_2 are true axial and tangential strains.

Instantaneous thickness t_i and the instantaneous internal diameter d_i were calculated as follows: In Appendix B it is shown that the instantaneous wall thickness t_i is approximately

$$t_i = \frac{t}{1 + e_1 + e_2} \ . \tag{4.3}$$

The internal diameter d_i as shown in Appendix B, is

$$d_i = (d + 2t)(1 + e_2) - 2t_i \quad , \tag{4.4}$$

where d and t are initial internal diameter and initial thickness, respectively. The thickness strain (ϵ_3) was found from

$$\epsilon_3 = \log_e \left(\frac{t_i}{t} \right) \quad . \tag{4.5}$$

The axial and tangential stresses were calculated according to:

$$\sigma_1 = \frac{p d_i^2 + 4 L/\pi}{4 t_i (d_i + t_i)} \tag{4.6}$$

and

$$\sigma_2 = \frac{p d_i}{2 t_i} \quad , \tag{4.7}$$

where σ_1 = axial stress,

σ_2 = tangential stress,

L = axial load recorded by the Instron and

p = internal pressure.

IV.5 Plane Strain Compression

The tests described thus far provide points in the first and fourth quadrants of the yield locus. In order to provide additional support for the proposed yield criterion, it was decided to obtain some information in the third quadrant of the yield locus.

A strip of 6-inch length and 1 1/2 x 1/4 inch cross section was machined from 1 1/2-inch diameter PVC rod. It was compressed between two parallel flat and polished dies, which were forced into the strip from both sides. "Molyslip" was used as a lubricant for minimum friction as suggested by Williams and Ford [72].

Initial tests were conducted on the 500 kg capacity Instron machine. High-speed tool bits of 1/4 x 1/4 inch section were used as dies; they were finish ground on the loading faces. The compression of the material was measured by mounting the extensometer on the dies. As the material deformed, the movement of the "incompressible" dies corresponded to the deformation of the polymeric specimen. This movement was sensed by the extensometer and a plot of applied load against compression motion was obtained. Note that with a large capacity load cell, this small machine could be loaded to about 2000 lbs. before the clutch slipped. In this way it was possible to obtain quite sensitive data in the elastic range where total deformation is relatively small.

Identical tests were conducted on a 10,000 lb. Instron machine to obtain the latter part of the load-deformation curve. In essence, this picked up where the smaller machine reached its limit. Here, the applied load was recorded against time; a cross-head speed of 0.02 inch/min was used with both machines. As described in the direct compression test the deformation was obtained by knowing the cross-head and chart speed, and correcting for machine stiffness. Since the strain amplifier was out of order the extensometer could not be used. Stress and strain values were computed according to:

$$\sigma_d = \frac{L}{h(w)} \quad \text{and} \quad \epsilon = \log_e \left(\frac{t_a}{t_o} \right) , \tag{4.8}$$

where σ_d is direct stress,

ϵ is thickness strain,

L is applied load,

h and w are tool and specimen width, respectively and

t_a and t_o are instantaneous and original thicknesses, respectively.

Plane strain compression tests were conducted for the PVC only since the supplies of PC and PE were all consumed at this point of the study.

IV.6 Evaluation of Yielding Under Multiaxial Stress States

To plot a yield locus it is necessary to define the boundary between the elastic and plastic regions. It is impossible to pinpoint this boundary line exactly and several definitions of yielding have found use. Among these are the proportional limit, elastic limit, proof stress, offset method, and backward extrapolation.

In the present study, yielding is defined by the percent offset method. Figure 8 illustrates the selection of offset method under uniaxial stress state; there the "tensile yield strength" of PC is specified for an offset of 0.3 percent. This approach is reasonably consistent with the definition used by Dibenedetto [40] and Rusch [37] in their studies of yield behavior of glassy amorphous polymers; they used the actual departure of linearity for defining the onset of yielding. Argon et al. [76] and Brady and Yeh [32] have shown that the initiation

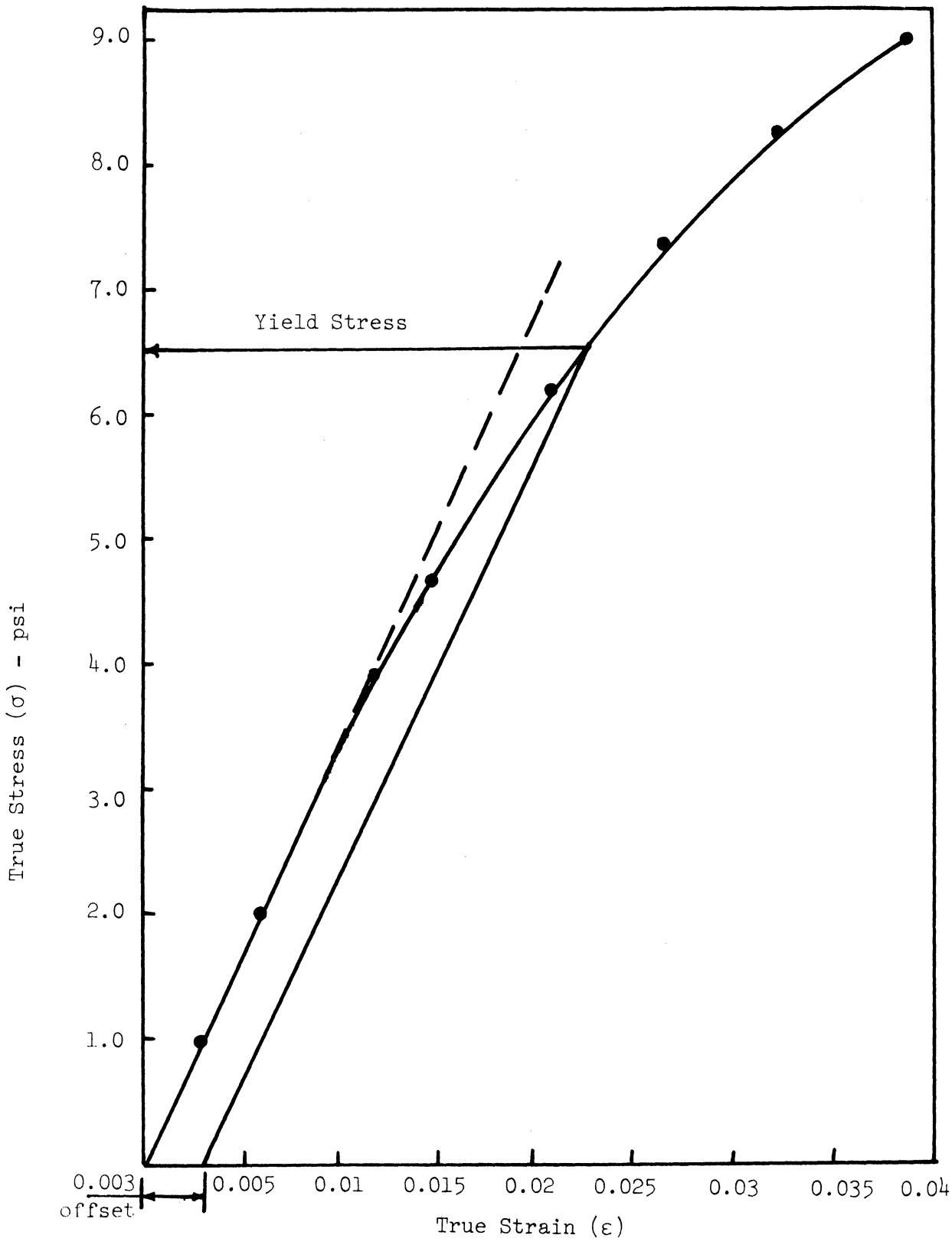

FIG. 8 TENSILE TRUE STRESS-TRUE STRAIN CURVE FOR PC SHOWING HOW THE YIELD STRESS WAS DETERMINED WHEN USING 0.3 PERCENT OFFSET.

of deformation bands which is a manifestation of localized plastic flow in PS also coincides with the strain where departure from linearity occurs.

In the yielding studies of polymeric materials as discussed in Chapter III, "yield point" has often been defined as the maximum load in the load-elongation curve divided by the initial cross-sectional area. This definition of yield stress has certain inherent disadvantages. For brittle materials such as PS and PMMA this load maxima coincides with the breaking load. Bowden and Jukes [16], in their yield locus studies of PMMA, could not get such data when the higher of the two principal stresses in the fourth quadrant of the yield locus was tensile. In this stress-state, where specimens were tested under a Ford-type [72] test accompanied with an axial pull, the specimens broke and no drop in the load was observed.

Also, when polymers are tested under high temperatures or high strain rates this maximum in the load-deflection curve vanishes. Again, when the material is substantially oriented (cold-rolled, cold-drawn or hot-drawn) this maximum does not manifest itself. Due to these reasons, Rawson and Rider [77], in the high temperature yield studies of hot stretched PVC had to use two definitions of yielding: (1) maximum load and (2) backward extrapolation.

In order to alleviate these complications, yield stress in the present studies is selected by offset method and this concept is extended to multiaxial stress state by defining an "effective" strain function. This meets two basic requirements: (1) that for the uniaxial state of

stress it becomes equal to the strain in the tension test, and (2) for Poisson's ratio of 1/2 it reduces to a strain function identical to that used for metals where Poisson's ratio is observed to be 1/2 during plastic flow. In effect, this "strain" function is a weighted average of all three principal strains.

The mathematical form of this strain function is expressed here as:

$$\bar{\epsilon} = \frac{1}{\sqrt{2}\,(1+\nu)} \sqrt{(\epsilon_1 - \epsilon_2)^2 + (\epsilon_2 - \epsilon_3)^2 + (\epsilon_3 - \epsilon_1)^2} \quad . \qquad (4.9)$$

where ν is Poisson's ratio. Expressing the stress-strain relationships in terms of Lame's constant, λ, the stress in the radial direction is:

$$\sigma_3 = \lambda(\epsilon_1 + \epsilon_2) + (\lambda + 2G)\epsilon_3 \quad , \qquad (4.10)$$

where $\lambda = E\nu/(1+\nu)(1-2\nu)$ and G and E are the shear and Young's moduli.

For the plane stress condition which pertains to thin-wall tubes, $\sigma_3 = 0$, thus (4.10) becomes:

$$\epsilon_3 = -\lambda(\epsilon_1 + \epsilon_2)/(\lambda + 2G)$$

and

$$\epsilon_3 = -(\epsilon_1 + \epsilon_2)/(1 + 2G/\lambda) \quad ,$$

but

$$2G/\lambda = (1 - 2\nu)/\nu \quad .$$

Hence

$$\epsilon_3 = -\frac{(\epsilon_1 + \epsilon_2)}{\left(\frac{\nu + 1 - 2\nu}{\nu}\right)} = -\frac{\nu(\epsilon_1 + \epsilon_2)}{1 - \nu} \quad . \qquad (4.11)$$

Equation (4.9) can now be revised to give:

$$\bar{\epsilon} = \frac{1}{\sqrt{2}\,(1+\nu)} \sqrt{\epsilon_1^2 + \epsilon_2^2 - 2\epsilon_1\epsilon_2 + \epsilon_1^2 + \epsilon_2^2 + 2\epsilon_3[\epsilon_3 - (\epsilon_1 + \epsilon_2)]} \quad . \tag{4.12}$$

Substituting (4.11) into (4.12) and rearranging terms, leads to the following form of (4.9) for the case of plane stress:

$$\bar{\epsilon} = \frac{1}{1+\nu} \sqrt{\epsilon_1^2 + \epsilon_2^2 - \epsilon_1\epsilon_2 + [\nu/(1-\nu)^2](\epsilon_1 + \epsilon_2)^2} \quad . \tag{4.13}$$

If ν is 1/2, (4.13) reduces to:

$$\bar{\epsilon} = \sqrt{4/3(\epsilon_1^2 + \epsilon_1\epsilon_2 + \epsilon_2^2)} \tag{4.14}$$

which is the effective strain function for the von Mises criterion for the case of plane stress and with constancy of volume.

Now for the thin-wall tube tests, $\bar{\epsilon}$ can be found by using (4.13) with ϵ_1 and ϵ_2 being determined from equations (4.1) and (4.2). The measured values of Poisson's ratio for the rods used in this study were 0.42 for PC, and 0.38 for both HDPE and PVC.

Curves of σ_1 and σ_2 were plotted as functions of $\bar{\epsilon}$, and the arbitrary magnitude of offset was applied to the curve of the larger of the two stresses. The reason for this choice is discussed in Section V.1.3. The magnitude of the smaller stress was then found by using the stress ratio for that particular test. In the present investigation an arbitrary value of 0.3 percent effective strain was again used as

offset. Figure 9 illustrates this point. It may be noted that other offset values (0.6 and 0.9 percent) were also investigated but the absolute values of "yield" stresses so determined, did not alter the findings in regard to normalized yield loci. For that reason, emphasis was concentrated on the 0.3 percent values only.

As pointed out earlier, in the yield studies of polymeric materials, many investigators have defined the yield "point" at the instability load. But, when the state of stress is multiaxial (such as in pressured tube tests), the ease of locating this instability point disappears since difficulties are encountered in trying to maintain a constant stress ratio in the region of instability. In addition, when $\sigma_2 > \sigma_1$, a pressure instability may develop thereby introducing an added complexity.

IV.7 Hydrostatic Pressure Studies

IV.7.1 Description of Apparatus. Figure 10 is an overall view of the apparatus used for hydrostatic pressure studies while Figs. 11a and 11b are line drawings which depict the setup used for tension and compression tests. The pressure chamber, whose internal diameter is 1 inch, had a wall thickness of 1 inch and working length of about 6 inches. Each end contained two stuffing boxes; one large and one small. Each stuffing box pressed against a Nylon sleeve which in turn compressed an O-ring seal. The Nylon sleeves prevented extrusion of the O-rings under high pressure. Inside the pressure chamber were two 0.375 inch diameter pistons labeled as compression and tension pistons. The top piston was used in compression testing whereas the bottom was used for tension tests. When one piston was in use, the other was idle. However, both pistons were connected in

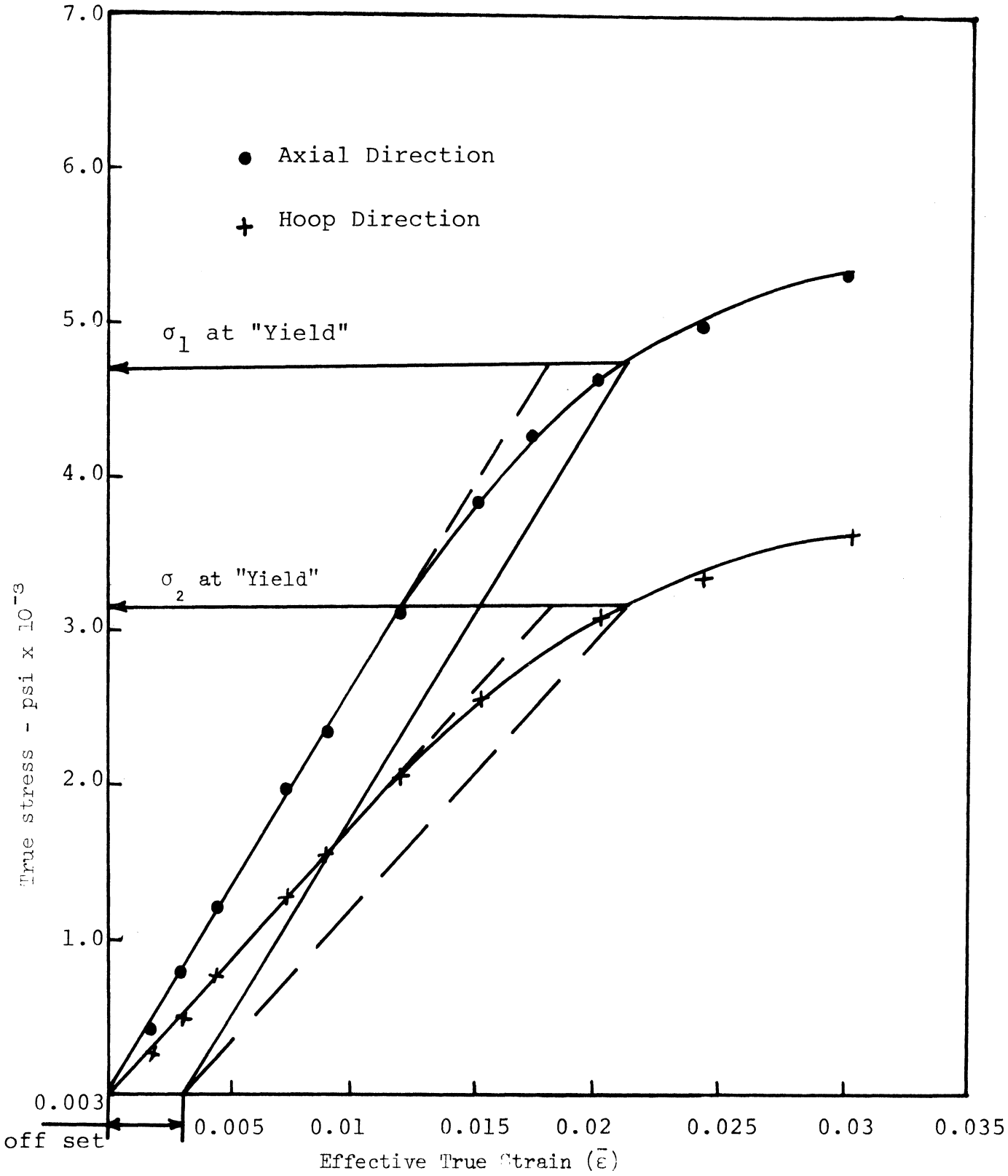

FIG. 9 BIAXIAL TEST RESULTS WITH PVC TUBE WITH σ_1 AND σ_2 PLOTTED AGAINST THE EFFECTIVE STRAIN $\bar{\epsilon}$; THESE DATE ARE FOR A STRESS RATIO (σ_1/σ_2) OF -1.5.

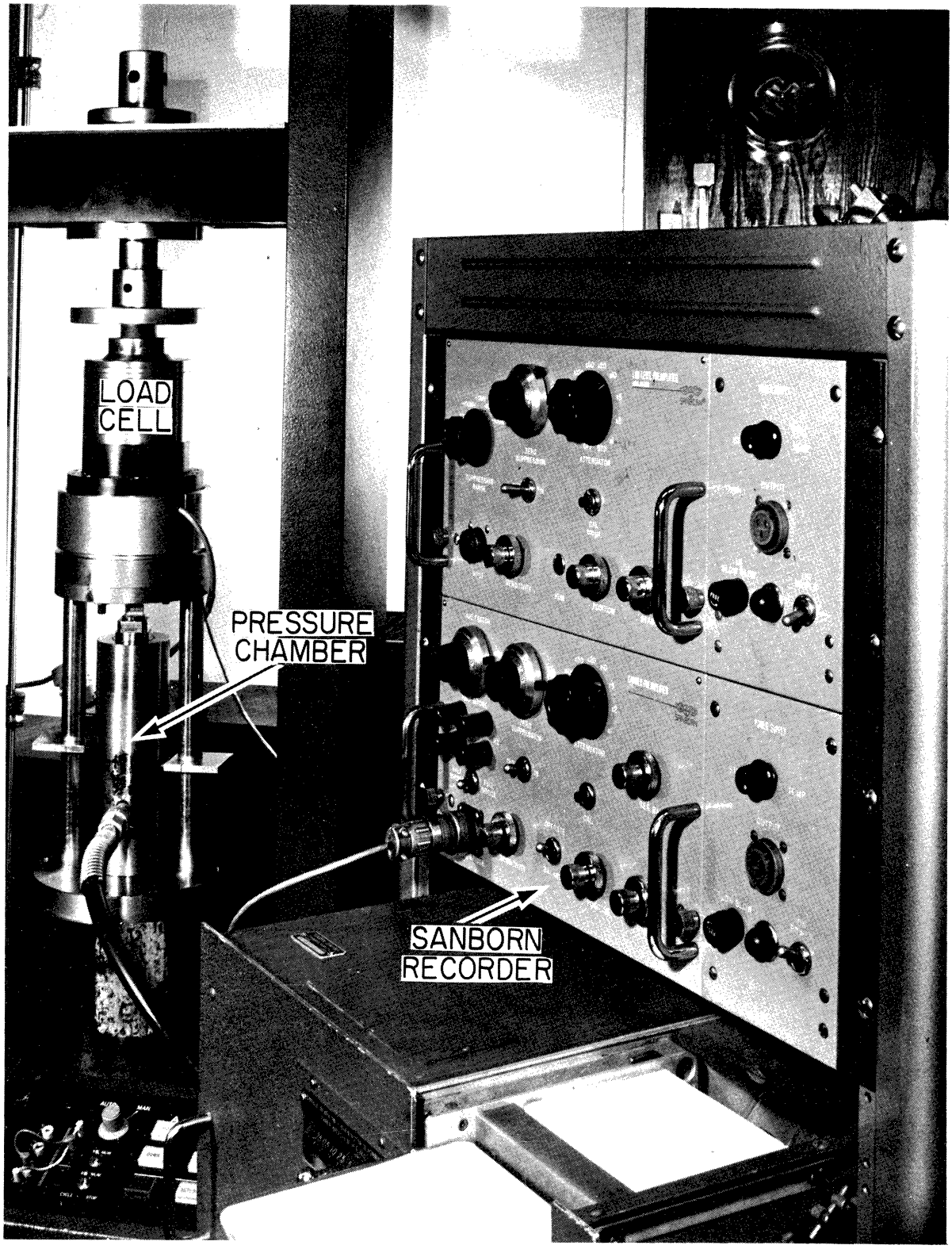

FIG. 10 GENERAL VIEW OF TESTING UNDER HYDROSTATIC PRESSURE.

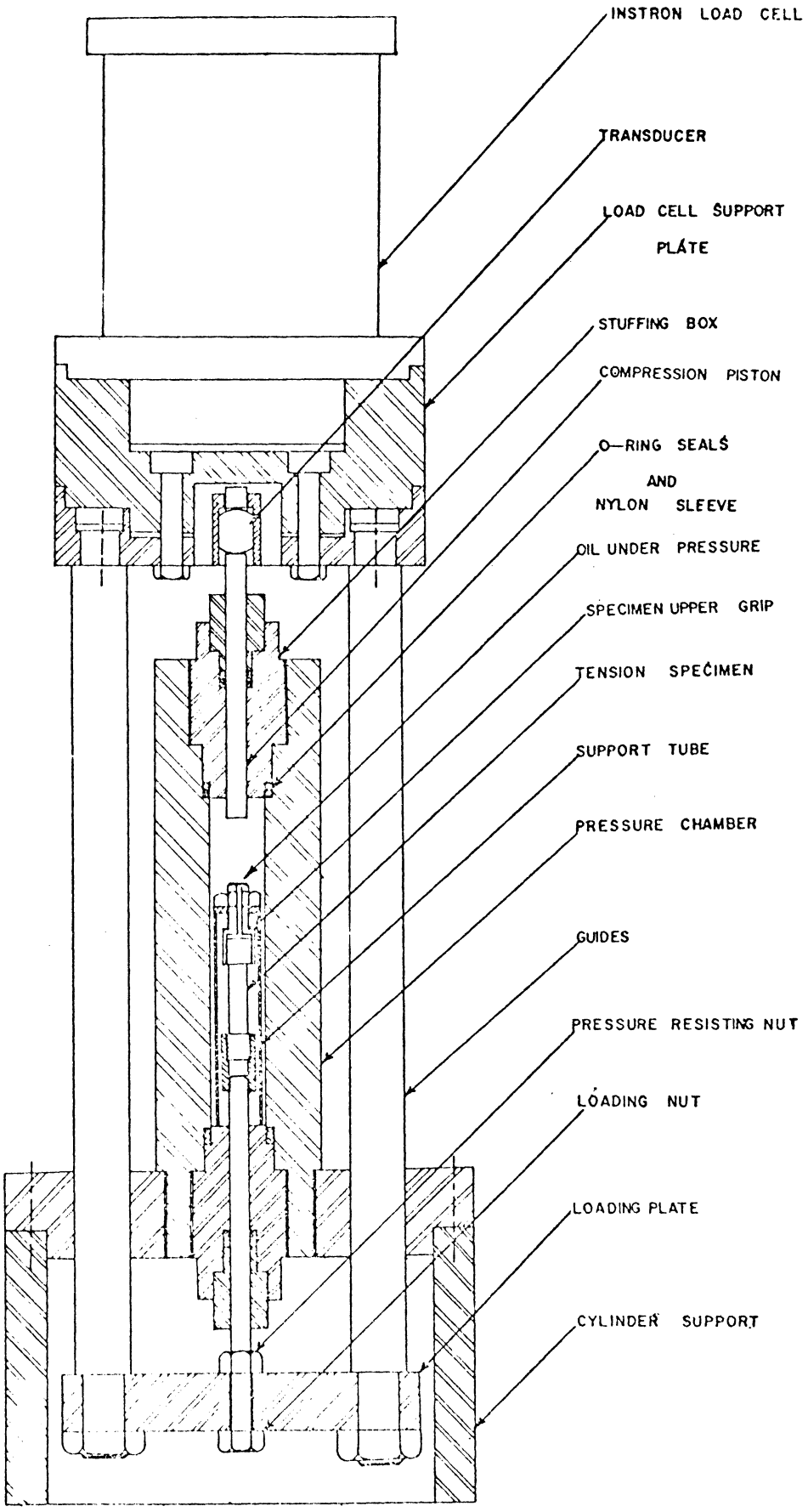

FIG. 11a SKETCH OF OVERALL SETUP USED FOR CONDUCTING TENSILE TESTS UNDER HYDROSTATIC PRESSURE.

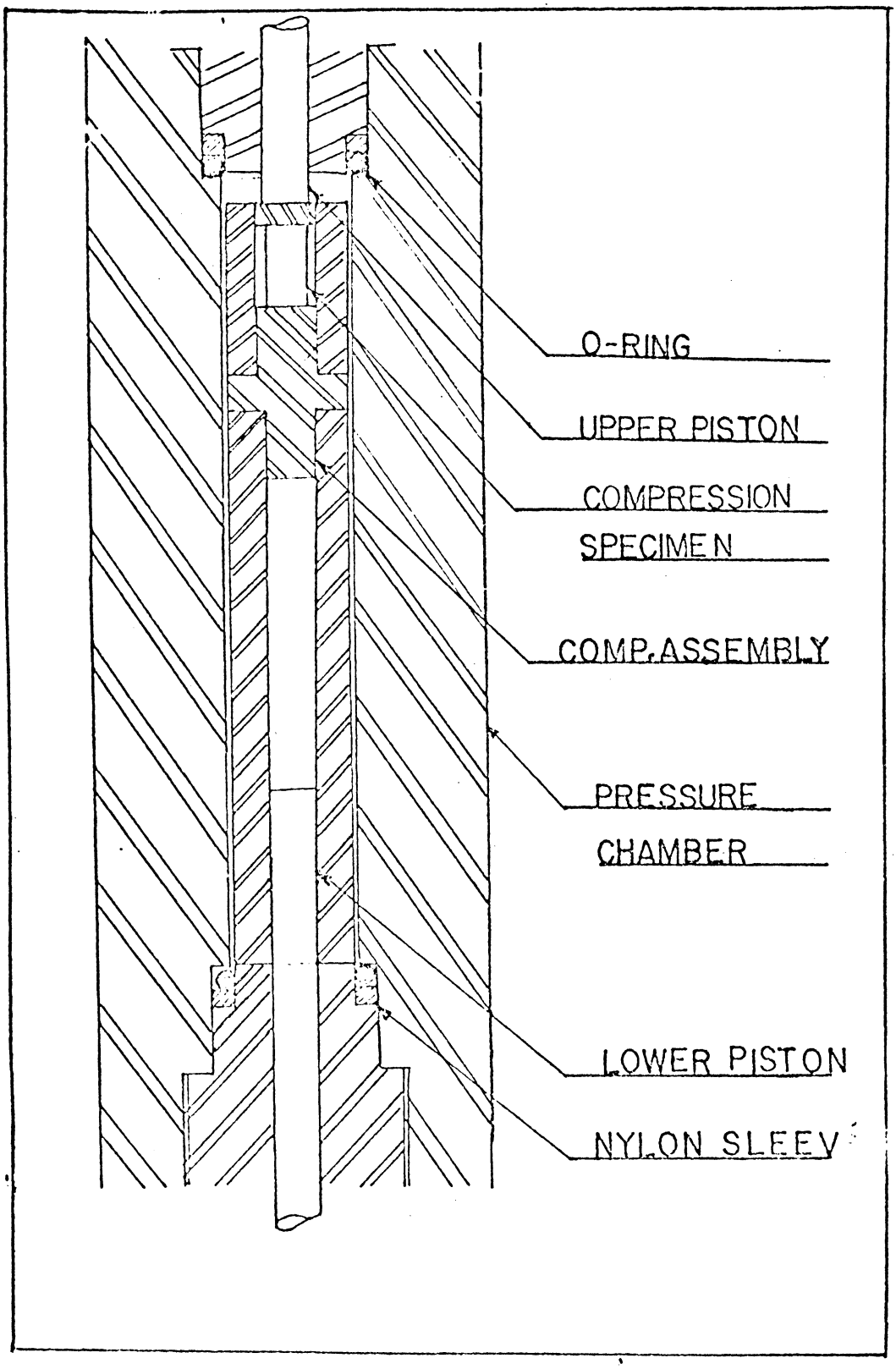

FIG. 11b DETAILED SKETCH ILLUSTRATING THE SETUP USED FOR CONDUCTING COMPRESSION TESTS UNDER HYDROSTATIC PRESSURE.

parallel through a pair of guide rods, hence during an experiment both pistons moved the same amount. As one moved in the other moved out thereby ensuring a constant volume of fluid in the chamber during a test.

The upper end of the top piston rested against a transducer which was secured inside an aluminum casing that was held in place by 1/8 inch diameter screws (these are not shown in Fig. 11). The upper and lower surfaces of the transducer were spherical to obviate loading linearity problems. As the pressure increased, the top piston pressed against the transducer which in turn transmitted the force to a carbide insert. This insert itself pressed against the upper plate. When there was no pressure in the cylinder, there was clearance between the carbide insert and the upper plate. The transducer was held between the two top plates which were bolted together as shown in Fig. 11a. The Instron load cell was supported on the upper plate. As the Instron cross-head pressed against the load cell and this external load was transmitted to the specimen, (either for tensile or compressive testing) this load was recorded on the Instron chart.

IV.7.2 Tension Test Under Pressure. Tensile specimens with 0.300 inch diameter and 1 1/2 inch gage length were used. The ends were 1/2 inch diameter and 1/2 inch long. One end of the specimen was connected to the lower piston through a threaded fastener. The other end was connected to another threaded fastener which in turn was connected to a steel sleeve by a nut. The lower piston was connected to the lower plate by means of two nuts. The upper nut transmitted the pressure force to the assembly while the lower nut transmitted the external load applied by the Instron.

The Instron load was applied to the one end of the specimen with the reaction to the other end of the specimen being provided by the steel sleeve. Hence in this way tensile load was applied to the specimen. The difference between the load indicated by the Instron and the friction force was that which was actually applied to the specimen.

IV.7.3 Computation of True Stress-True Strain. It was extremely difficult to measure the elongation of the specimen directly. An indirect approach was adopted to evaluate the longitudinal strain. Two tensile specimens with identical dimensions were tested. One specimen was tested outside the chamber and the elongation was measured with an extensometer. The other specimen was tested inside the chamber with no fluid pressure. During the first test, a load-deflection plot was obtained directly from the Instron. For the second test, the load was recorded against time. From these two plots, it became possible to convert the load-time plot to load-elongation plot. For identical loads, the different values of elongation and chart movement expressed in centimeters were determined and plotted as a graph as shown in Fig. 12. It should be noted that PE is plotted on one scale while PC and PVC are on different scales for convenience. In this way it was possible to compute true strain.

It was not possible to measure the contraction in diameter directly for computing the instantaneous area. However, the instantaneous cross-sectional area was computed by using Poisson's ratio; true stress values could then be determined. The values used for Poisson's ratio for each of the polymers has been given earlier after equation (4.14).

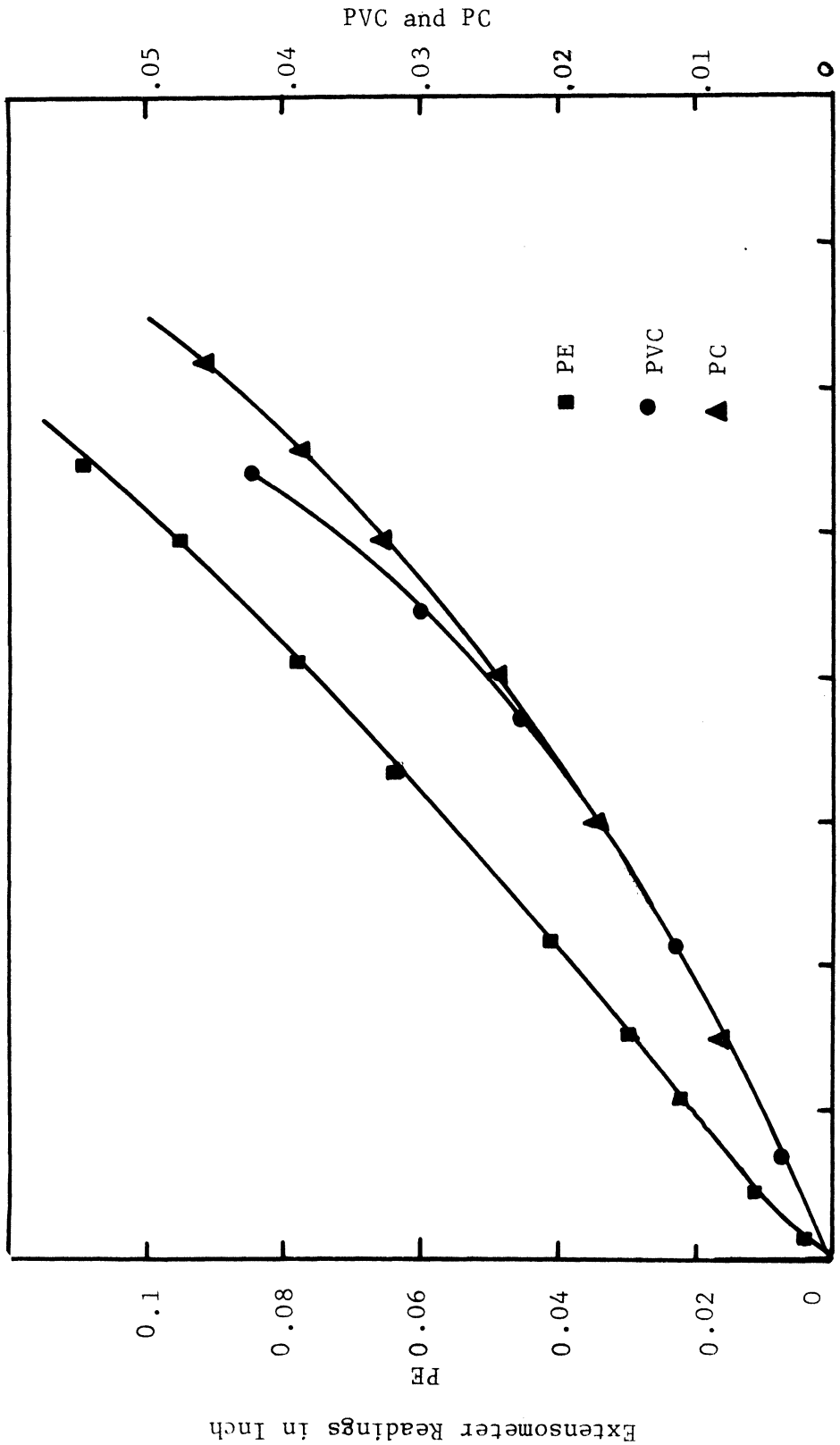

FIG. 12 CALIBRATION CURVES USED TO CONVERT THE INSTRON CHART MOVEMENT TO EQUIVALENT EXTENSOMETER ELONGATION.

IV.7.4 Compression Test Under Pressure. A compression test under hydrostatic pressure is shown in Fig. 11b. Figure 11b shows only the pressure chamber part of the Fig. 11a. During compression the upper piston is used while the lower piston remains idle. The compression specimen is supported inside the changeable assembly designated as the compression assembly in Fig. 11b. This assembly fits snugly inside the support tube which rests on the rigid seat. The compression specimen is secured inside the assembly by means of molyslip grease between the specimen and the seat.

Compression specimens of 3/8 inch diameter and 5/8 inch height were machined in the axial direction of the bar stock. The specimen was supported on the seat mounted inside the chamber. Molybdenum disulphide was used as the lubricant. An Instron of 500 kg nominal capacity was used during these tests and it was calibrated up to 2000 lbs by using a larger capacity load cell. During compression testing the top piston applied the load to the specimen while the lower piston remained idle. The load was recorded on the chart moving at known speed. The load was also recorded directly by the transducer interposed between the loading piston and the Instron load cell. Differences in the magnitudes of the load sensed by the Instron load cell and the transducer provided an estimate of the friction force. True stress was computed by using Poisson's ratio of 0.42 for PC and 0.38 for PVC and PE. The compression specimen was compressed under no pressure inside the chamber and the Instron load was recorded with respect to time. For different loads the true stress was calculated.

Corresponding to different stress values the strain was picked up from compression stress-strain curves already obtained for all three materials. In this way the chart drive was calibrated in terms of strain. It was assumed that this calibration procedure was valid at higher pressures.

CHAPTER V. EXPERIMENTAL RESULTS

V.1 Development of Yield Loci

As pointed out earlier, a yield locus is a dividing line between the elastic and plastic regions. In order to establish this boundary it is necessary to formulate a functional relationship between stresses and strains. Several possibilities exist and the question as to which is most suitable is a matter of considerable argument and diverse opinion. In the present investigation, the two largest of the three principal stresses have been plotted against the effective strain as defined in the preceding chapter. Then, yielding was based upon an offset method for 0.3 percent strain.

V.1.1 Tensile Results. All materials were subjected to standard tensile tests as described in Chapter III; these gave tensile behavior in the axial direction of the test rods. Using the equivalent of pressurized open-ended tubes, tensile behavior in the tangential (hoop) direction was determined for all materials; details may again be found in Chapter III. A single test using an unpressurized tube of PC was conducted to determine the axial tensile behavior of a tube; this could then be compared with the results found with the standard tensile specimen of this same material.

Figure 13 shows the tensile behavior of PC for the various orientations and specimens; as can be seen, the PC was decidedly isotropic. Figure 14 illustrates the behavior of PVC; note that for

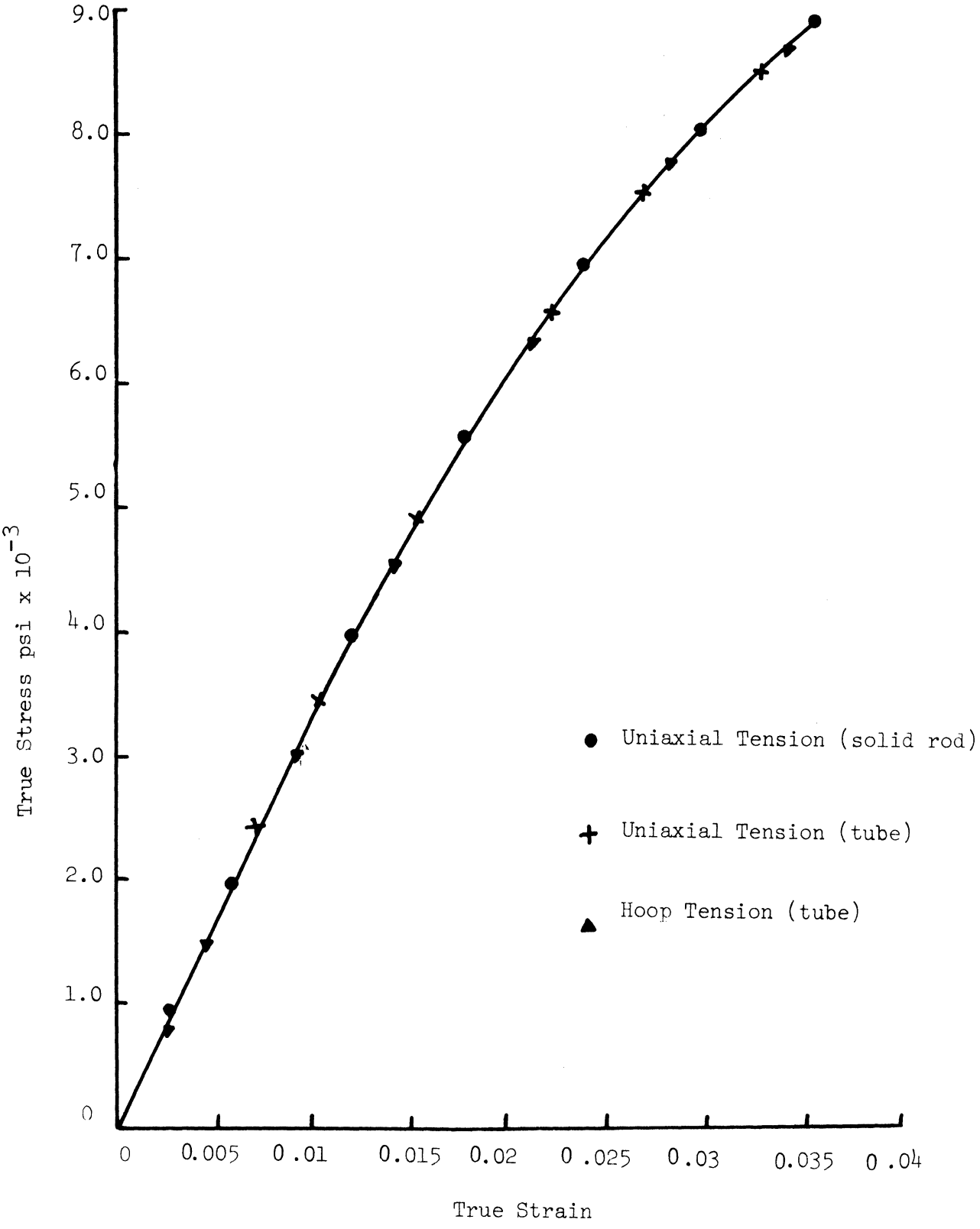

FIG. 13 TRUE STRESS-TRUE STRAIN CURVES FOR PC SUBJECTED TO VARIOUS TENSILE TESTS.

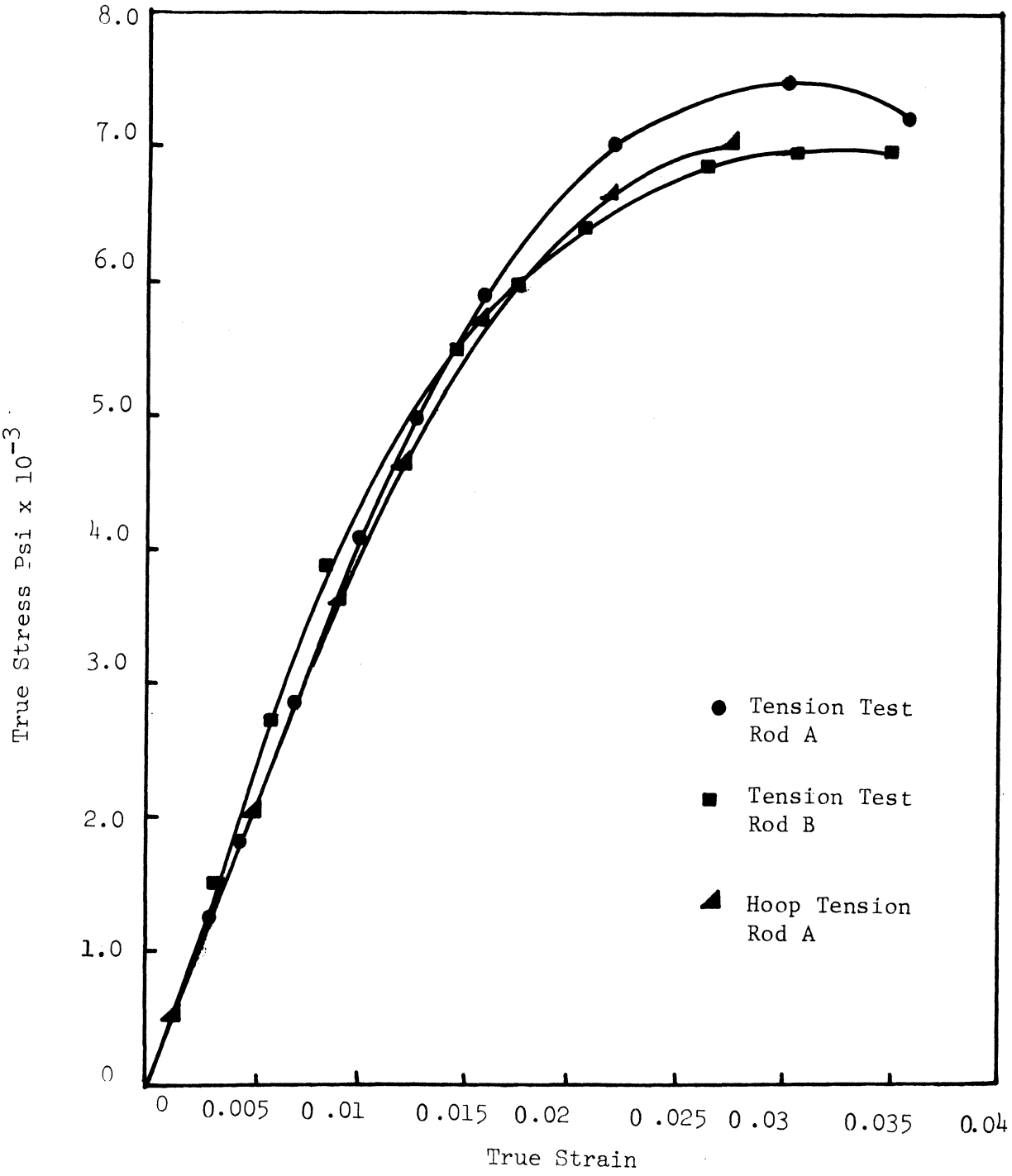

FIG. 14 TRUE STRESS-TRUE STRAIN CURVES FOR PVC SUBJECTED TO VARIOUS TENSILE TESTS. A AND B INDICATE DIFFERENT BARS OF "AS RECEIVED" MATERIAL.

rod A the axial and tangential behavior is similar at low strains but shows divergence as the strain increases. Additionally the axial tensile behavior of rod B differs from rod A. Figure 15 contains typical axial tensile results for the three rods of HDPE. Rods designated as A and C produced nearly identical results; in comparison rod B was very similar at low strains but displayed some divergence at higher strains. Tangential tensile behavior was investigated only for rod C due to material shortage. Both axial and tangential results for this rod were similar at low strains but showed some divergence at large strains. These findings suggested anisotropy which was later confirmed with the compression results.

V.1.2 Compression Results. To employ the proposed yield criterion, values of compressive yield strength were required. Direct compression tests, as detailed in Chapter III, were conducted in the axial and radial directions of the test rods for each of the three polymers. Figure 16 for PC includes the data for both the axial and radial direction tests; both test rods were used and again, as with the tensile results, this material exhibited a decidedly isotropic and homogeneous behavior. (Note that no distinction is made here between the two rods.) Figure 17 indicates the findings with PVC. There it can be seen that both rods displayed isotropic behavior but the properties differed between the two rods. Figures 18 through 21 contain the findings for HDPE. The first three of these plots show the individual results for each of the three test rods (A, B, and C). To plot all of these

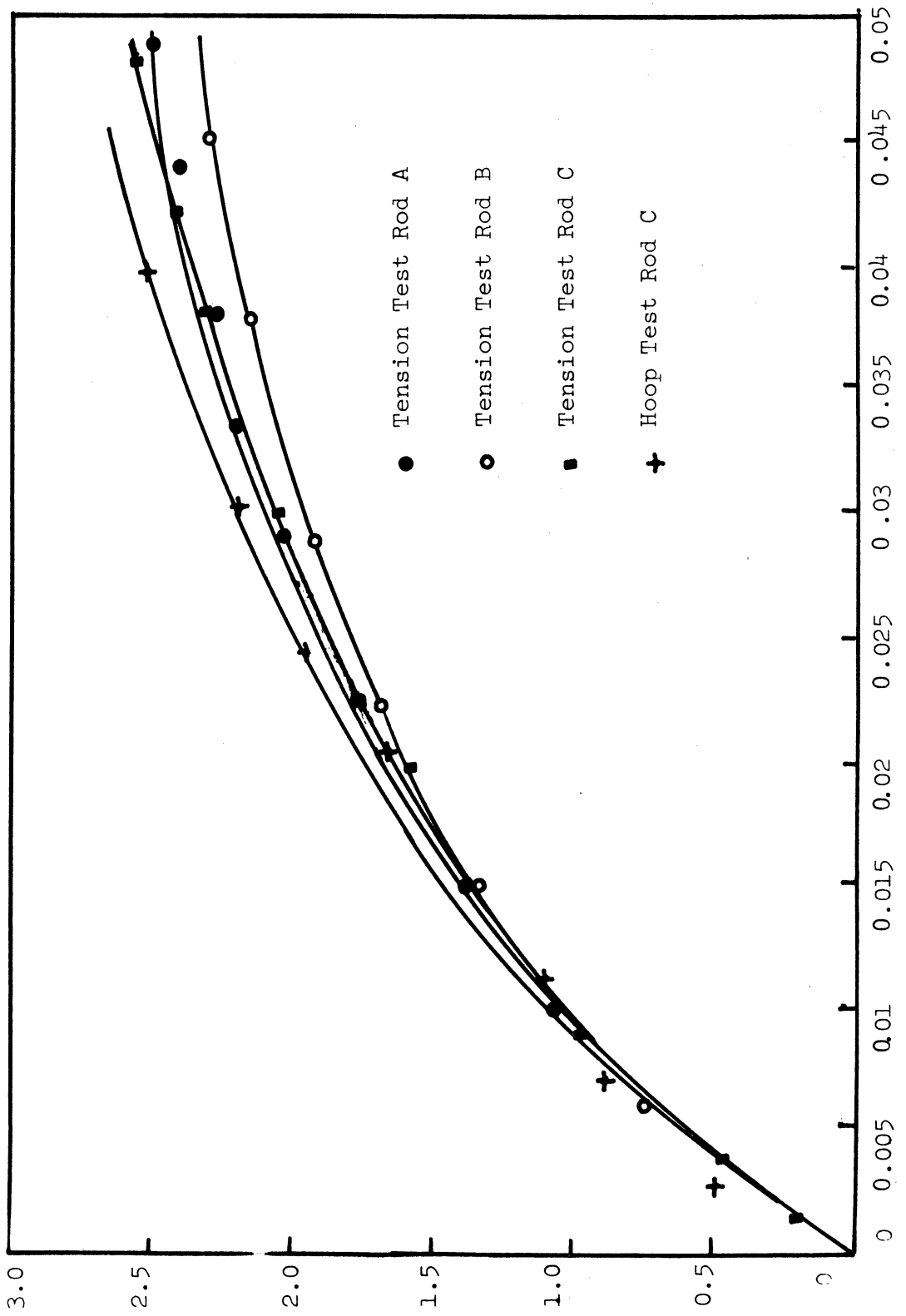

FIG. 15 TRUE STRESS-TRUE STRAIN CURVES FOR PE SUBJECTED TO VARIOUS TENSILE TESTS. A, B AND C INDICATE DIFFERENT BARS OF "AS RECEIVED" MATERIAL.

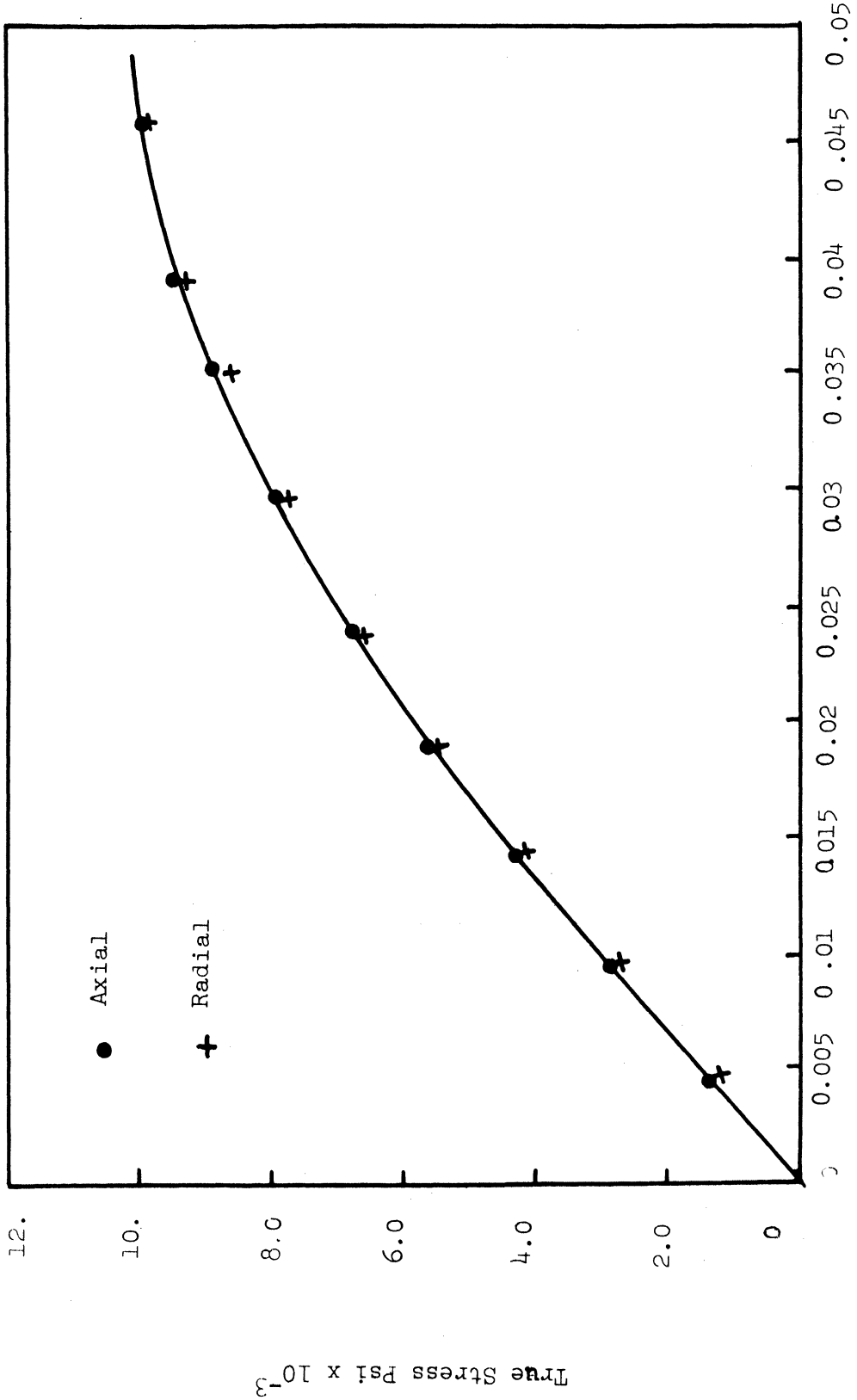

FIG. 16 COMPRESSIVE TRUE STRESS-TRUE STRAIN BEHAVIOR OF PC TESTED IN TWO DIRECTIONS.

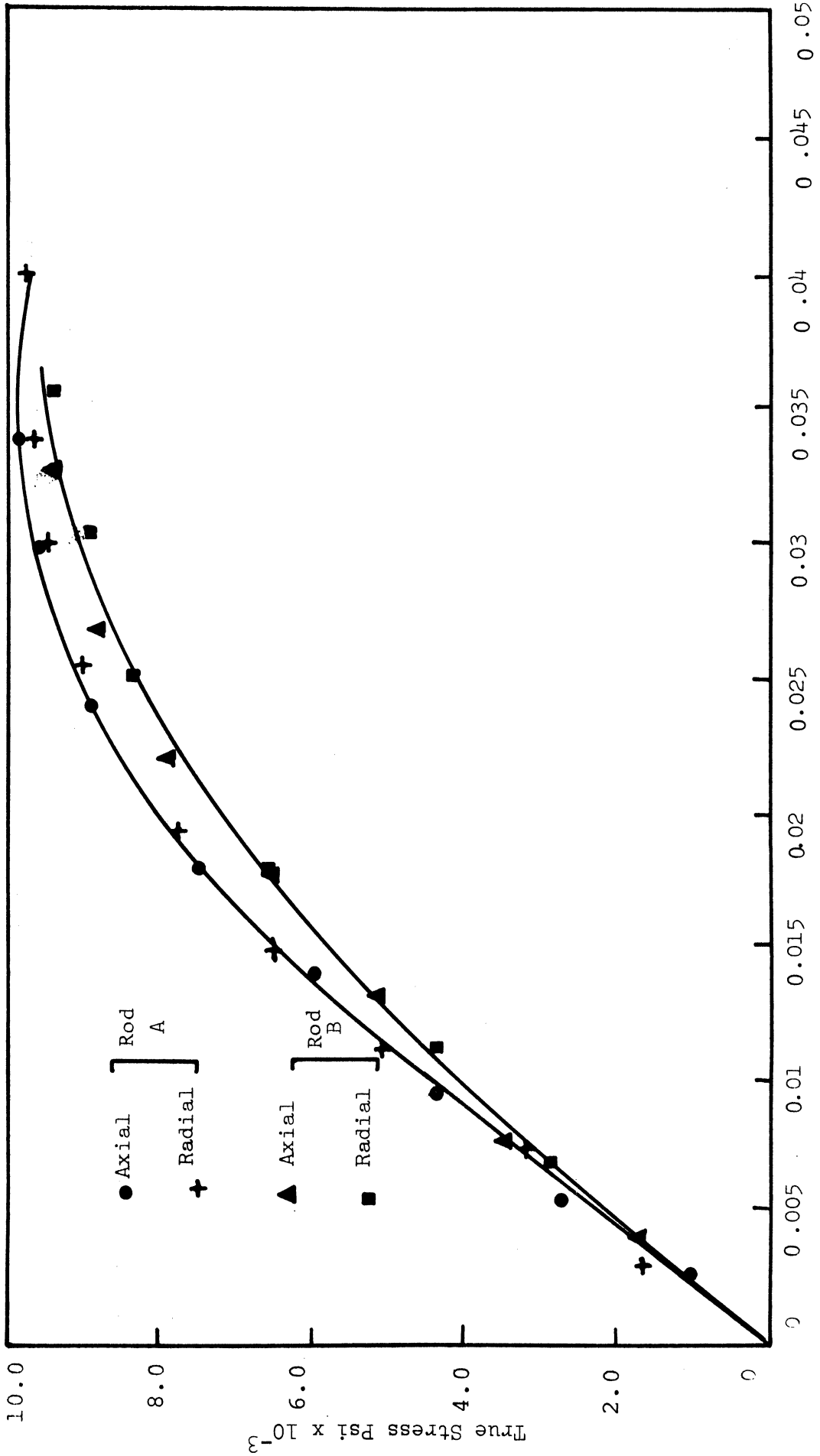

FIG. 17 TRUE STRESS-TRUE STRAIN CURVES FOR PVC SUBJECTED TO VARIOUS COMPRESSION TESTS. A AND B INDICATE DIFFERENT BARS OF "AS RECEIVED" MATERIAL.

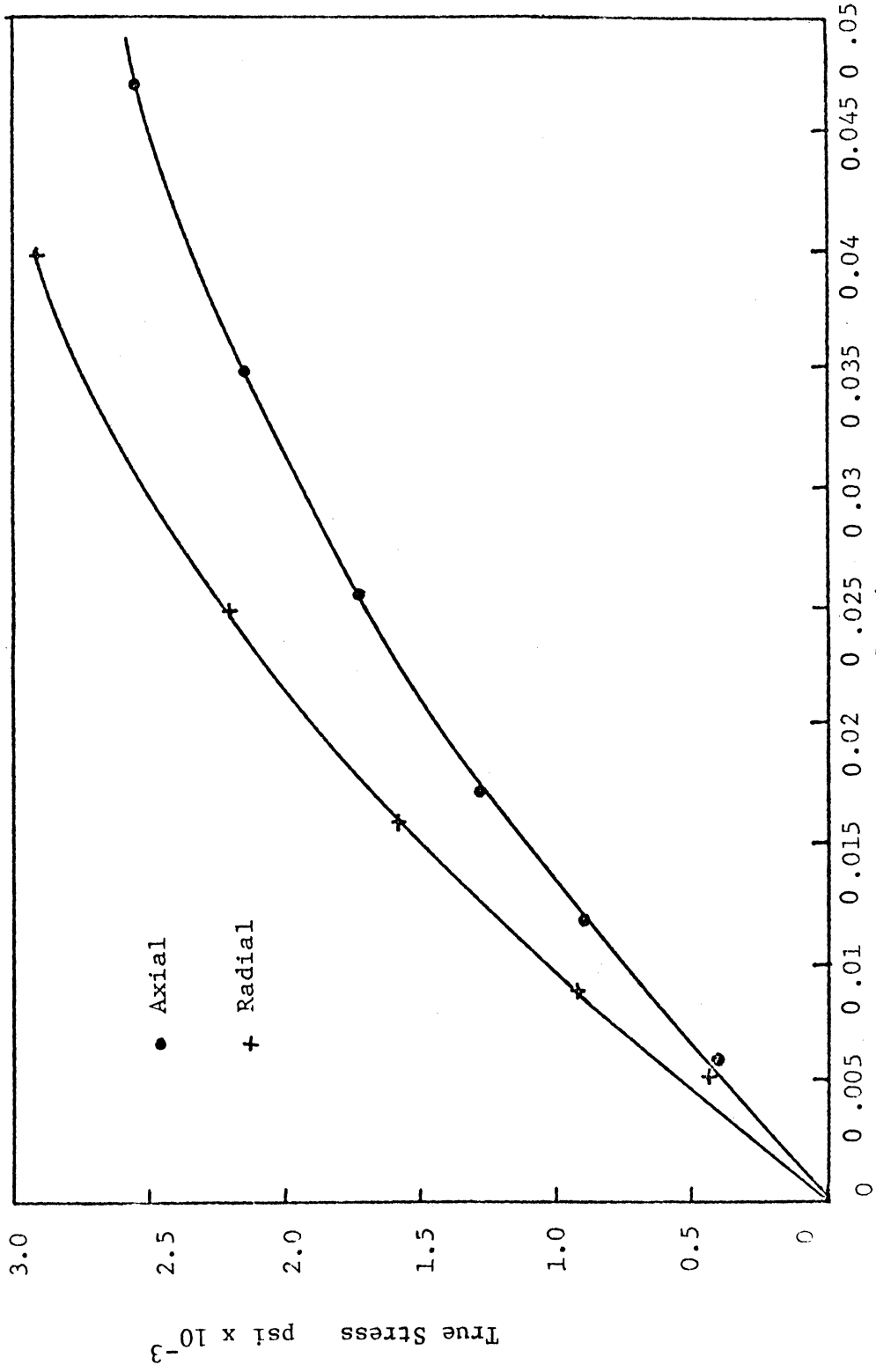

FIG. 18 COMPRESSIVE TRUE STRESS-TRUE STRAIN CURVES FOR HDPE (BAR A) TESTED IN TWO DIRECTIONS.

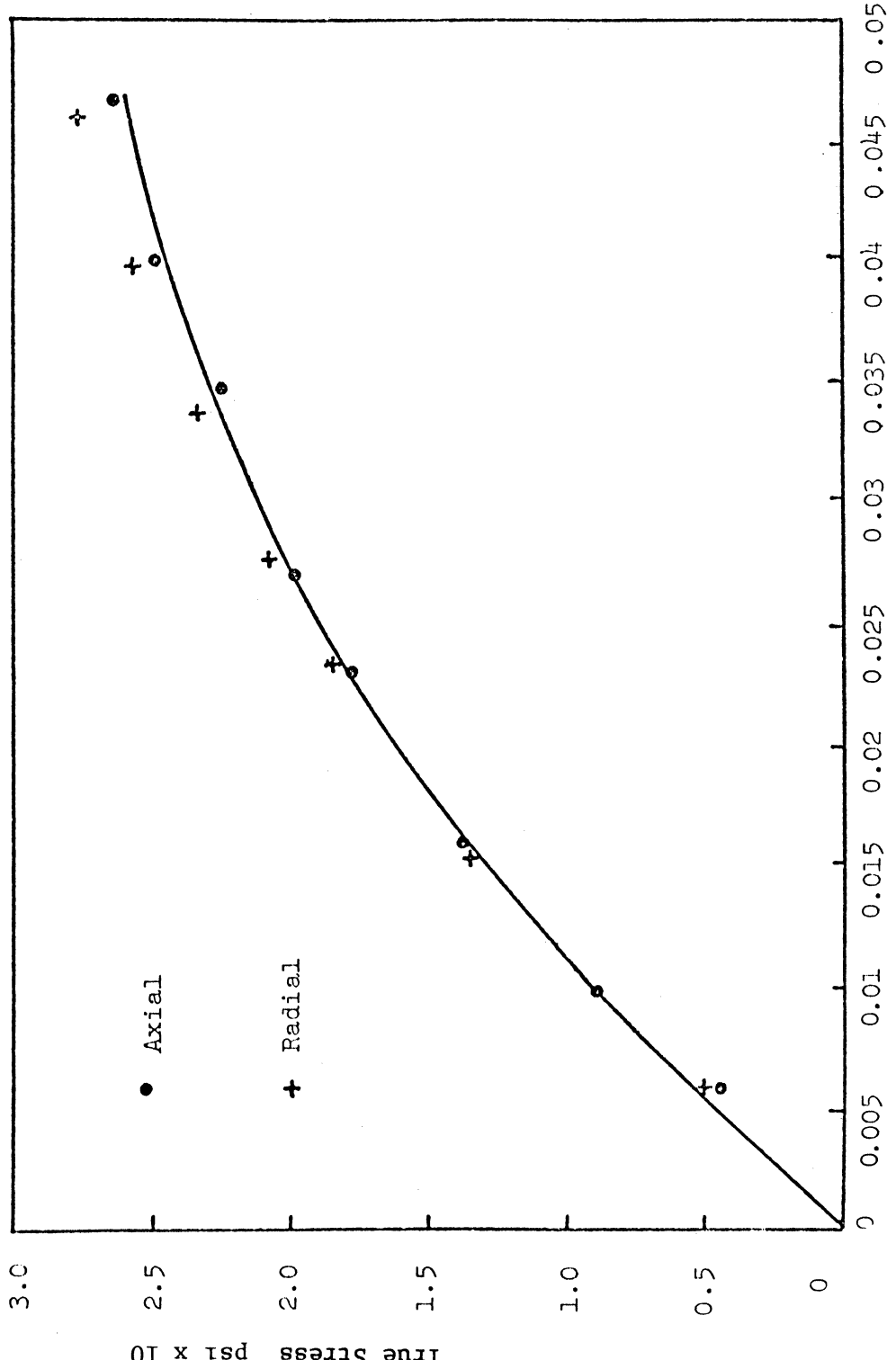

FIG. 19 COMPRESSIVE TRUE STRESS-TRUE STRAIN CURVES FOR HDPE (BAR B) TESTED IN TWO DIRECTIONS.

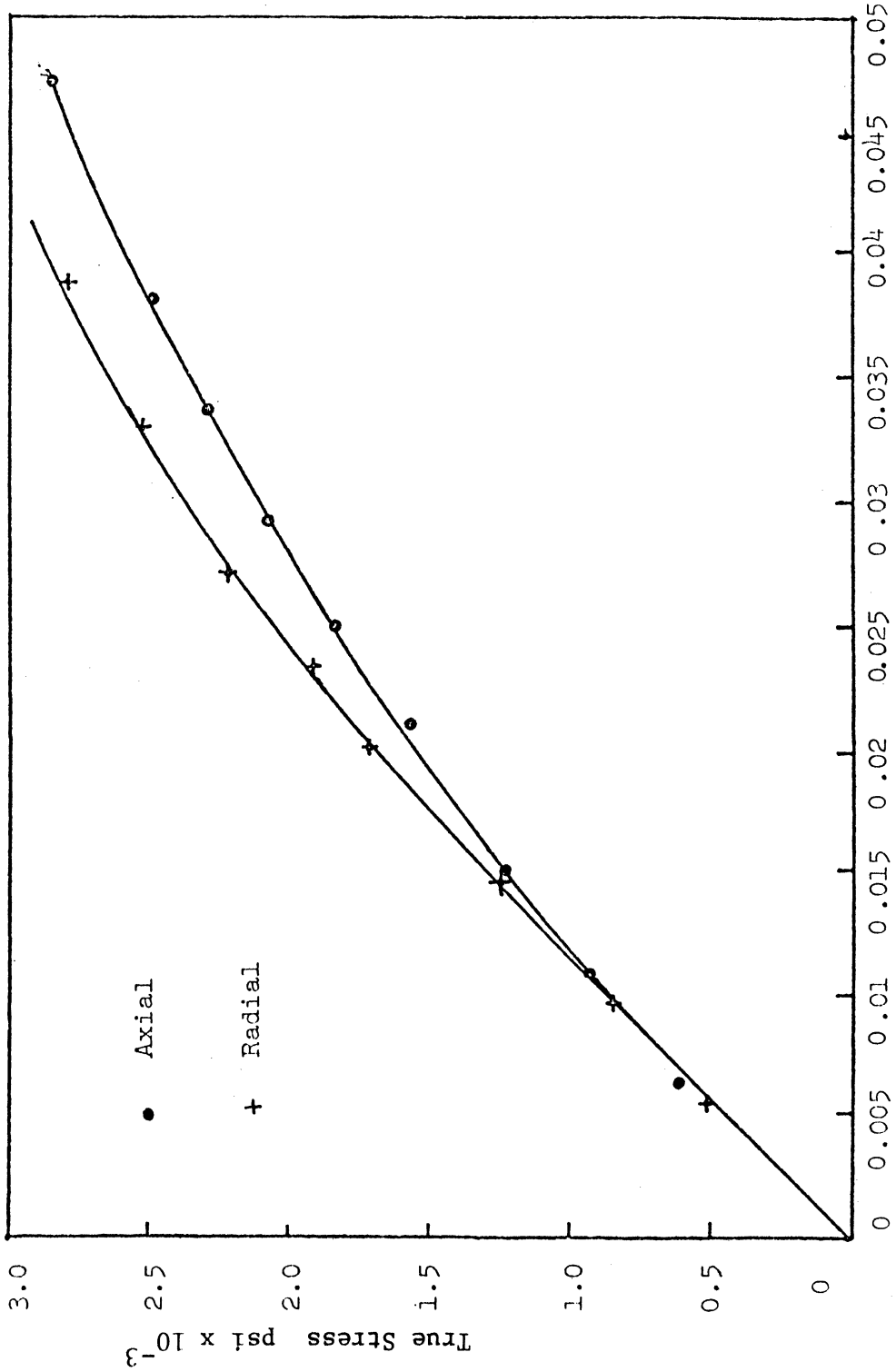

FIG. 20 COMPRESSIVE TRUE STRESS-TRUE STRAIN CURVES FOR HDPE (BAR C) TESTED IN TWO DIRECTIONS.

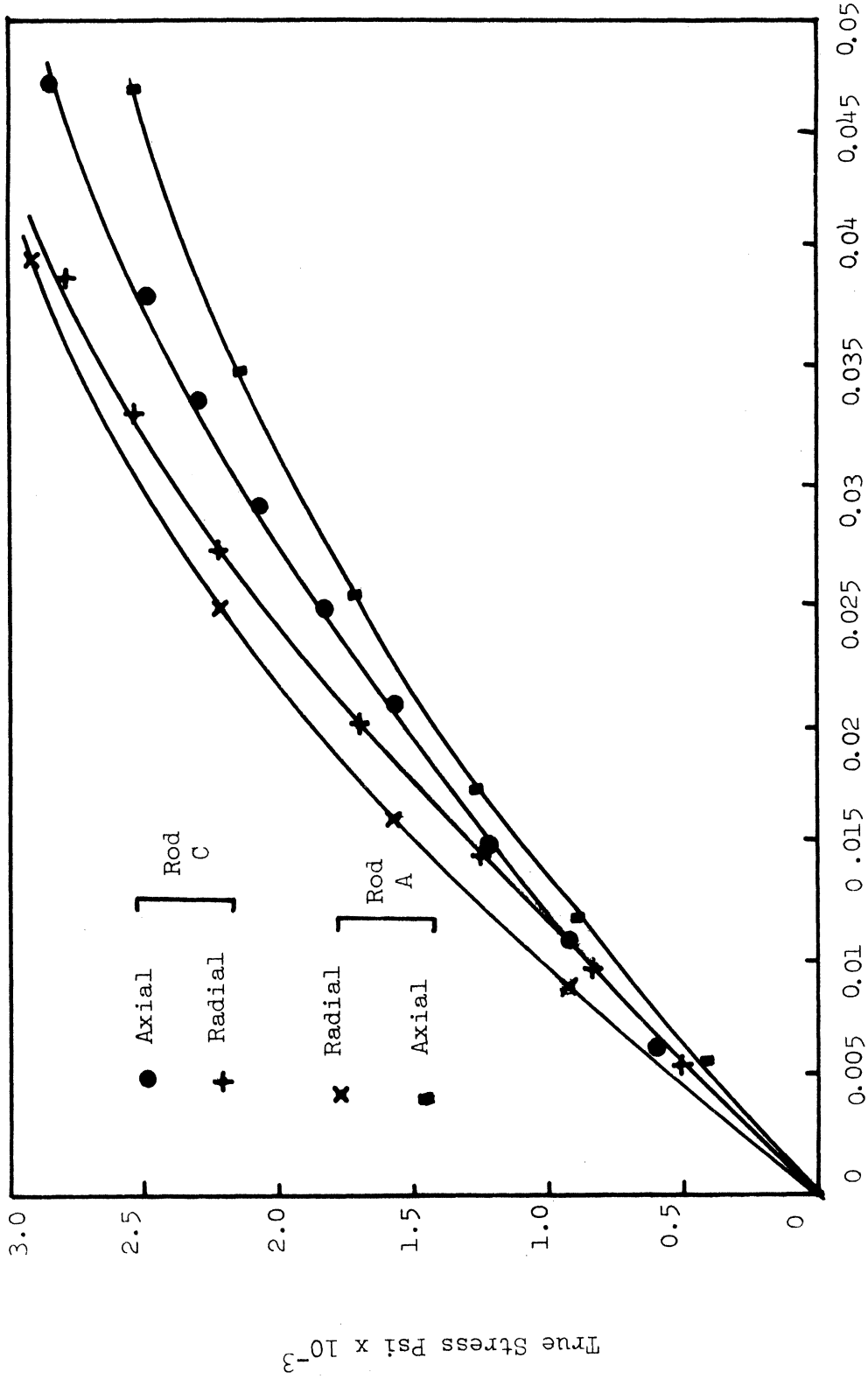

FIG. 21 COMPOSITE OF FIGURES 18 AND 20 ILLUSTRATING THE VARIOUS COMPRESSIVE BEHAVIOR OF HDPE.

results on a single figure would cause a loss of clarity but to indicate the variations among the three bars, Fig. 21 is included. This contains a composite of Figs. 18 and 20 ; note that the test results on Fig. 19 would fall within the extreme lines of Fig. 21. The HDPE appears to be more anisotropic and less homogeneous than the other two materials. With regard to all of the findings from these tests, use was made of the axial compression curves for purposes of defining a "compressive yield strength" as used in the yield loci plots.

V.1.3 Biaxial Stress Results. The thin-wall tubes, as described earlier, were loaded along different constant stress ratio paths. The curves of the two major principal stresses were drawn against the effective strain function, the yield stress being selected from the largest stress-effective strain curve for a 0.3 percent offset strain. The corresponding value of the smaller stress was then determined from the known stress ratio.* Some typical curves for the three polymers using stress ratios of approximately +1.0 and -1.0 are shown in Figs. 22 through 27. The results for other stress ratios are tabulated in Tables V.1 through V.3.

* Checks indicated that if the offset were applied to the curve of the lower of the two principal stresses and the stress ratio invoked to compute the larger stress, practically identical values of σ_1 and σ_2 were obtained. It was felt that greater accuracy could be attained by using the larger stress curve since there was generally less scatter of the test data.

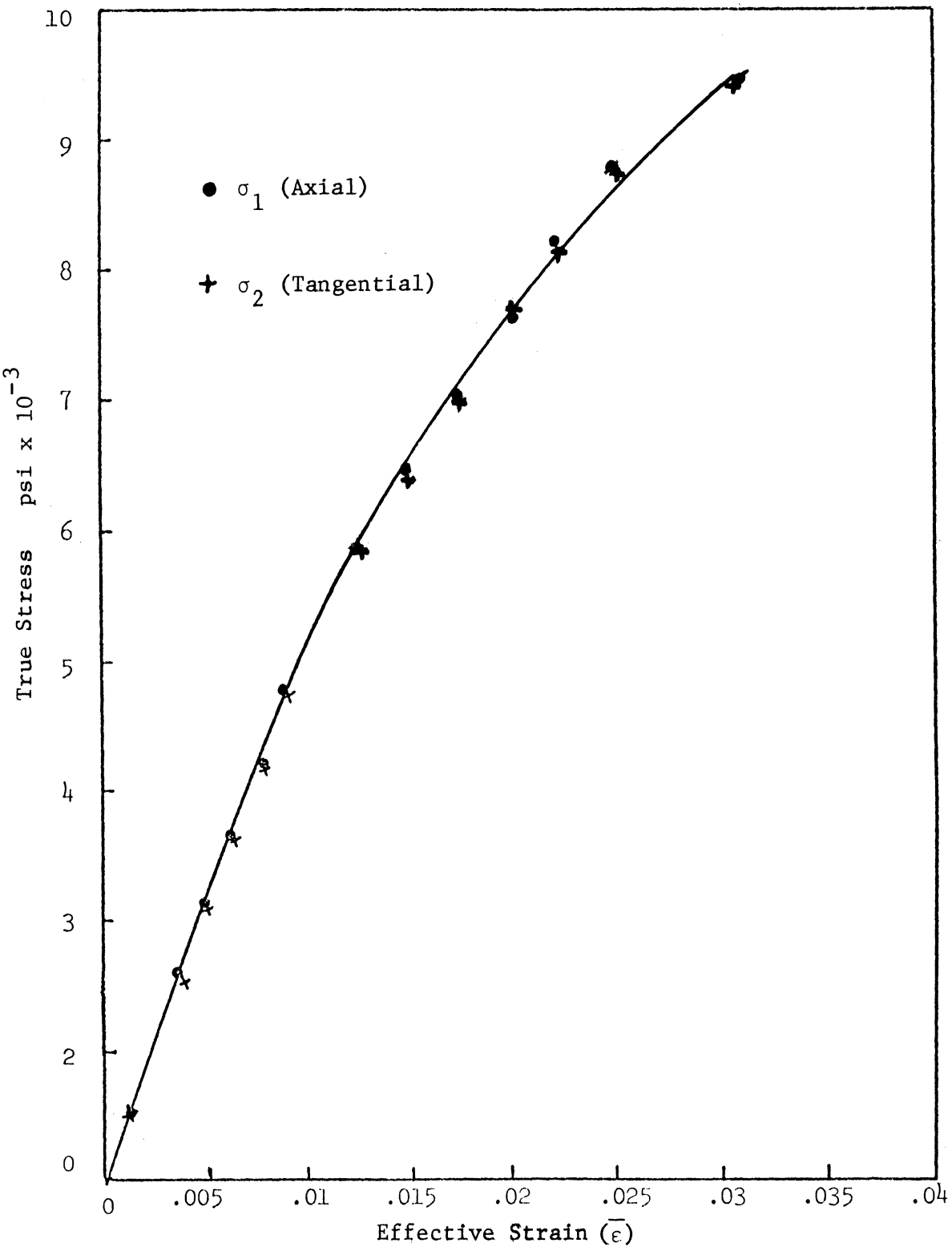

FIG. 22 TRUE STRESS-EFFECTIVE STRAIN CURVE OF PC UNDER TENSILE AXIAL LOAD AND INTERNAL PRESSURE WITH STRESS RATIO OF ABOUT +1.0.

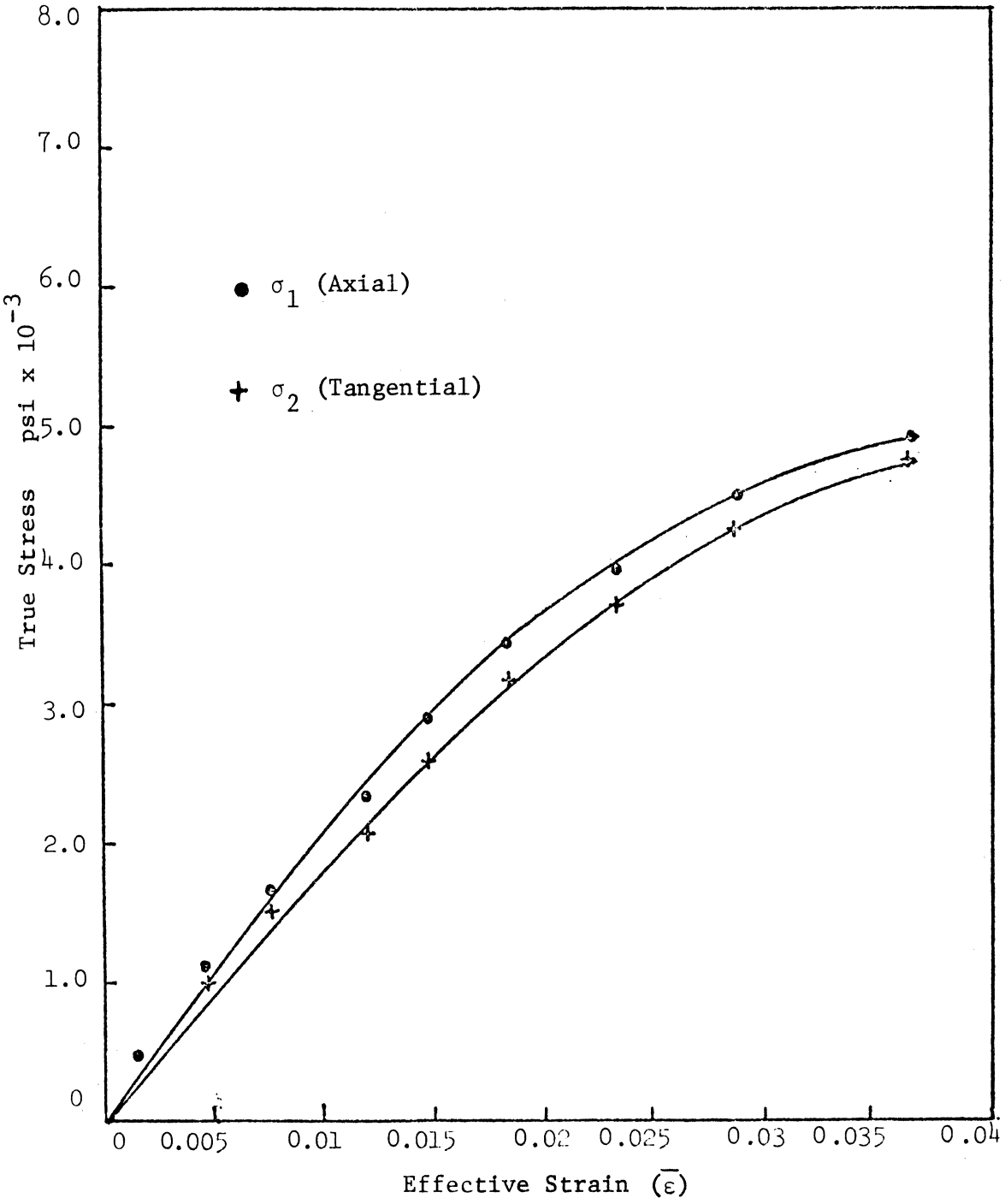

FIG. 23 TRUE STRESS-EFFECTIVE STRAIN CURVE OF PC UNDER AXIAL COMPRESSIVE LOAD AND INTERNAL PRESSURE WITH STRESS RATIO OF ABOUT -1.0.

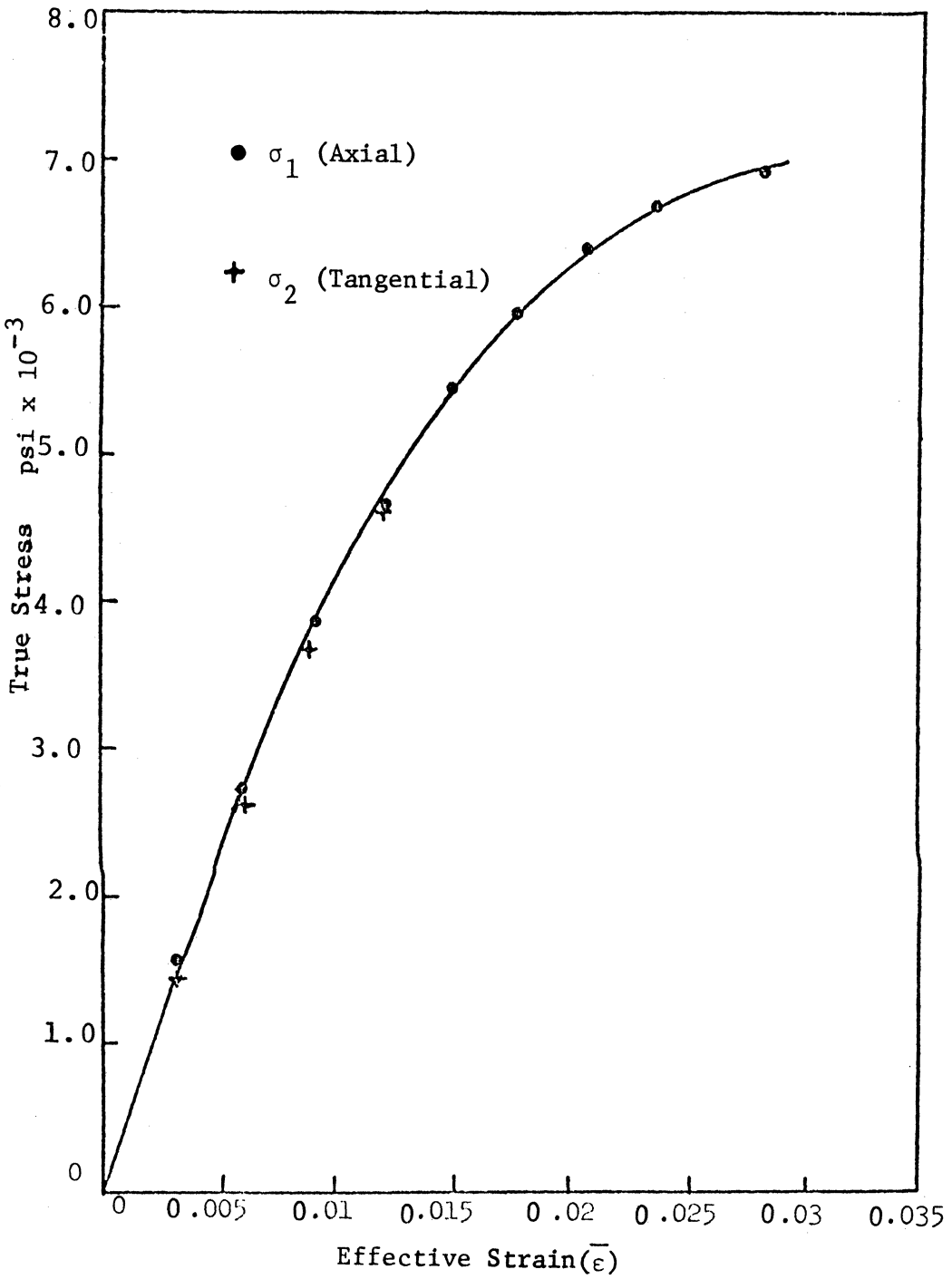

FIG. 24 TRUE STRESS-EFFECTIVE STRAIN OF PVC (A) UNDER AXIAL TENSILE LOAD AND INTERNAL PRESSURE WITH STRESS RATIO OF ABOUT 1.0.

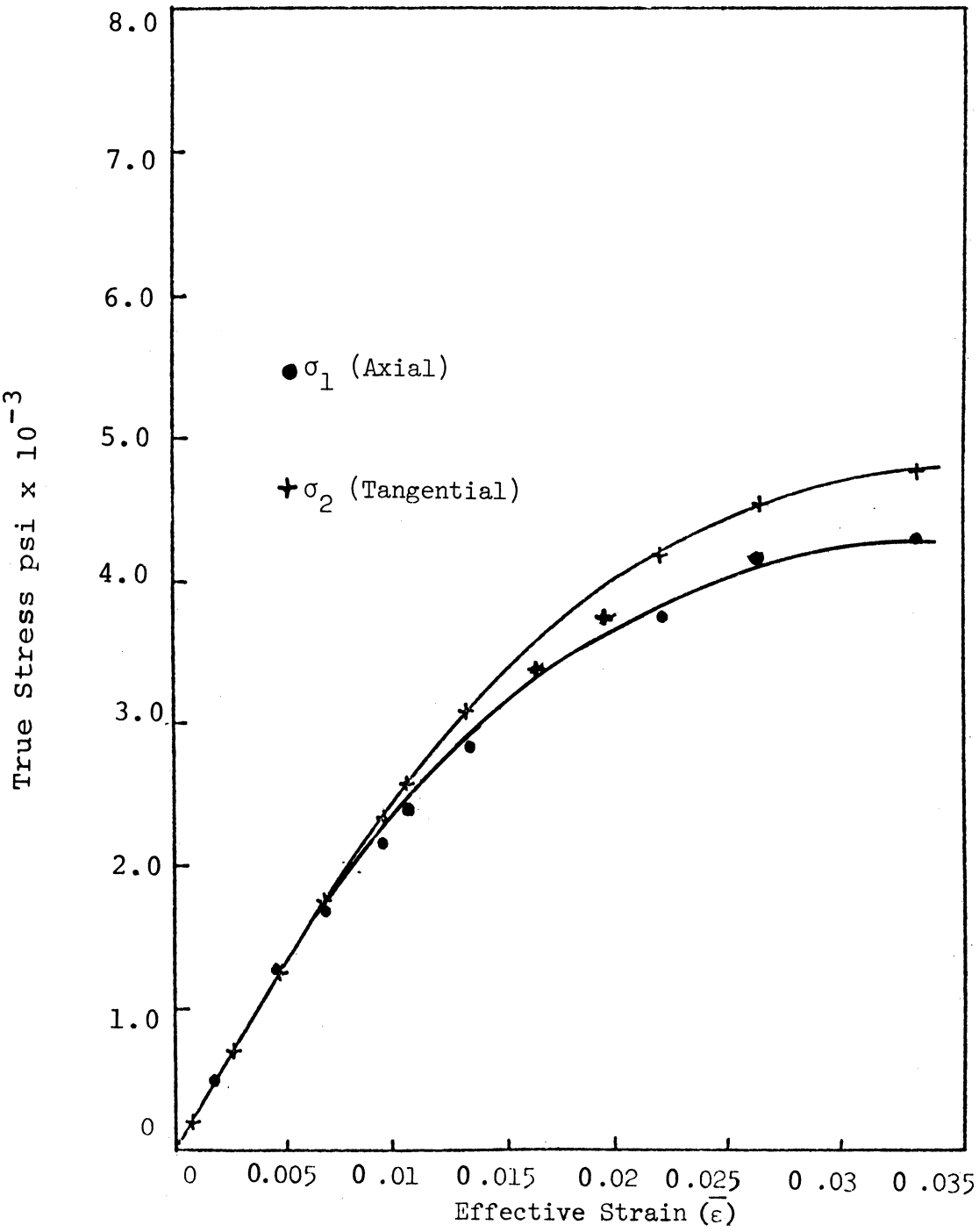

TRUE STRESS-EFFECTIVE STRAIN CURVE OF PVC (B) UNDER AXIAL COMPRESSIVE LOAD AND INTERNAL PRESSURE WITH STRESS RATIO OF ABOUT -1.0.

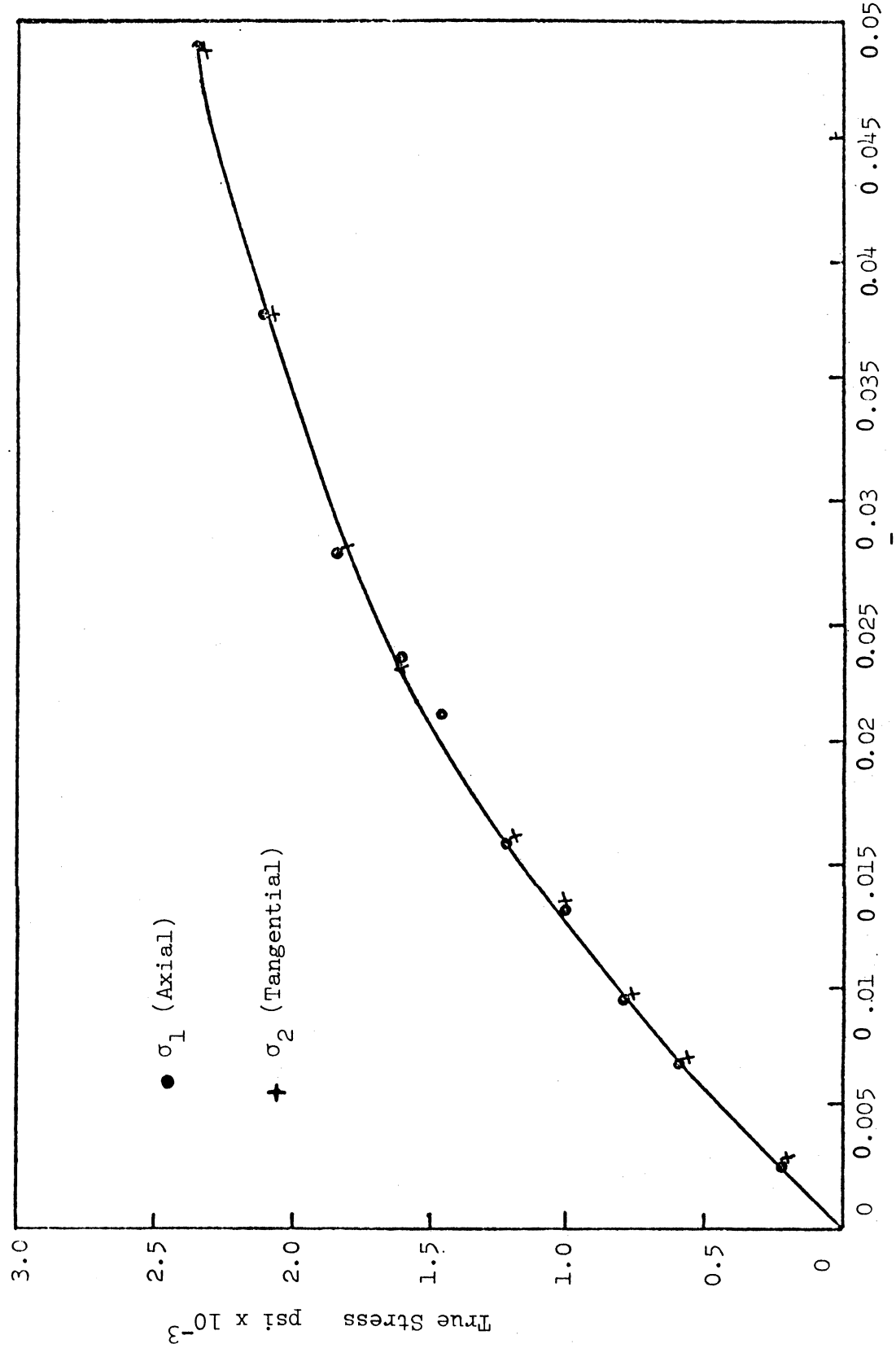

FIG. 26 TRUE STRESS-EFFECTIVE STRAIN CURVE OF PE (A) UNDER AXIAL TENSILE LOAD AND INTERNAL PRESSURE WITH STRESS RATIO OF ABOUT 1.0.

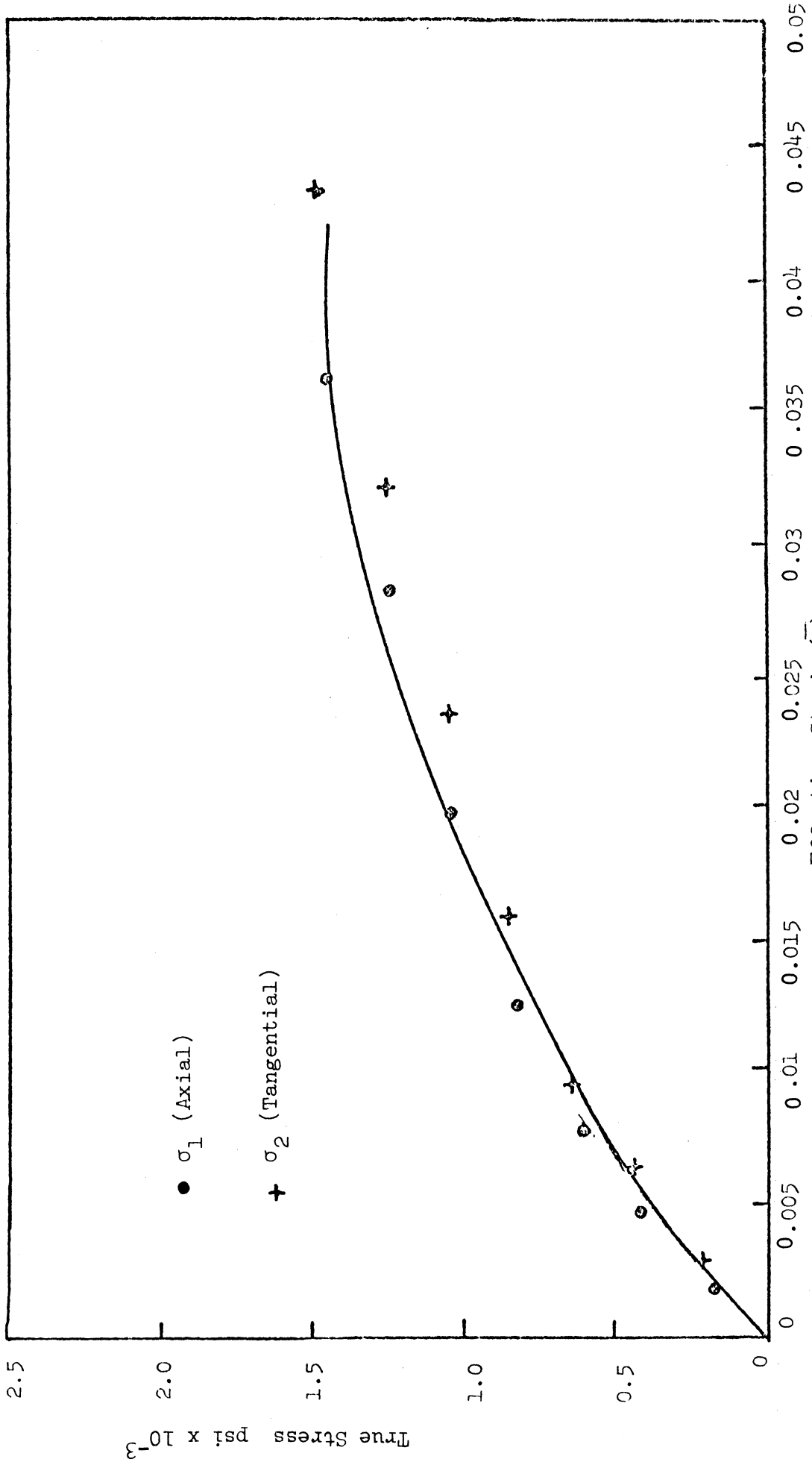

FIG. 27 TRUE STRESS-EFFECTIVE STRAIN CURVE OF PE (B) UNDER AXIAL COMPRESSIVE LOAD AND INTERNAL PRESSURE WITH STRESS RATIO OF ABOUT -1.0.

Table V.1

Yield Stress Values of PC Under Different States of Stress

Material	σ_1 psi (axial)	σ_2 psi (tangential)	$R_1 = \frac{\sigma_1}{T}$	$R_2 = \frac{\sigma_2}{T}$
PC	6600	0	1.0	0
	7100	3750	1.08	0.565
	7000	4750	1.06	0.72
	6000	6000	0.91	0.91
	4900	7000	0.74	1.06
	3500	7000	0.53	1.06
	1800	7100	0.27	1.07
	0	6600	0	1.0
	-1650	5600	-0.25	0.85
	-4450	4100	-0.675	0.62
	-5000	3400	-0.76	0.515
	-5200	2600	-0.79	0.4
	-5600	2300	-0.85	0.35
	-6500	1800	-0.99	0.272
	-7800	0	-1.2	0

Table V.2

Yield Stress Values of PVC Under Different States of Stress

Material	σ_1 psi (axial)	σ_2 psi (tangential)	$R_1 = \frac{\sigma_1}{T}$	$R_2 = \frac{\sigma_2}{T}$
PVC-A	6300	0	1.0	0
	6350	3200	1.0	0.505
	3300	6700	0.52	1.06
	5600	5600	0.89	0.89
	6900	1900	1.1	0.3
	0	6250	0	1.0
	-8200	0	-1.3	0
PVC-B	5400	0	1.0	0
	-3400	3500	-0.63	0.65
	-2400	4700	-0.45	0.87
	-5750	1650	-1.06	0.31
	-4750	3200	-0.88	0.59
	-1500	5400	-.278	1.0
	-6950	0	-1.32	0
PVC-B (Plane Strain)	0	8900	0	1.65

Table V.3

Yield Stress Values of PE Under Different States of Stress

Material	σ_1 psi (axial)	σ_2 psi (tangential)	$R_1 = \frac{\sigma_1}{T}$	$R_2 = \frac{\sigma_2}{T}$
HDPE-A	1325	0	1.0	0
	-1675	0	-1.28	0
	1325	650	1.0	0.5
	1200	1200	0.905	0.905
HDPE-B	1275	0	1.0	0
	-1675	0	-1.32	0
	-800	800	-0.63	0.63
	-550	1025	-0.43	0.87
	-1075	475	-0.845	0.37
HDPE-C	1325	0	1.0	0
	-1650	0	-1.28	0
	0	1400	0	1.05
	1350	425	1.0	0.32
	-1525	425	-1.15	0.32

Tables V.1 through V.3 give actual values of σ_1 and σ_2 for different states of stress; in addition normalized values are tabulated. Table V.2 also includes the result using PVC under plane strain loading conditions. Plane strain tests for the other two materials could not be carried out since all of the test material had been exhausted and it was felt unnecessary to obtain still another "batch" of each of these two polymers.

V.1.4 Plane Strain Compression Results. A plane strain compression test was conducted on PVC using a Ford-type test as mentioned earlier. The true stress-effective strain curve is shown in Fig. 28. From this test two tangents to the yield locus can be drawn in the third quadrant. From the normality rule, the normal* to the yield locus (at any point) makes an angle ϕ with the σ_2 axis. The tangent of this angle can be expressed as

$$\tan \phi = \frac{d\epsilon_1}{d\epsilon_2} , \qquad (5.1)$$

where $d\epsilon_1$ and $d\epsilon_2$ are plastic strain increments in the axial and tangential directions, respectively.

With the test strip length oriented with the rod axis, the thickness coincided with the radial direction; compression thereby coincided with the radial direction of rod. Practically no deformation occurred in the width direction during compression. Thus in equation (5.1) $d\epsilon_2$ can be taken as zero and ϕ becomes 90 degrees at the point A.

---

* For example, the projection of the "total" strain increment in the $\sigma_1 - \sigma_2$ plane.

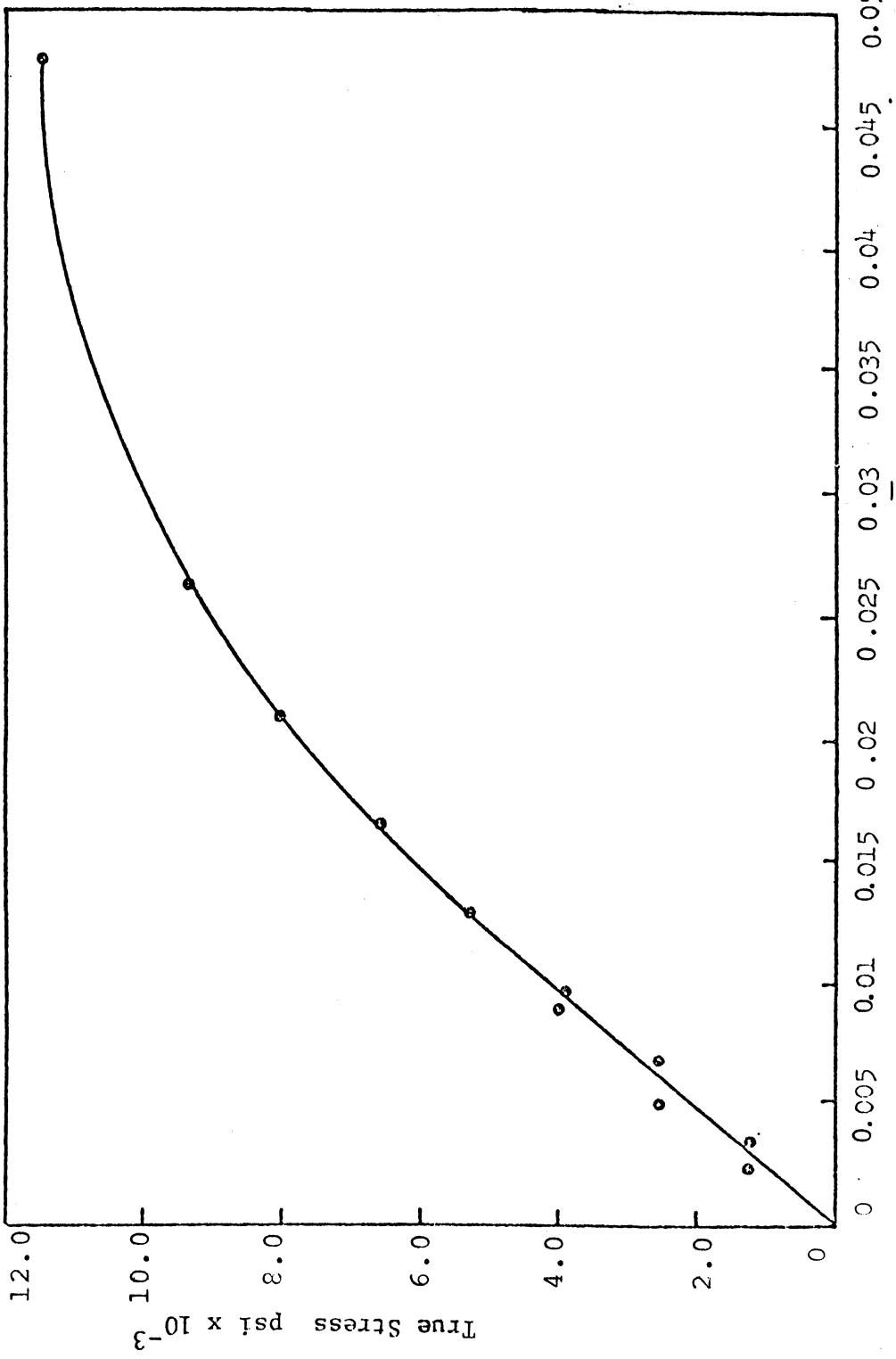

FIG. 28 TRUE STRESS-EFFECTIVE STRAIN BEHAVIOR OF PVC (BAR B) SUBJECTED TO PLANE STRAIN LOADING.

Physically, this means that the normal to the yield locus makes a 90 degree angle with the σ_2 axis. (With this isotropic material, the corresponding tangent at point B can be drawn as shown in Fig. 31.)

V.2 Comparison of Results with Suggested Yield Criterion

From the results obtained in the preceding section, yield loci for the three polymers were drawn as shown in Figs. 29 through 32. Since, except for PC, the properties of the materials obtained in two different batches were not identical, only normalized yield loci were plotted for PVC and HDPE. Besides a normalized yield locus, a regular yield locus (i.e., based upon absolute values of stress) was plotted for PC. This is shown in Fig. 29. The solid line indicates the theoretical locus determined with equation (2.26) and the experimental points are superimposed. The ratios of yield strengths in compression to tension, as determined experimentally, were 1.2 and 1.3 for PC and PVC, respectively. The ratio of yield strength in compression to tension has been reported to be 1.12 for PC by Bauwens et al. [18] and Christiansen [78]; this is not very far from the value of 1.2 found in this work and the discrepancy could be due to the different definitions of yield stress. Bauwens et al. [18] report the ratio of compressive yield to tensile as 1.3 for PVC which is identical to the one found in the present work. It can be seen from Figs. 29 through 31 that the correlation between theoretical and the experimental results is excellent for PC and PVC.

The normalized yield locus for polyethylene is drawn in Fig. 32. The solid line is the yield locus for a ratio of compressive to tensile

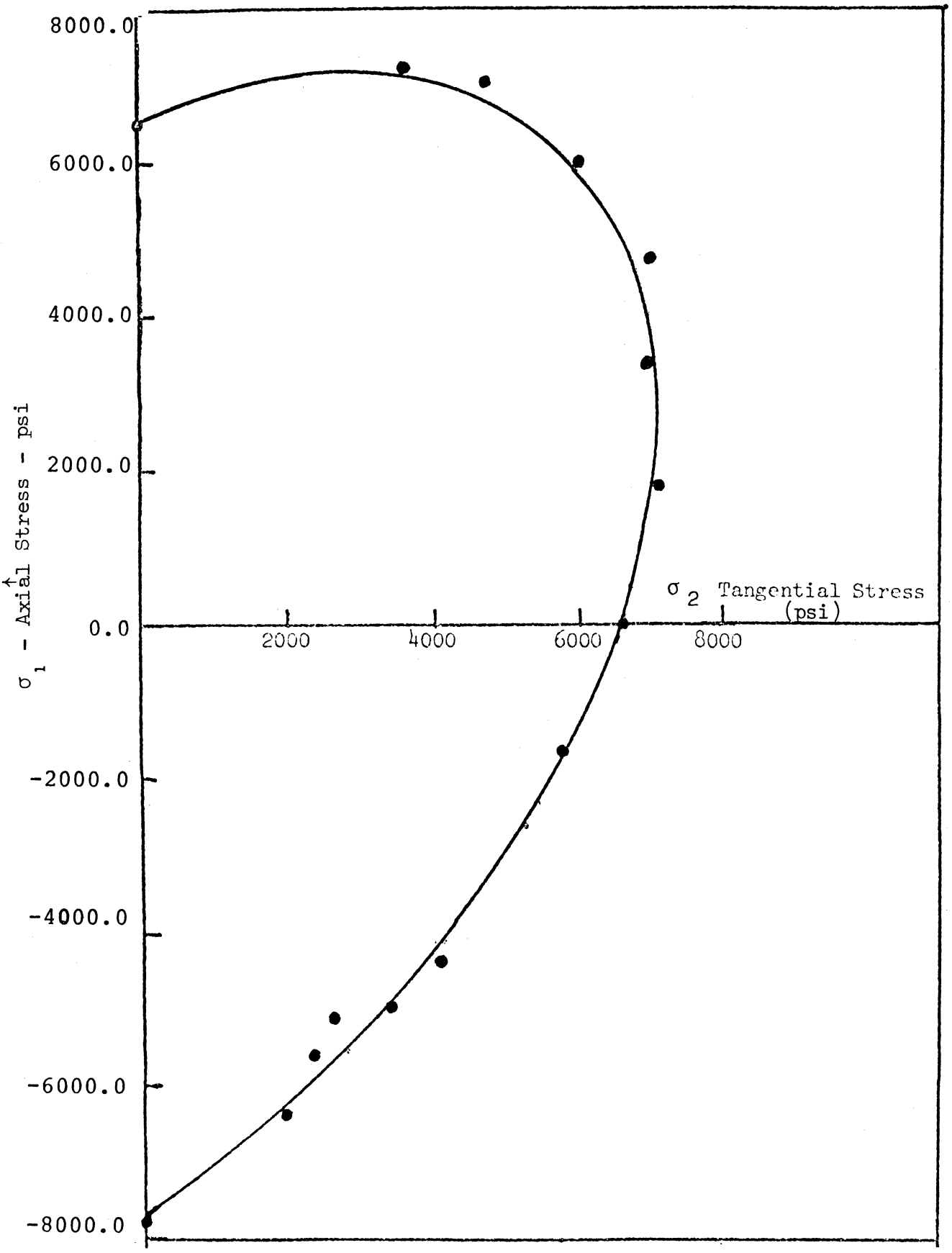

FIG. 29 YIELD LOCUS OF PC SHOWING EXPERIMENTAL POINTS AND CURVE BASED UPON PREDICTIONS OF MODIFIED VON MISES CRITERION (EQUATION (2.26)).

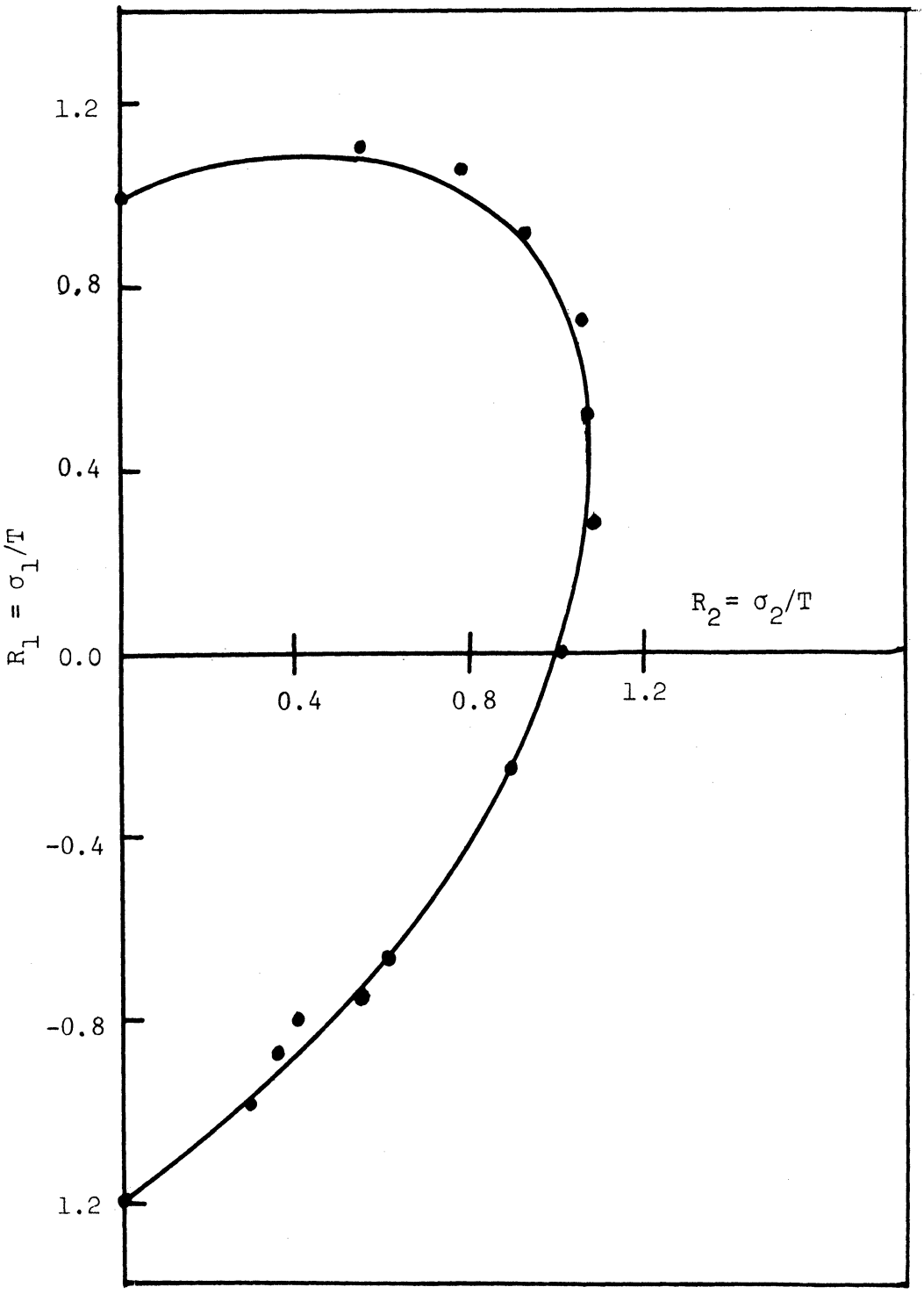

FIG. 30 NORMALIZED YIELD LOCUS OF PC SHOWING EXPERIMENTAL POINTS AND CURVE BASED UPON MODIFIED VON MISES CRITERION (EQUATION 2.28) FOR C/T = 1.2.

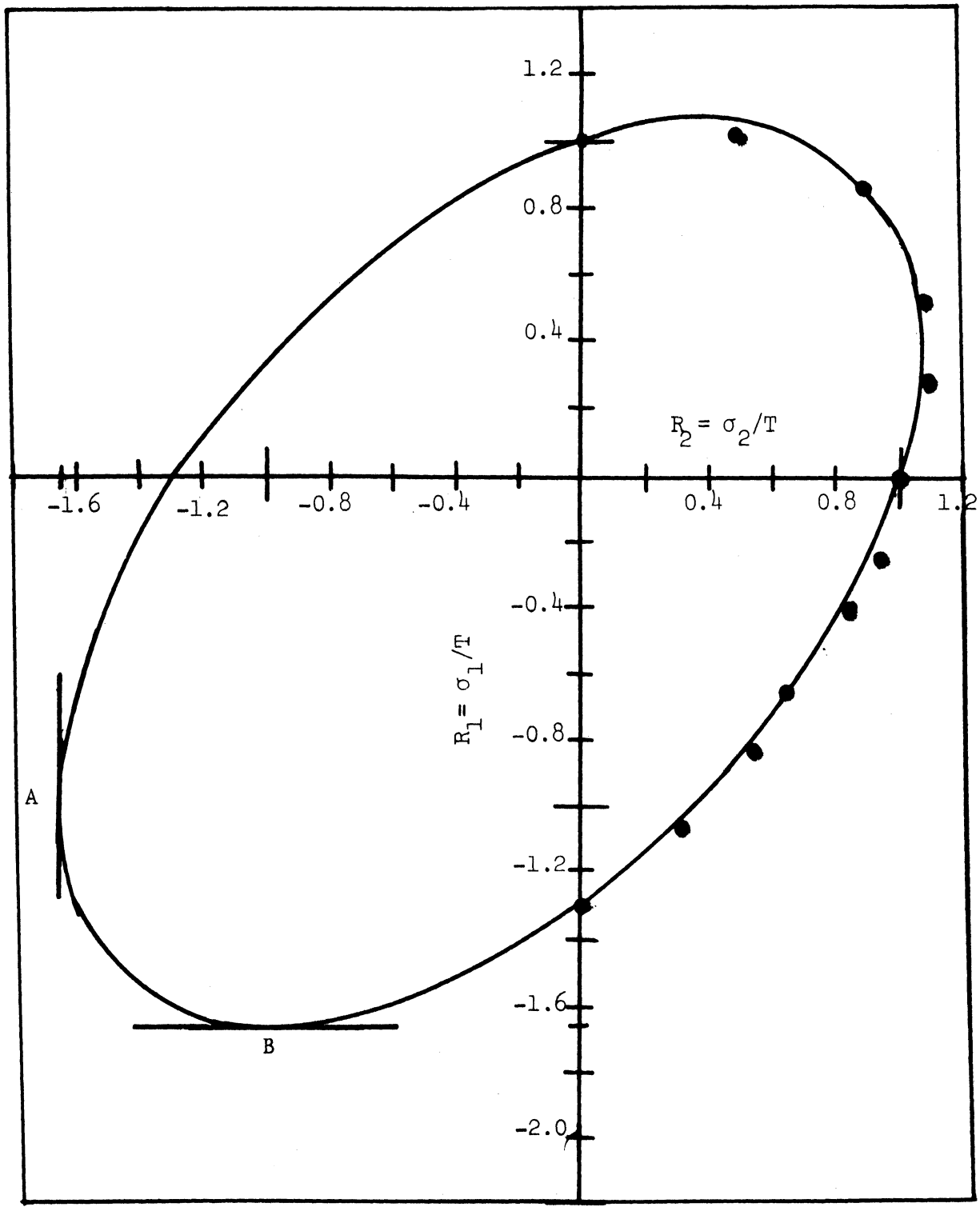

FIG. 31 NORMALIZED YIELD LOCUS OF PVC SHOWING EXPERIMENTAL POINTS AND CURVE BASED UPON MODIFIED VON MISES CRITERION (EQUATION 2.28) FOR C/T = 1.3.

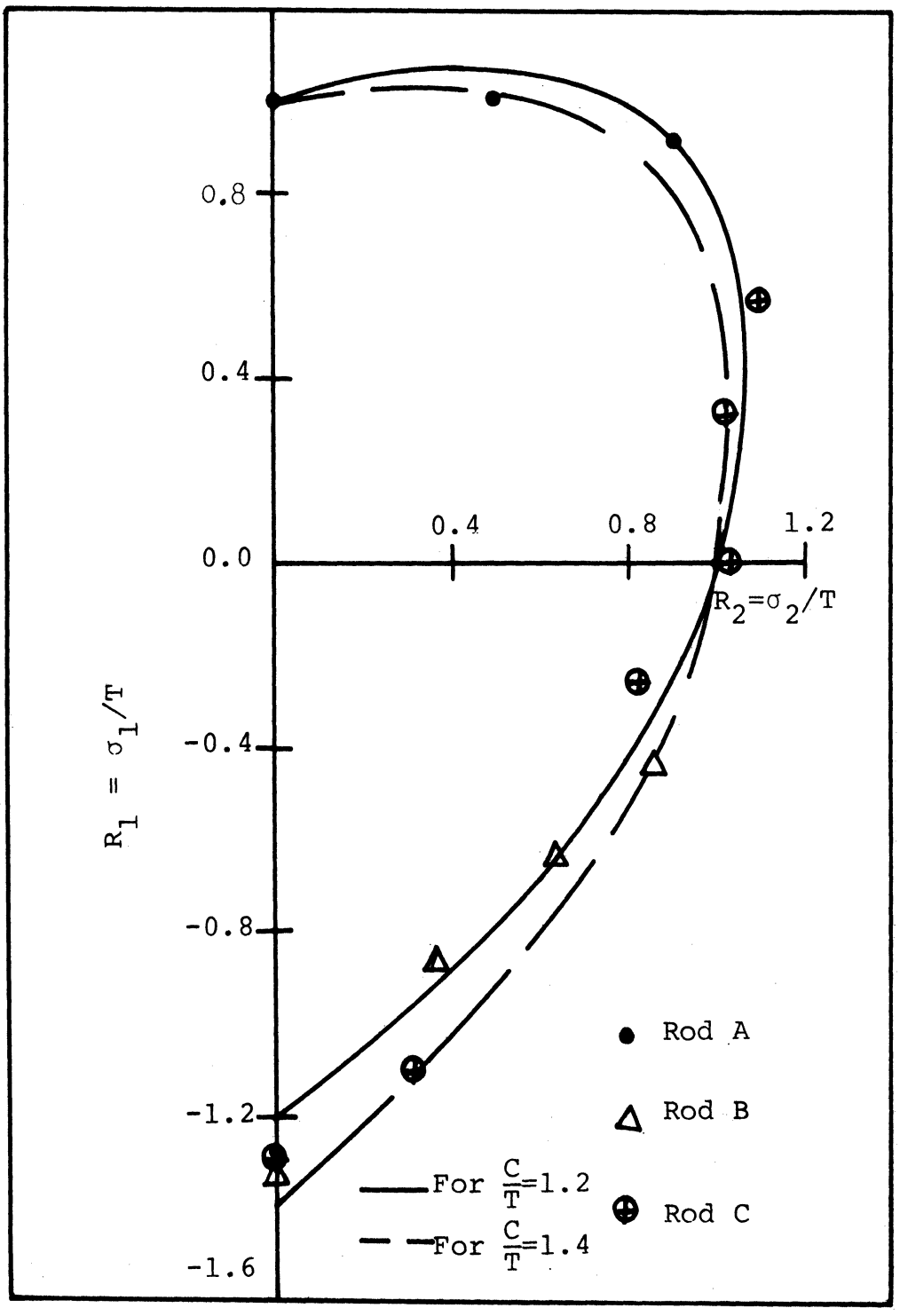

FIG. 32 NORMALIZED YIELD LOCI OF HDPE SHOWING EXPERIMENTAL POINTS AND TWO CURVES BASED UPON C/T RATIOS OF 1.2 AND 1.4 (EQUATION 2.28).

yield strength of 1.2 while the dotted line is for a ratio of 1.4 The actual ratio was different for the three different polyethylene rods used in this study and varied from 1.28 to 1.32. The experimental results fit fairly well in the band which is bounded by ratios of 1.2 and 1.4. For polyethylene, the correlation between the theoretical and the experimental results, although not as good as that observed for the other two materials, is still satisfactory. The observed scatter may be due to the presence of anisotropy in the material, which increases as deformation proceeds. The trend of the experimental results indicates that the proposed criterion predicts the yielding behavior of a variety of polymers (amorphous to crystalline) fairly well.

V.3 Comparison of Yield Criteria

Using equations (2.27) and (2.28) it is instructive to compare predicted yield loci for various C/T ratios using each of these equations. At small C/T ratios the difference seems trivial, however, for higher values of this ratio the difference becomes significant. Figure 3 demonstrated this. Points determined from equation (2.27) lie outside those found with equation (2.28) in the third quadrant whereas no appreciable difference is found in the other three quadrants. As discussed by Tschoegl [67] first quadrant point are quite insensitive in regard to describing a most appropriate "failure" surface. To determine with reasonable certainty which of these two criteria are most accurate in predicting yield behavior, tests that lead to third quadrant points are essential.

Figure 33 shows the published results of different workers for various amorphous polymers. It can be seen that the experimental data

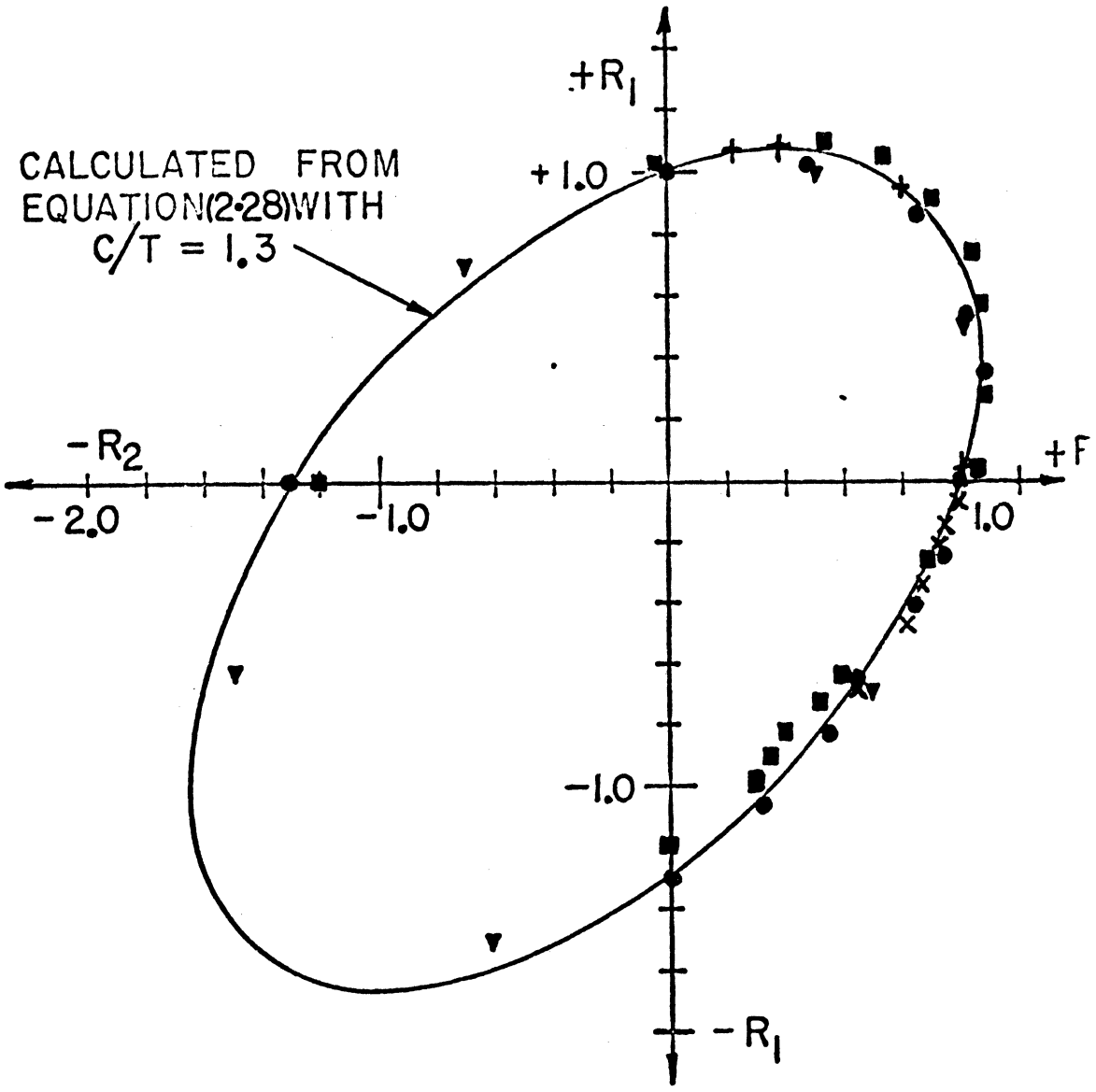

SYMBOL	SOURCE OF DATA	MATERIAL	C/T RATIO
●	PRESENT STUDY	PVC	1.30
■	PRESENT STUDY	PC	1.20
▼	WHITNEY (13)	PS	1.30
×	BAUWENS (18)	PVC	1.30
+	STERNSTEIN (15)	PMMA	1.30

FIG. 33 A COMPOSITE OF EXPERIMENTAL DATA FROM VARIOUS SOURCES COMPARED WITH THE NORMALIZED YIELD LOCUS PREDICTED FROM THE MODIFIED VON MISES CRITERION (EQUATION 2.28) FOR C/T RATIO OF 1.3.

shows excellent agreement with the theoretical curve. Unfortunately, except for Whitney's [13] work with PS, no information relating to the third quadrant was found in the published literature.

V.4 Fracture Under Multiaxial Stress States

This section discusses the fracture of polycarbonate and polyvinylchloride. It is very difficult, if not impossible, to document the fracture modes for all the stress ratios used but an attempt is made to discuss the fracture mode of PC and PVC for certain specific stress ratios.

The fracture of tubes under stress states in the first quadrant is entirely different from those in the fourth quadrant. For the first quadrant, the tubes fail by cracking while in the fourth quadrant they "fail" by buckling which produces a peripheral bulge.

The process of fracture is dictated primarily by the stress state and the material. Generally speaking PVC tends to be "more brittle" than PC in its behavior. Thomsen [79] assumed that fracture of tubes takes place on the planes where the shear stress reaches a maximum. An attempt has been made to classify the fracture behavior into three categories for the first and fourth quadrant loading as shown in Fig. 34; the three possible failure modes are shown in that figure.

Figure 35 shows the failure mode of two PC tubes for stress ratios of 3/4 and 1/2. For the stress ratio of 3/4 a neck developed parallel to the axial direction and propagated in the tangential direction. For the stress ratio of 1/2 the neck development was not so conspicious but a sharp crack developed at an angle of about 5 degrees to the axis of the tube.

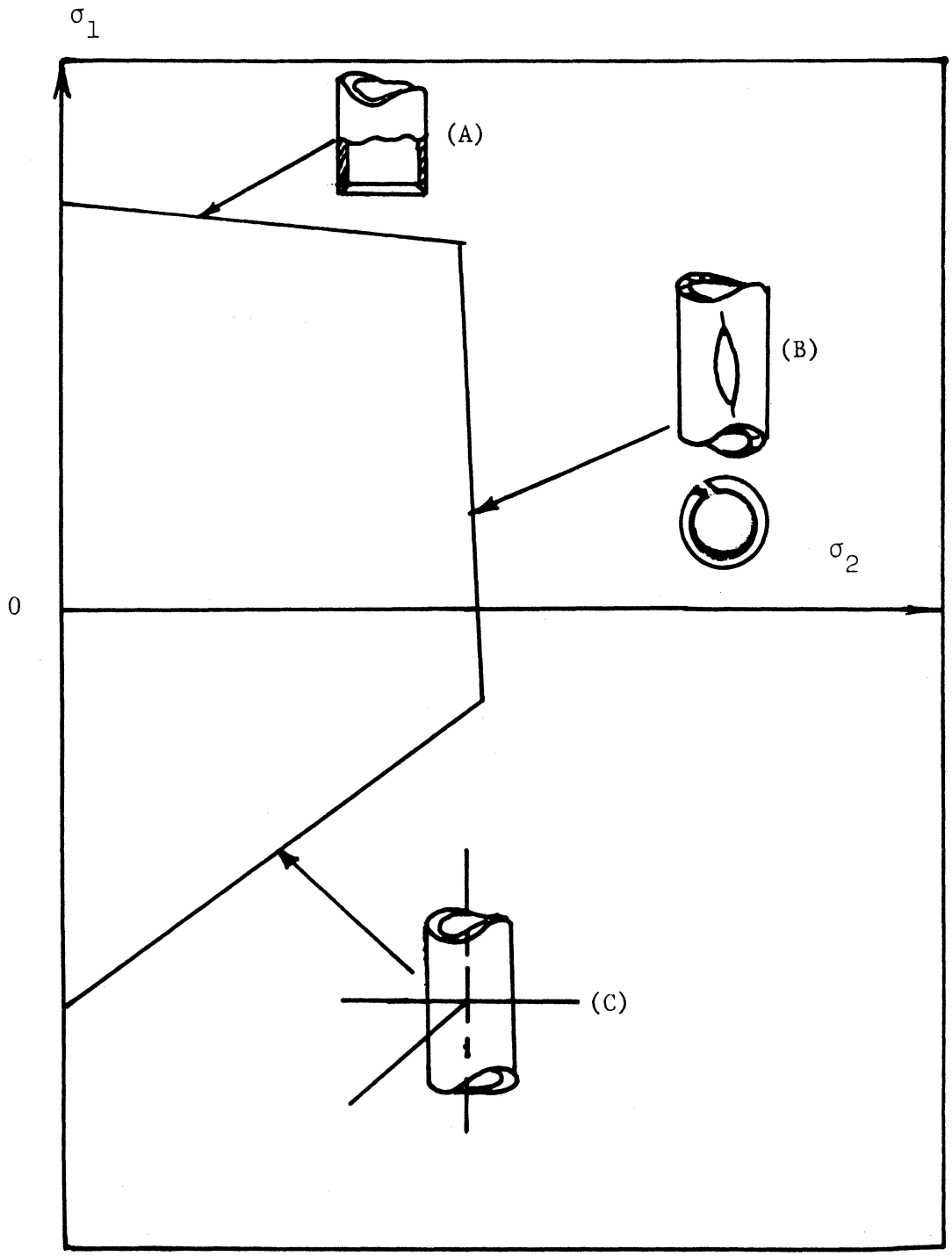

FIG. 34 PROBABLE MODES OF FRACTURE OF THIN WALL TUBES UNDER BIAXIAL STRESS FIELD [THOMSEN].

FIG. 35 FAILURE OF POLYCARBONATE TUBES IN BIAXIAL STRESS STATE.

Figure 36 shows the fracture of PVC tubes for the stress state of two and zero (i.e., stressed only in the hoop direction). For the stress ratio of two the fracture was not similar to mode (A) of Fig. 34, since the 45 degree angle as suggested in Fig. 34 was not observed. The fracture of the PVC tube under only the circumferential stress is very fascinating. It shows many important features. There is one main crack running along the tube axis. The crack does indeed incline at 45 degrees to the thickness and not in a true radial direction. However, there is no visible neck formation as observed for PC. Besides, there are subsidiary cracks running at about 45 degrees to the main crack. The fracture appears brittle. This fracture is very similar to the one reported by Davis [80] (see Nadai [7])for medium carbon steel tubes under pure circumferential stress (high stored energy test). It would appear that the fracture of PC is shear fracture while for PVC it may start as shear but it finally turns to brittle fracture.

The fourth quadrant stress state does not cause the fracture patterns suggested in Figure 34 rather, buckling takes place; this causes bulging in the circumferential direction. From the stress ratio of zero to -1.0 the maximum strain and stress are in the hoop direction. The instability condition is determined by the slope of the hoop stress and hoop strain curves.

Figure 37 shows the polycarbonate tubes for the stress ratio of -1.0 and -2.5. The distinct shear bands at about 45 degrees to the tube axis can be seen for the tube subjected to -1.0 stress state (pure-shear). For the stress ratio of -2.5 the tube developed a bulge. Figure 38 shows

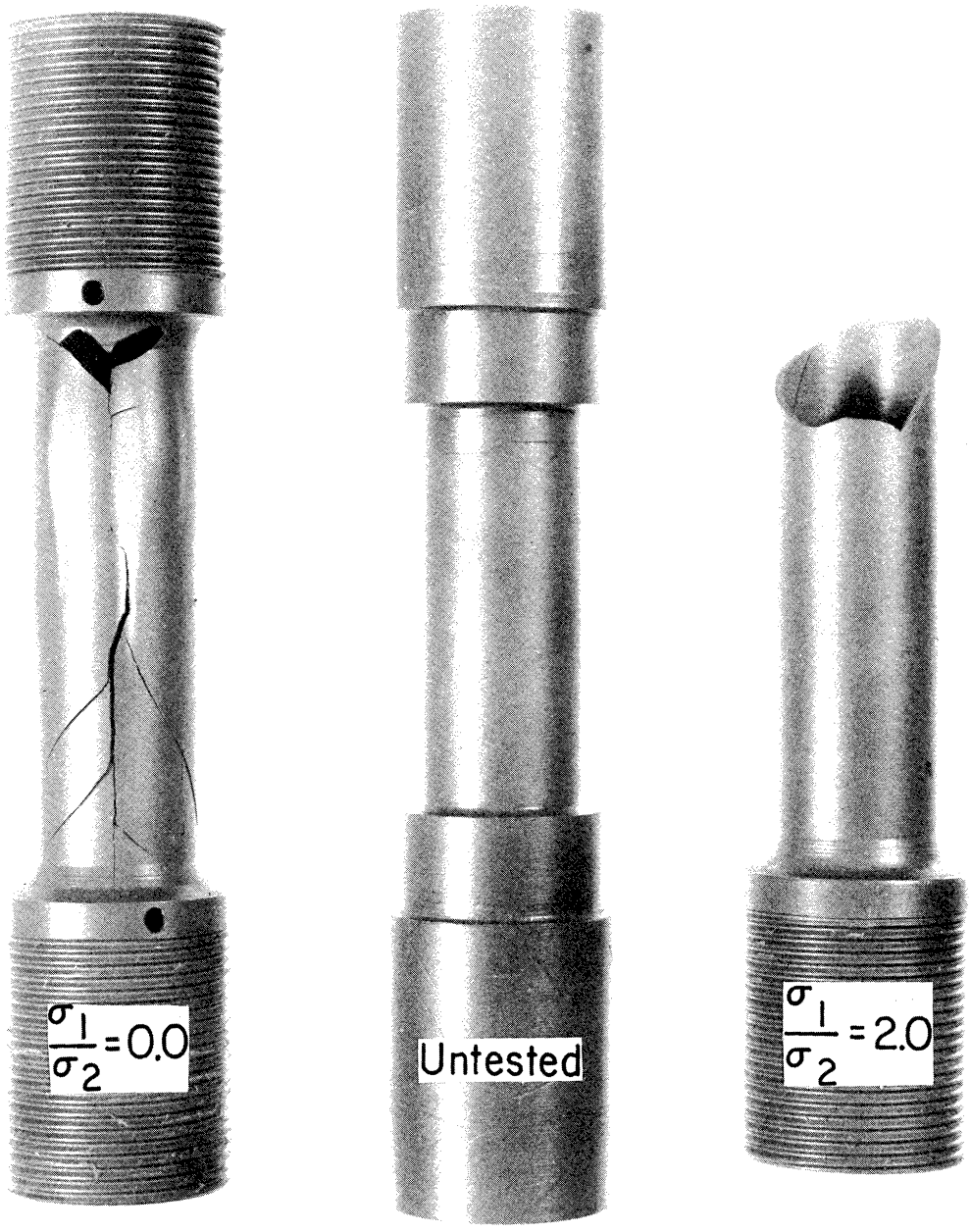

FIG. 36 FAILURE OF POLYVINYL CHLORIDE TUBES IN BIAXIAL STRESS STATE.

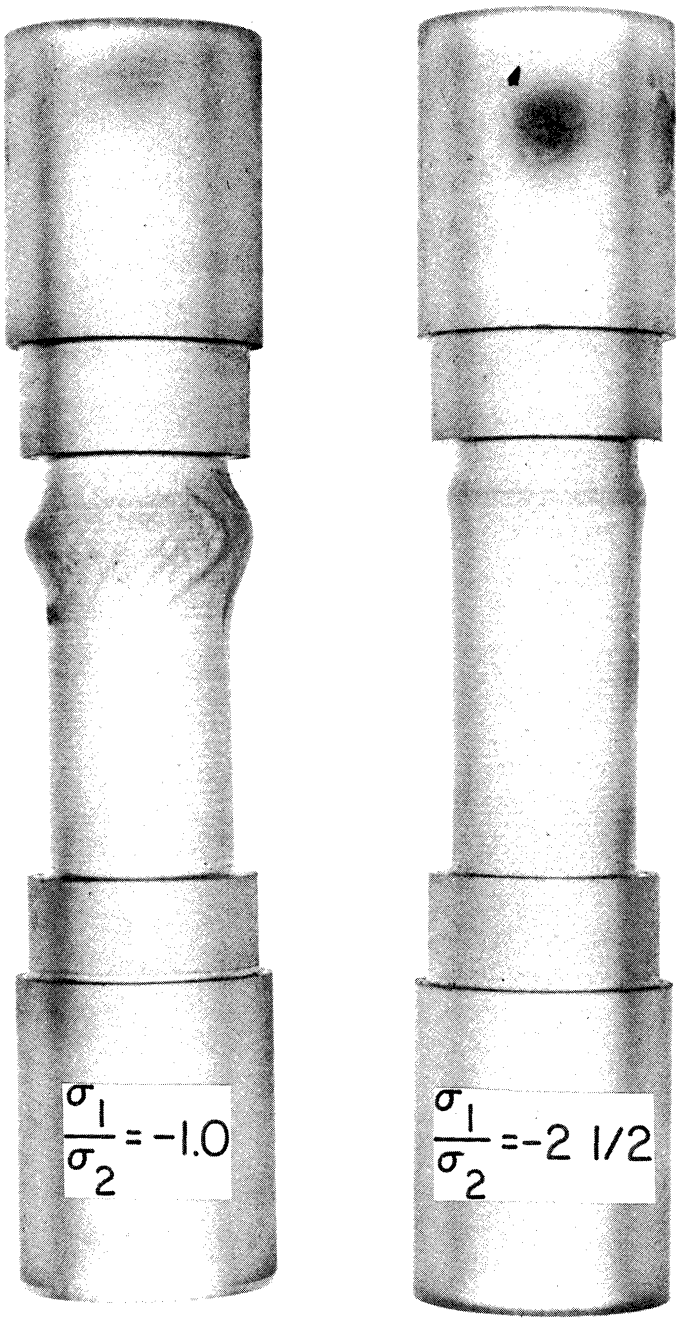

FIG. 37 BULGING OF POLYCARBONATE TUBES UNDER BIAXIAL STRESS STATE.

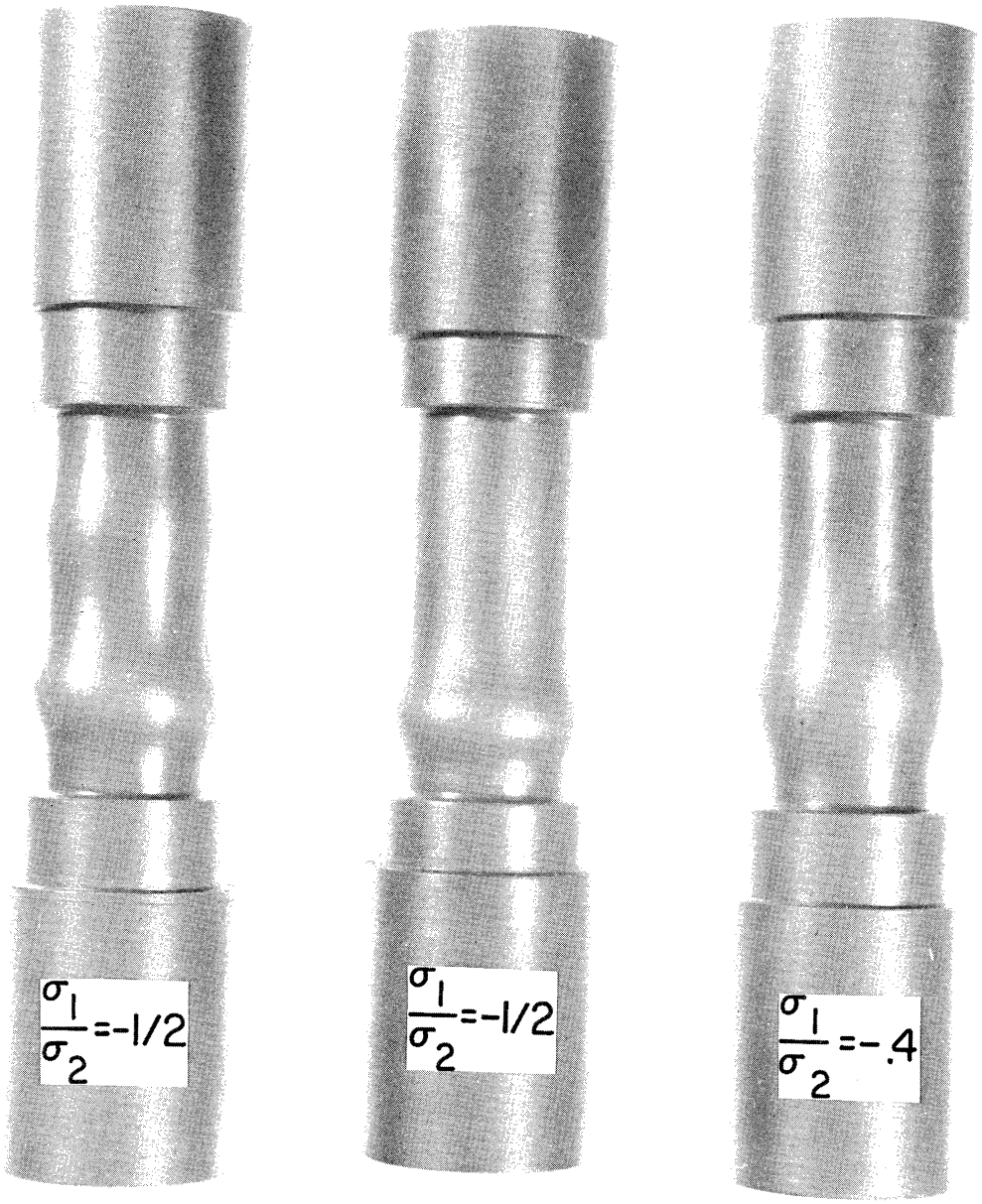

FIG. 38 BULGING OF POLYVINYLCHLORIDE TUBES UNDER BIAXIAL STRESS STATE.

the failure of PVC tubes; the first two tubes are for the stress ratio of -1/2, while the third is for -0.4. The first tube developed two bulges. At first the bottom bulge appeared. As loading continued, this bulge grew in size, and simultaneously the second bulge developed. The second tube was unloaded in the initial stages of the bulge development.

In conclusion, it appears that the "failure" modes of PVC and PC in the fourth quadrant are essentially identical, since bulging predominates. In the first quadrant however, the modes are somewhat different, shear failure predominating with PC contrasted with brittle behavior in PVC.

V.5 Results Related to Pressure Studies

The yield locus studies of polymeric materials can lead to predictions of the effect of hydrostatic pressure on yielding in an indirect manner. As pointed out in Chapter III, many investigators have tested various polymeric materials in tension, compression, and torsion under external hydrostatic pressure thereby evaluating the effect of pressure on yield strength. In the present study, the three polymers were subjected to hydrostatic pressures up to 9000 psi; tension and compression tests were then conducted. The purpose of these tests was twofold: (1) to determine the effect of hydrostatic pressure on the yield strengths of the three polymers and (2) to compare the increase in yield strengths in compression and tension for the same magnitude of hydrostatic pressure. Most studies in the past have been limited to either tension or compression tests, although Ainbinder et al. [48]

investigated both types of behavior. From that one study [48] no conclusive comparison could be made in regard to the relative increase in tensile and compressive yield strengths under external pressure.

V.5.1 Theoretical Prediction of Yield Strength Under External Hydrostatic Pressure. Variations of tensile yield stress and compressive yield stress can be investigated as either a function of external hydrostatic pressure (P) or mean normal stress (σ_m); and, the yield criteria expressed by (2.21) and (2.26) can be used for this purpose. Using normalized forms of these equations, one obtains (2.38) and (2.43) which can be used to predict variations in C and T as functions of σ_m whereas (2.39) and (2.44a and b) involve variations of C and T as a function of P. (Note that these normalized equations literally give R_T and R_C which must then be corrected to give absolute values of the tensile and/or compressive yield stress).

Figure 39 shows two curves which represent (2.39) and (2.44) for variations in normalized pressure. The one representing (2.44) predicts a linear increase in both R_T and R_C, where the ratio of R_C to R_T always equals X. In contrast, the curve representing (2.39) predicts a parabolic relationship between B and the two roots which are analogous to R_C and R_T. The ratio of R_C to R_T decreases as B (or pressure) increases, and for high values of B it approaches unity. It should be noted that as the pressure increases, the curve becomes nearly parallel to the abscissa. (For B = -2/3, equation (2.39) predicts the yield strength in tension equal to zero whereas compression gives R_C = -1.0 using equation (2.44), for B = -4/3 both tensile and compressive yield

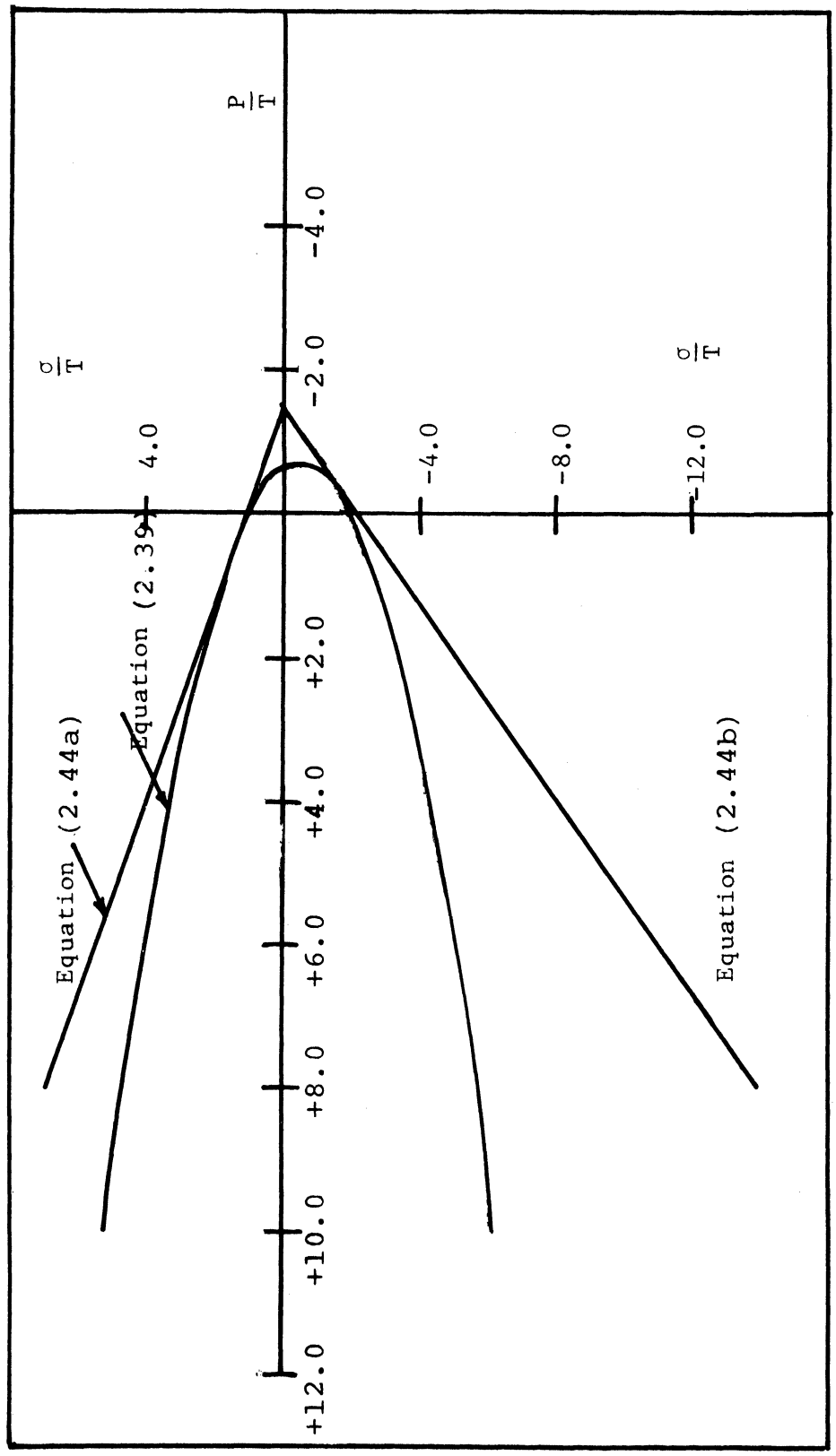

FIG. 39 PREDICTED EFFECT OF HYDROSTATIC PRESSURE ON TENSILE AND COMPRESSIVE YIELD STRESS (PLOTTED IN NORMALIZED FORM) USING EQUATIONS (2.39), (2.44a) AND (2.44b).

stresses are equal to zero. Note that in both of these examples, the "equivalent pressure" is less than atmospheric. This implies that practical use of these plots might be restricted to values of $B \geq 0.$) Figure 40 shows plots of equations (2.38) and (2.43) which relate the mean normal stress to the yield stress in tension and compression. There, both curves are symmetrical about the abscissa, thus, either curve gives identical values for the tensile and compressive "roots" (although these "roots" are not the same for both curves). These curves are two-dimensional plots of a cone and a paraboloid of revolution about the [111]-axis taken in three-dimensional space where the abscissa of Fig. 40 coincides with this [111]-axis. Lines parallel to the ordinate of Fig. 40 represent the diameter of the cone or paraboloid. It should be noted that for correlation of experimental results in tension and compression with this theory, one needs only the upper or lower half of these symmetric curves. Because of this the results obtained from experimental tests in this present study are all plotted on "one" side of the abscissa.

V.5.2 Comparison of Experimental Data with Theoretical Predictions. Reference [78] contains most of the experimental results included in an unpublished paper [81] which came to this author's attention. It should be noted that some of the data included in that paper [81] had been extracted from other sources [51],[52]. These data showed the effect of external pressure on the tensile yield strength. Comparisons of equations(2.39) and (2.44a) were made by constructing "theoretical" plots such as shown in "tensile" portion of Fig. 39. Since C and T

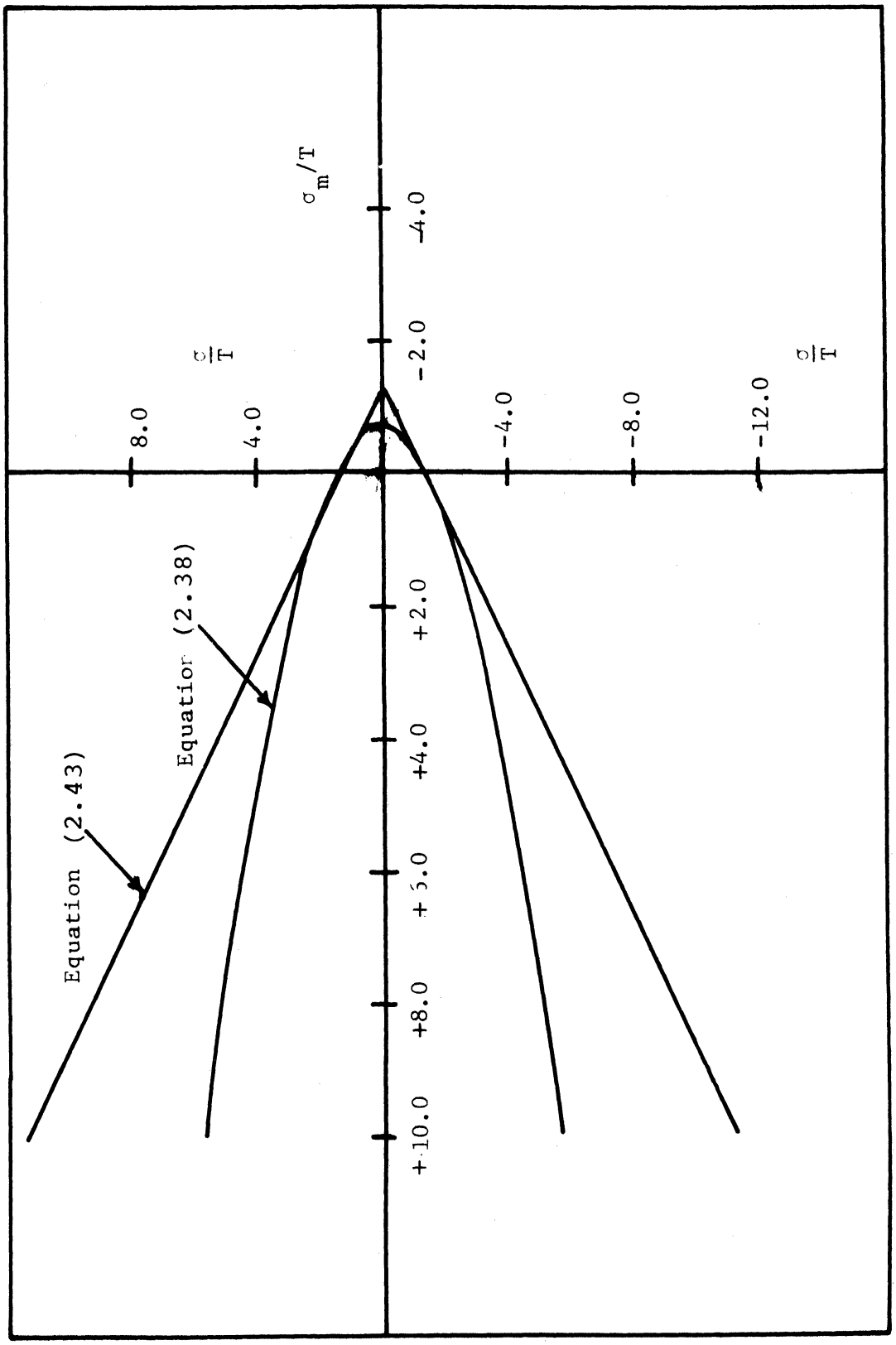

FIG. 40 PREDICTED EFFECT OF MEAN NORMAL STRESS ON TENSILE AND COMPRESSIVE YIELD STRESS (PLOTTED IN NORMALIZED FORM) USING EQUATIONS (2.38) AND (2.43).

were known for the polymers under consideration, it was only necessary to introduce a number of values for pressure, P, and compute the corresponding stress, σ. (Note that the values C, T, P and σ are represented by X, B and R in the two equations and are so plotted in the figures that follow.) Figures 41 and 42 show such comparisons for four polymers; note that POM is polyoxymethylene. It may be noted that in general the shape of the curve based upon the experimental points is more like the predictions based upon (2.39) than (2.44a).

The three polymers used in this present investigation were subjected to hydrostatic pressures of 6,000 and 9,000 psi and both uniaxial tensile and compressive tests were carried out under these pressures. The true stress-strain curves obtained using the higher pressure are compared with their counterparts when no pressure was applied. Figures 43 through 48 show these findings. It was felt unnecessary to include a plot of the results obtained with the 6,000 psi pressure but the yield values of interest were determined with that pressure and are included in Table V.4 along with the comparative measurements for 9,000 and zero psi pressure. Note that Table V.4 includes the 0.3 percent offset yield stress and the corresponding mean stress for the three polymers under three pressure conditions.

The values in Table V.4 of both tensile and compressive yield stress as a function of σ_m are plotted in Figs. 49 through 51. In addition, the theoretical curve based upon equation (2.35) is also shown. Note that as mentioned at the end of Section V.5.1 the symmetrical nature of the curve negates the need for plotting both the portion above

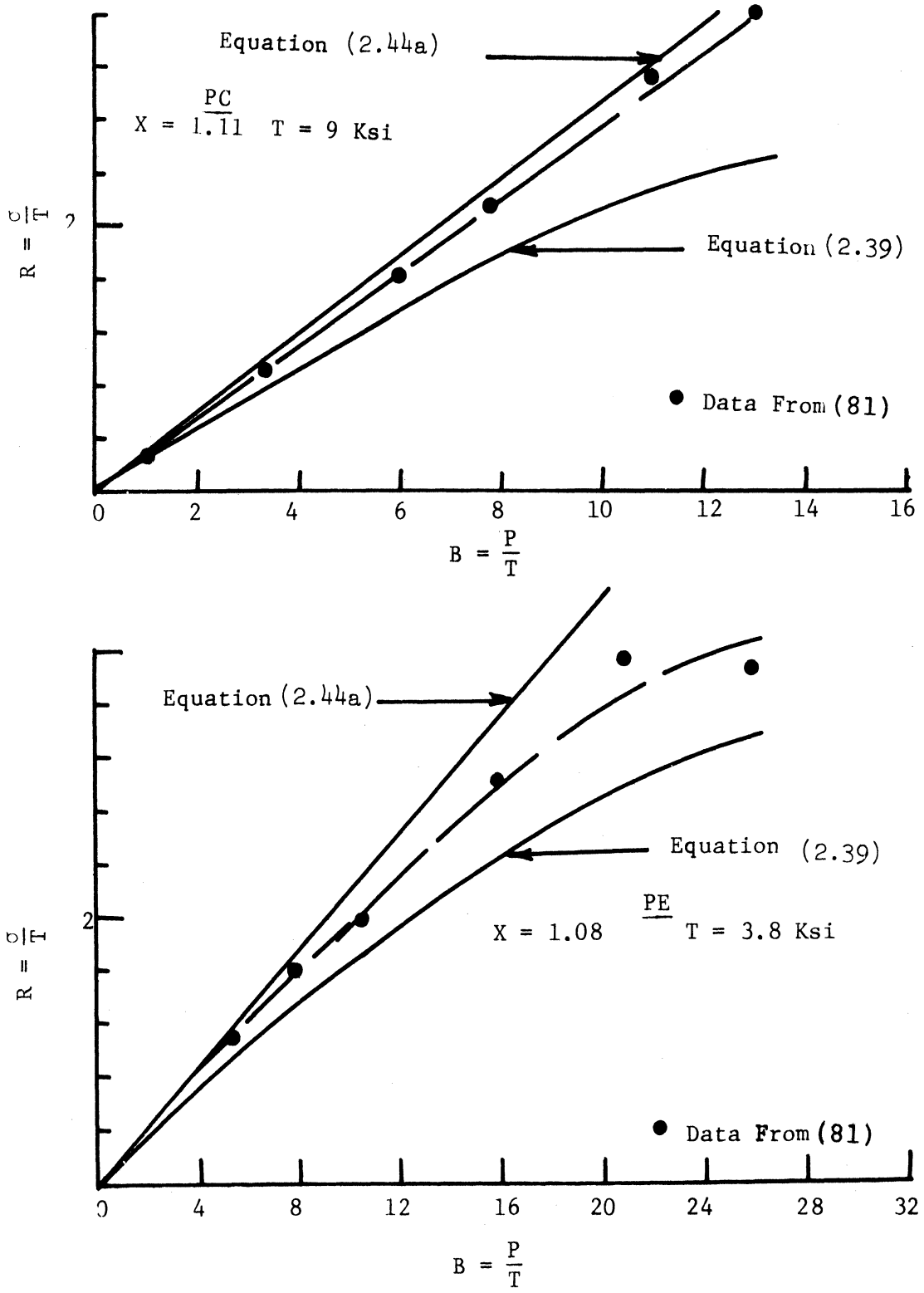

FIG. 41 EFFECT OF HYDROSTATIC PRESSURE ON TENSILE YIELD STRESS OF PC AND HDPE; COMPARISON OF PUBLISHED DATA WITH PREDICTIONS BASED UPON EQUATIONS (2.39) AND (2.44a).

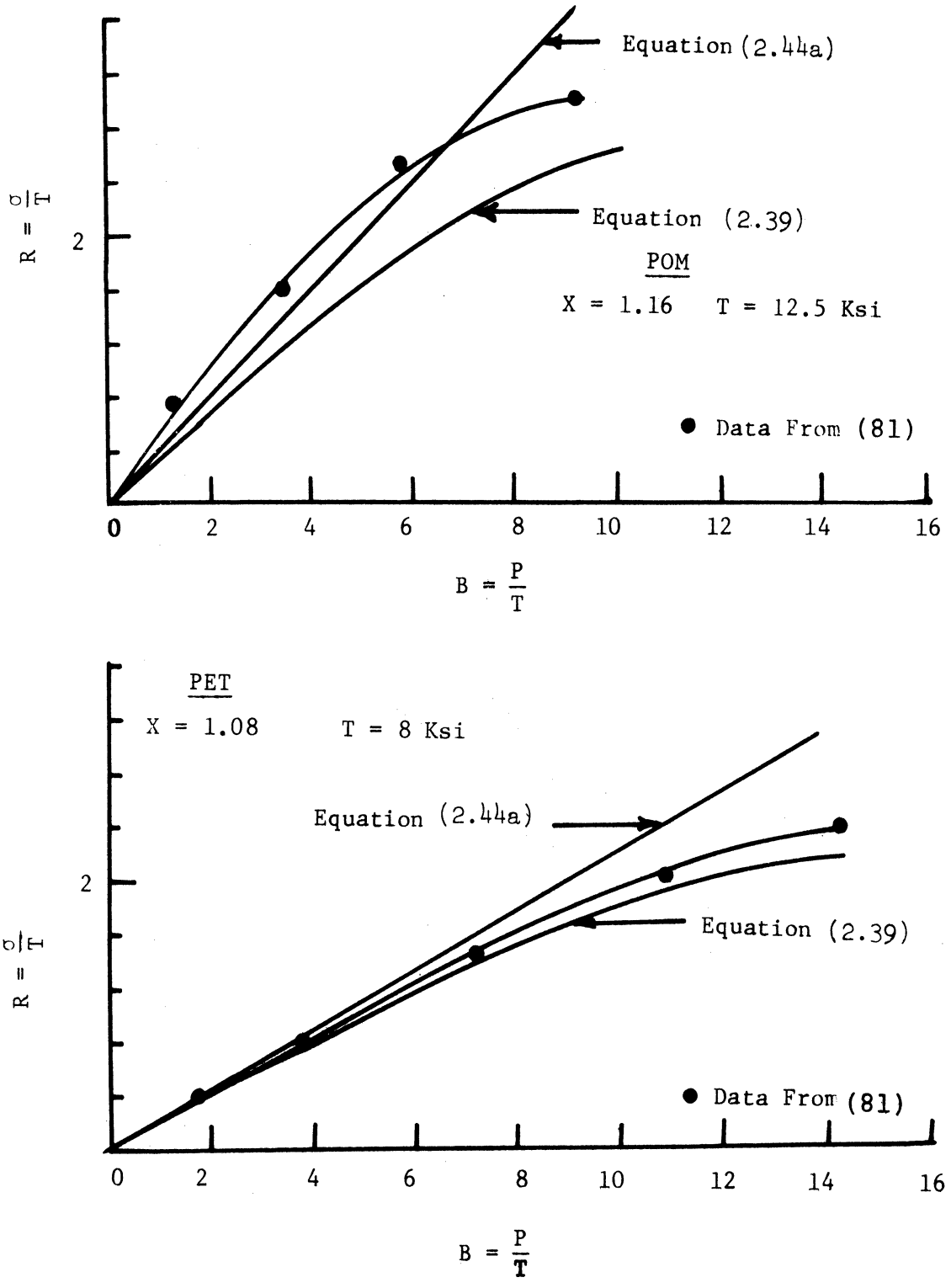

FIG. 42 EFFECT OF HYDROSTATIC PRESSURE ON TENSILE YIELD STRESS OF POM AND PET; COMPARISON OF PUBLISHED DATA WITH PREDICTIONS BASED UPON EQUATIONS (2.39) AND (2.44a).

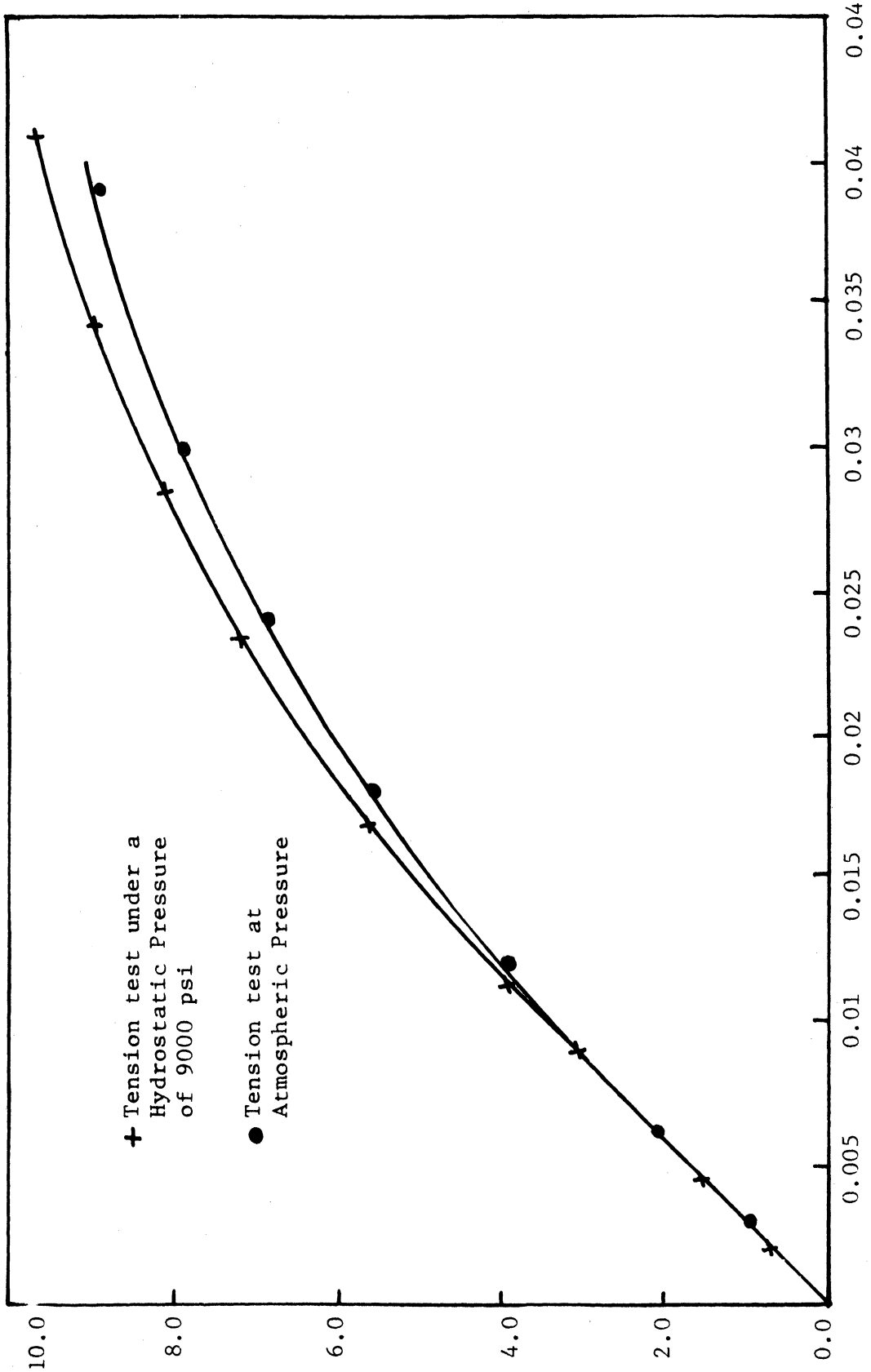

FIG. 43 TENSILE TRUE STRESS-TRUE STRAIN BEHAVIOR OF PC AT ATMOSPHERIC PRESSURE AND UNDER A HYDROSTATIC PRESSURE OF 9000 psi.

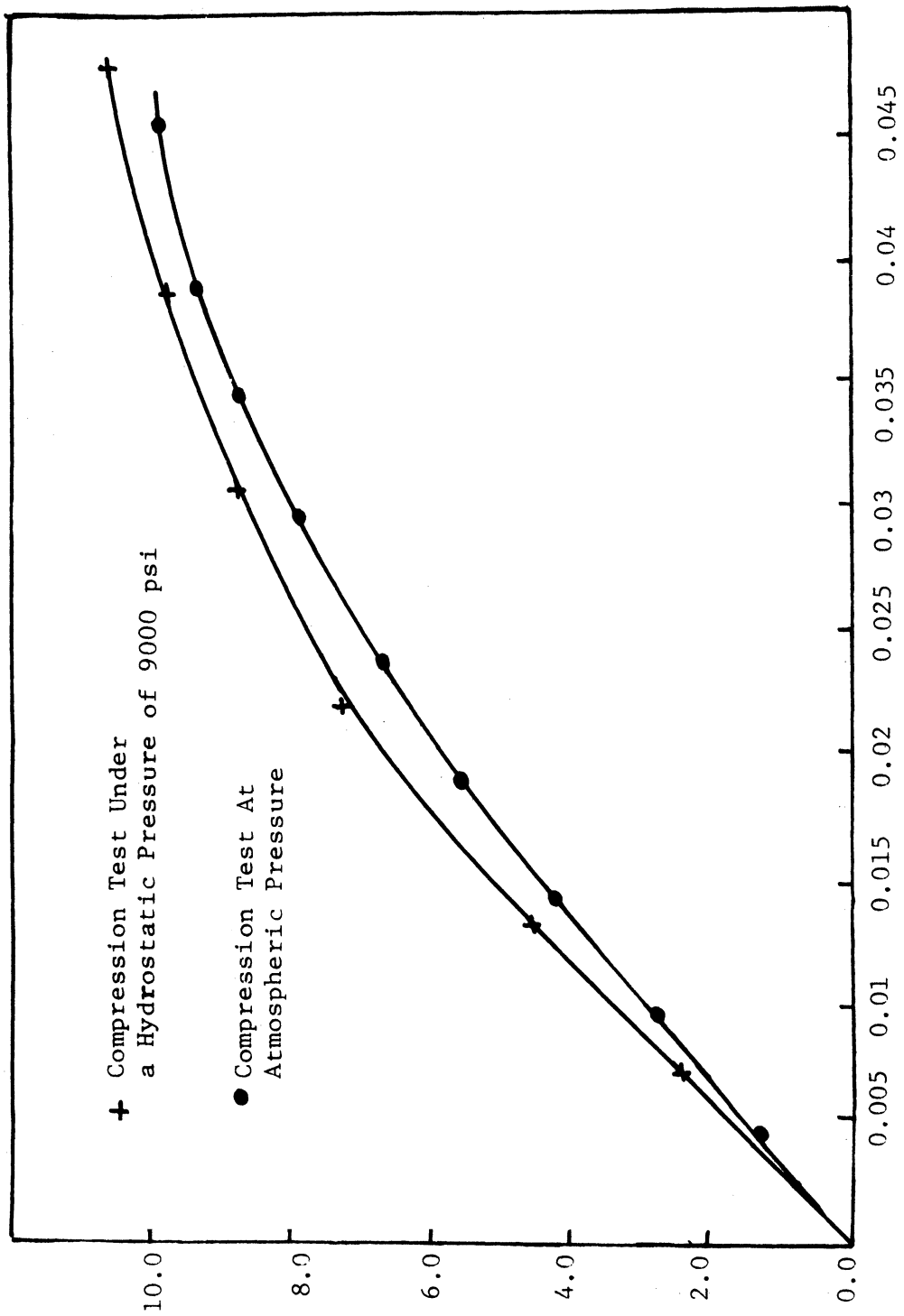

FIG. 44 COMPRESSION TRUE STRESS-TRUE STRAIN BEHAVIOR OF PC AT ATMOSPHERIC PRESSURE AND UNDER A HYDROSTATIC PRESSURE OF 9000 psi.

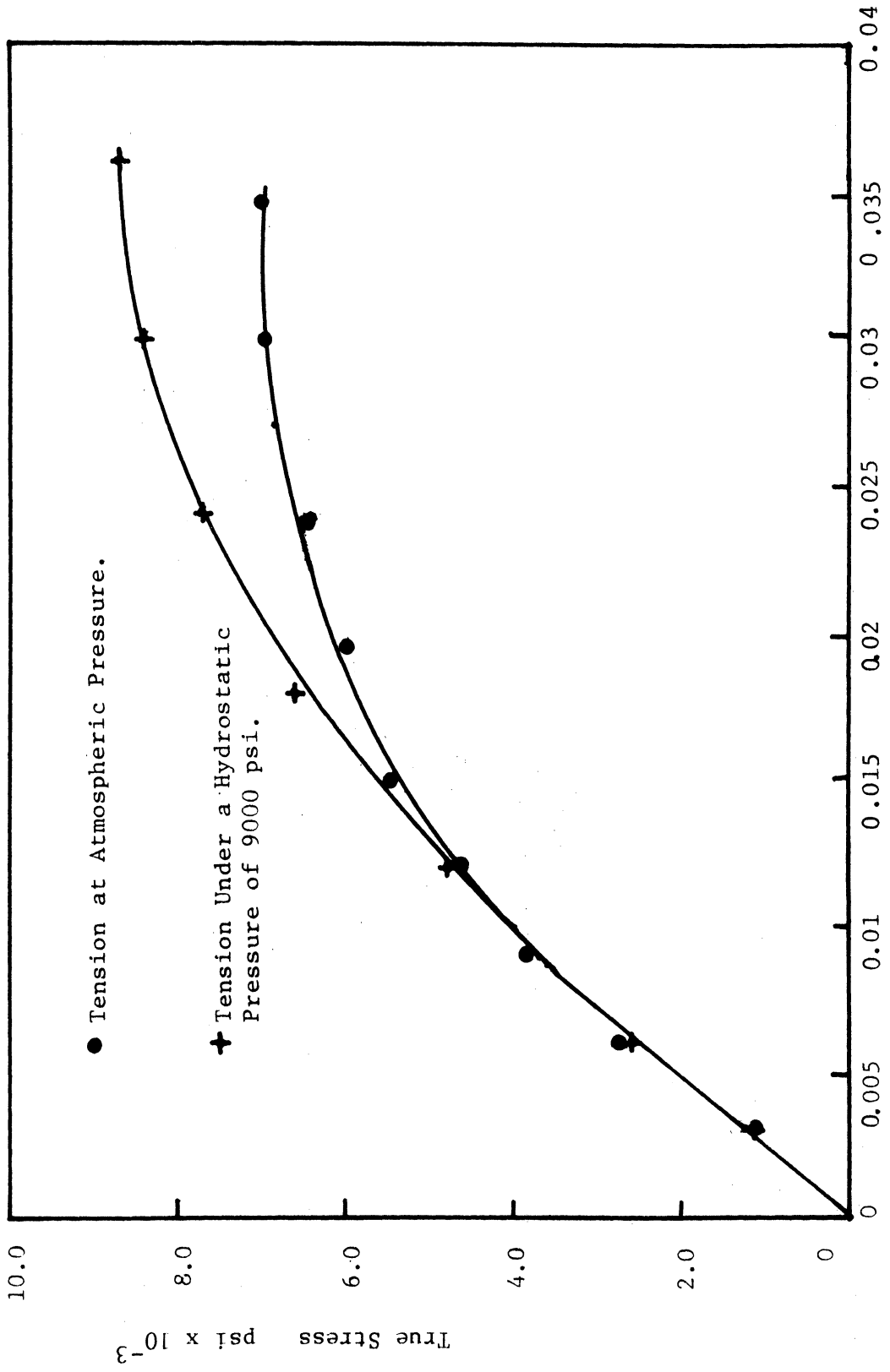

FIG. 45 TENSILE TRUE STRESS–TRUE STRAIN BEHAVIOR OF PVC (B) AT ATMOSPHERIC PRESSURE AND UNDER A HYDROSTATIC PRESSURE OF 9000 psi.

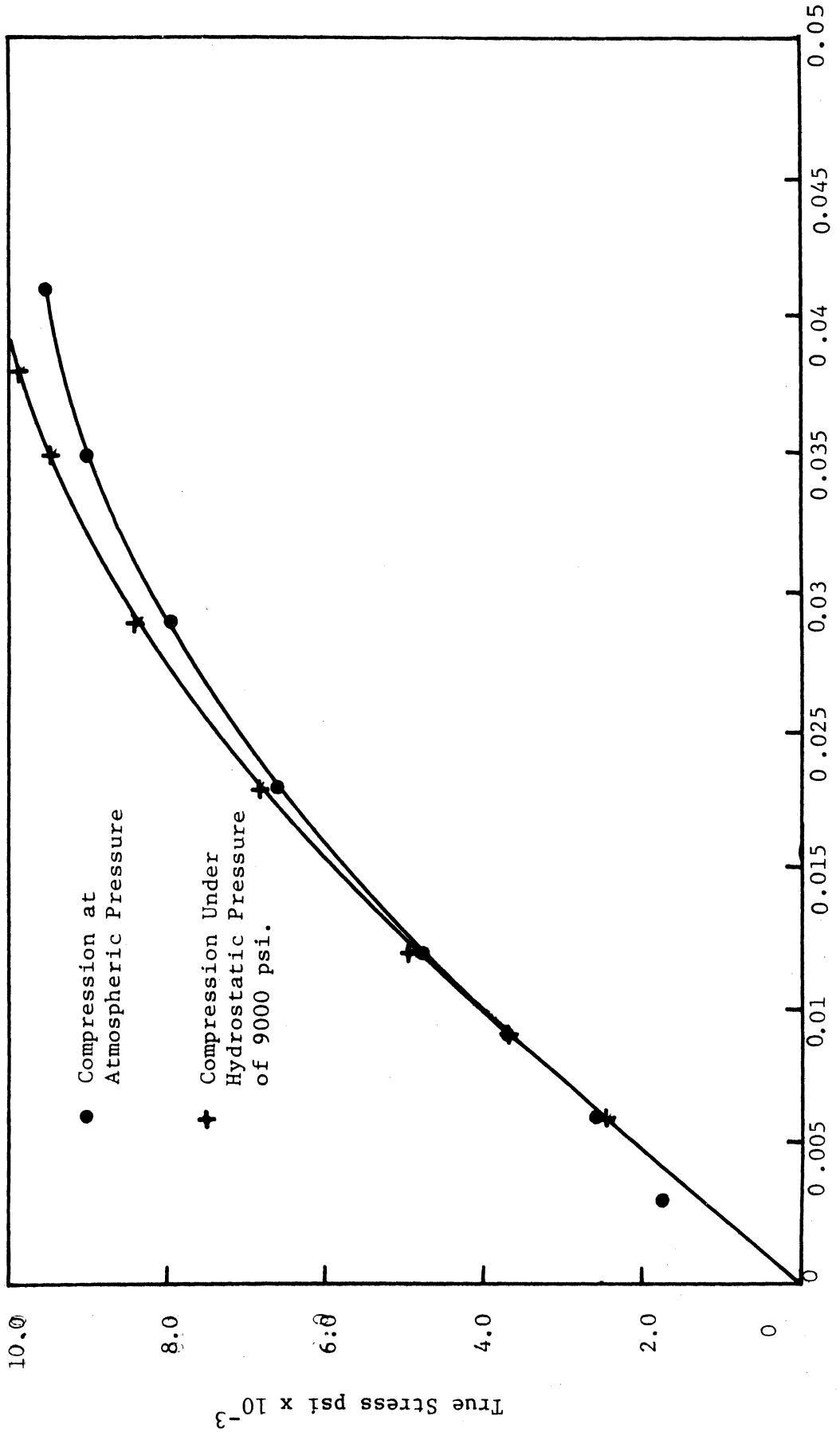

FIG. 46 COMPRESSIVE TRUE STRAIN BEHAVIOR OF PVC (B) AT ATMOSPHERIC PRESSURE AND UNDER A HYDROSTATIC PRESSURE OF 9000 psi.

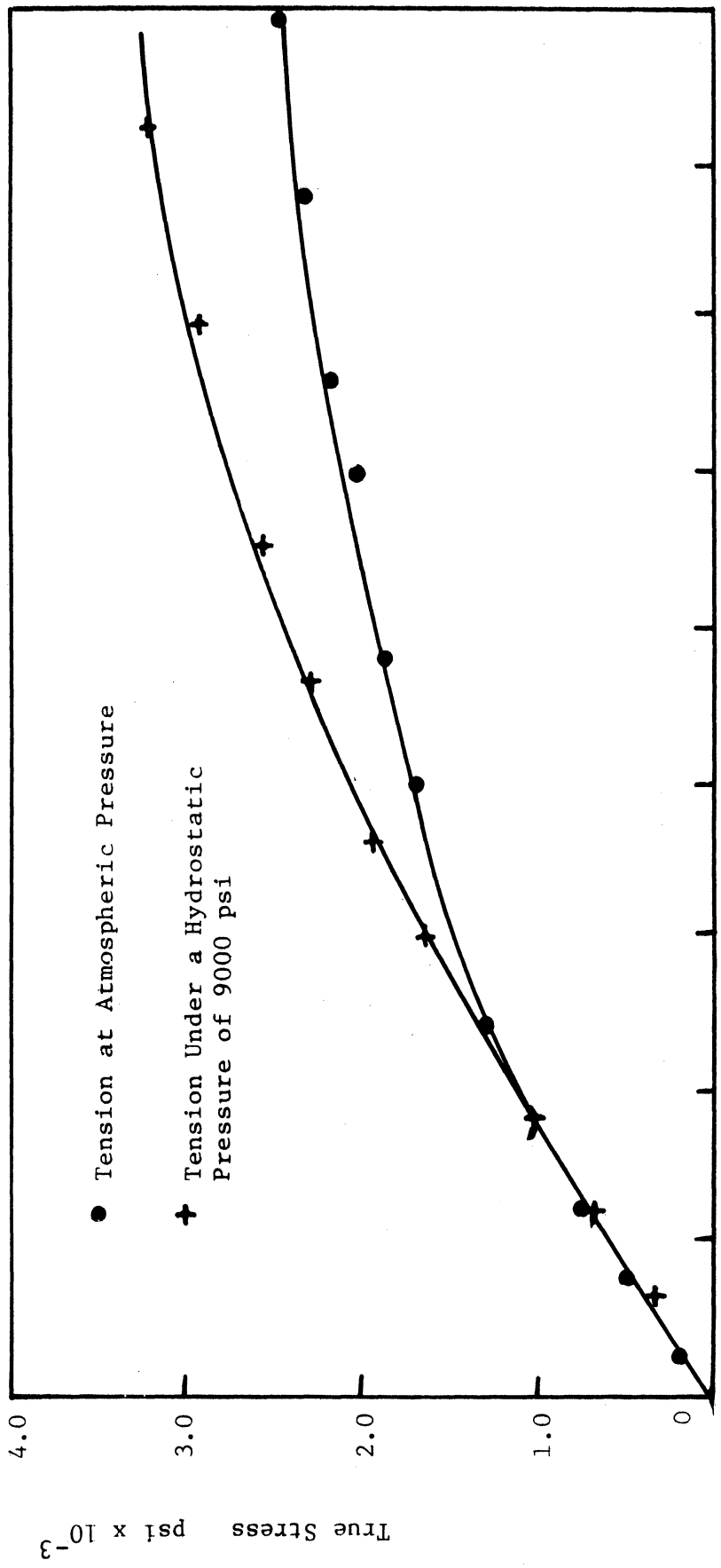

FIG. 47 TENSILE TRUE STRESS-TRUE STRAIN BEHAVIOR OF HDPE (C) AT ATMOSPHERIC PRESSURE AND UNDER A HYDROSTATIC PRESSURE OF 9000 psi.

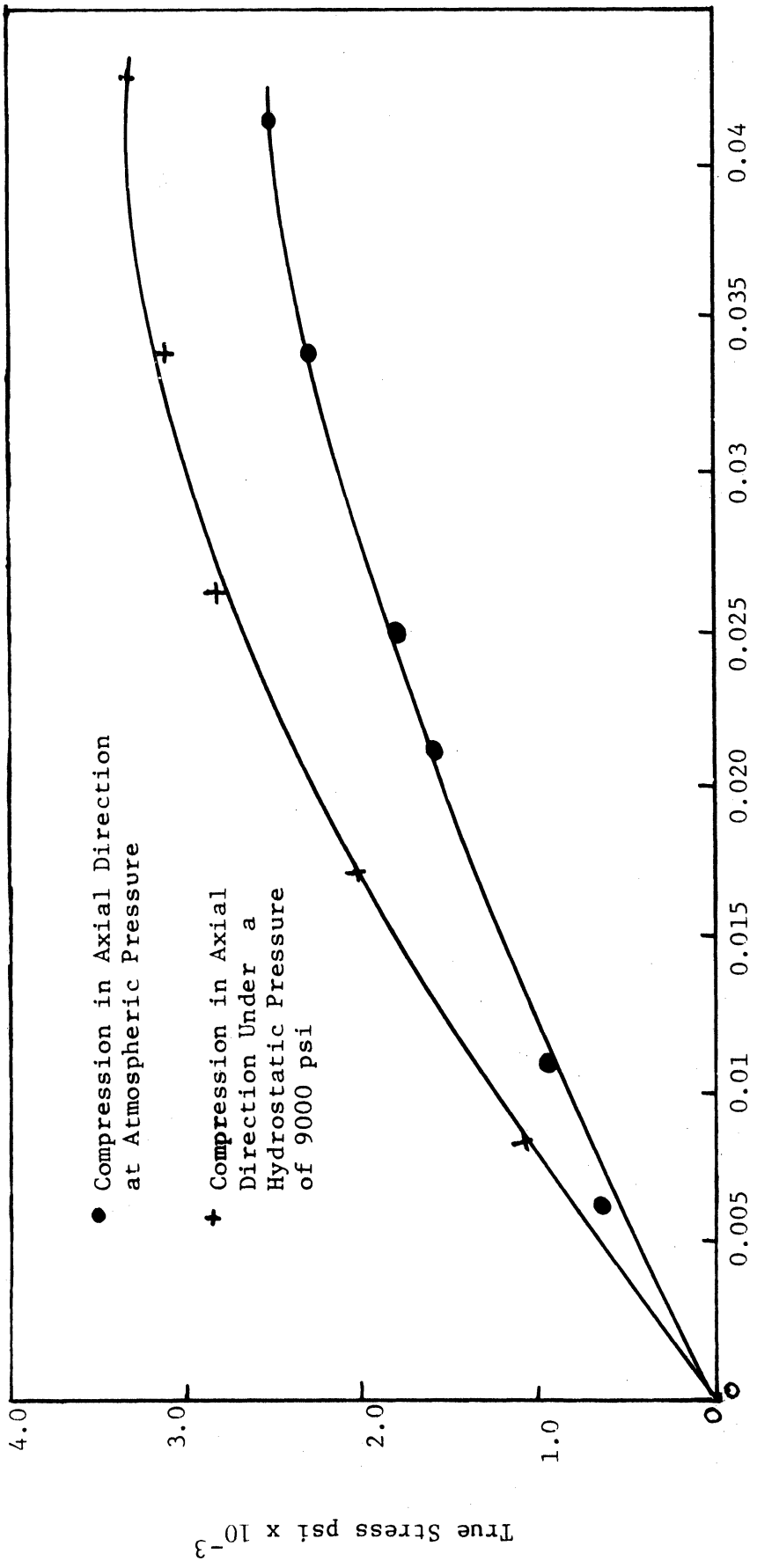

FIG. 48 COMPRESSIVE TRUE STRESS-TRUE STRAIN BEHAVIOR OF HDPE (C) AT ATMOSPHERIC PRESSURE AND UNDER A HYDROSTATIC PRESSURE OF 9000 psi.

Table V.4

Values of Tensile and Compressive Yield Strengths for Various Levels of Hydrostatic Pressure

Pressure (psi)	Test	PC		PVC-B		HDPE-C	
		σ (psi)	σ_m (psi)	σ (psi)	σ_m (psi)	σ (psi)	σ_m (psi)
0	Tension	6500	2200	5400	1800	1325	450
	Compression	-7800	-2600	-7000	-2300	-1650	-550
6000	Tension	6700	-3800	6400	-3900	2000	-5300
	Compression	-7500	-8500	-7500	-8500	--	--
9000	Tension	7000	-6650	7400	-6500	2250	-8250
	Compression	-8100	-11700	-8200	-11700	-2700	-9900

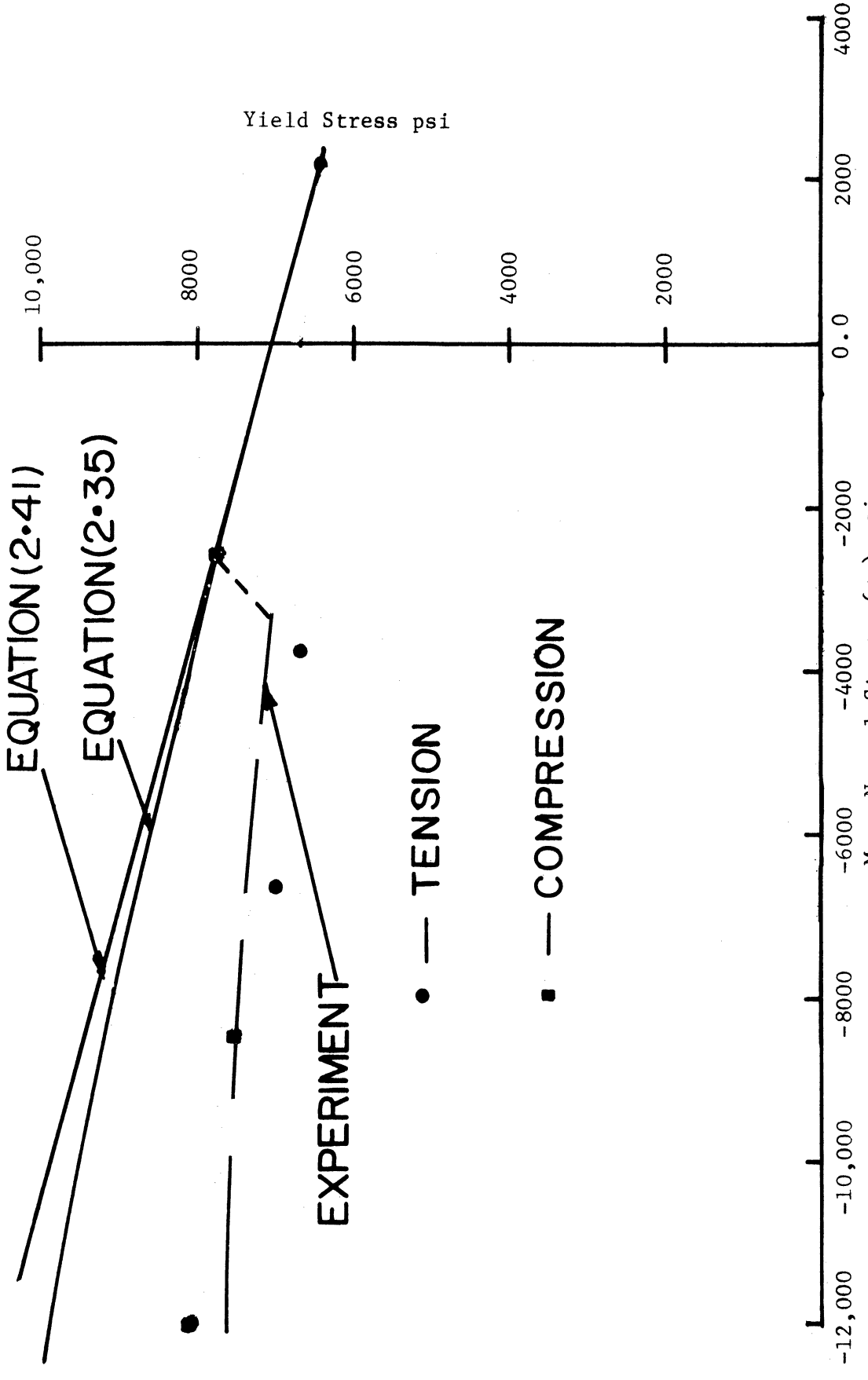

FIG. 49 COMPARISON OF EXPERIMENTAL RESULTS WITH THEORETICAL CURVES BASED UPON EQUATIONS (2.35) AND (2.41) SHOWING THE INFLUENCE OF MEAN NORMAL STRESS ON TENSILE AND COMPRESSIVE YIELD STRESS OF PC.

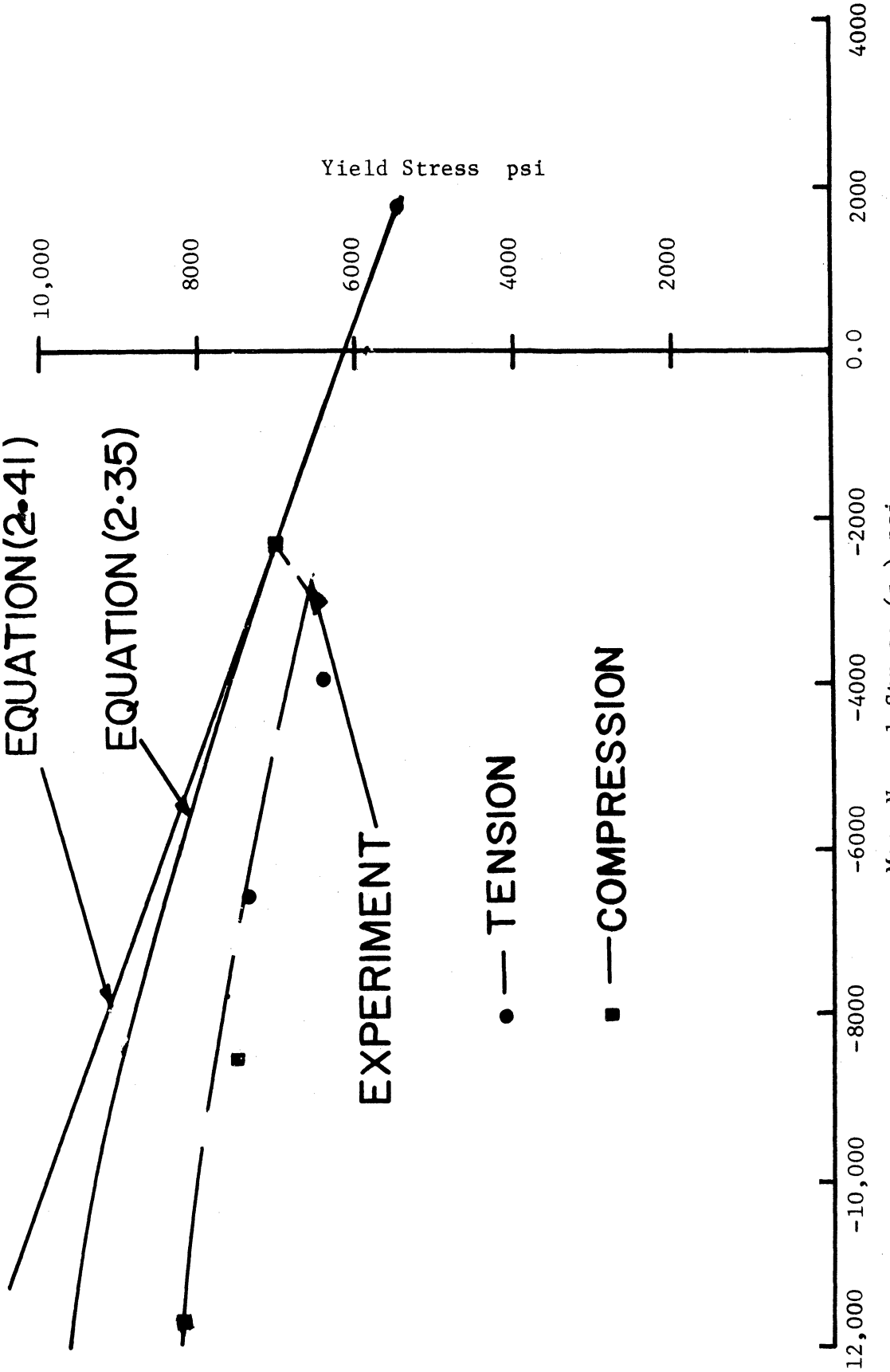

FIG. 50 COMPARISON OF EXPERIMENTAL RESULTS WITH THEORETICAL CURVES BASED UPON EQUATIONS (2.35) AND (2.41) SHOWING THE INFLUENCE OF MEAN NORMAL STRESS ON TENSILE AND COMPRESSIVE YIELD STRESS OF PVC (B).

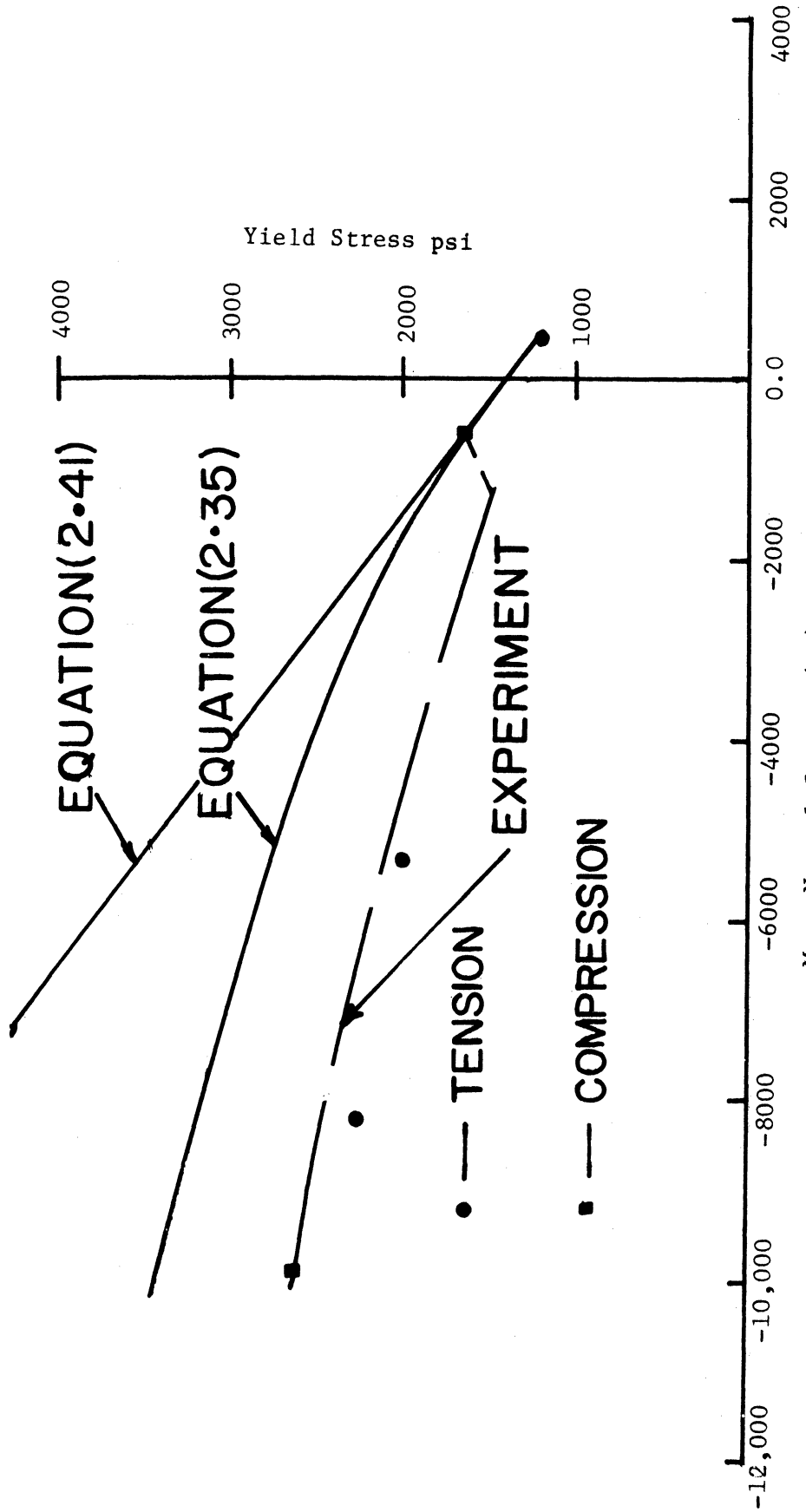

FIG. 51 COMPARISON OF EXPERIMENTAL RESULTS WITH THEORETICAL CURVES BASED UPON EQUATIONS (2.35) AND (2.41) SHOWING THE INFLUENCE OF MEAN NORMAL STRESS ON TENSILE AND COMPRESSIVE YIELD STRESS OF HDPE (C).

and below the abscissa. It can be seen that the theoretical curve lies above the experimental results. If a curve is drawn through all of the experimental points, except for those found under atmospheric pressure, that line is almost parallel to the theoretical curve until a sudden jump or transition takes place.

This transition may be caused by one of several possible sources. First, the calibration curves, shown in Fig. 12, which permitted a conversion from chart displacement to extensometer reading were obtained under atmospheric pressure conditions. Whether these identical curves would be obtained at elevated hydrostatic pressures is open to question, however, if they tended to shift toward the abscissa in Fig. 12 as pressure indcreased, the results would tend to raise the corresponding stress-strain curves in Figs. 43 through 48. The end effect of this would be to displace the "measured" points on Figs. 49 through 51 closer to the theoretical.

Second, in spite of all precautions taken in this study, the estimated value of the friction force may not be wholly accurate. With the small changes in yield stresses found at these relatively low hydrostatic pressures the possible error introduced by "friction" measurements could contribute to the deviations observed between measurement and prediction. Finally, it may be argued that the aforementioned transition is due to the effect of oil contact with the material; no such evidence was observed. PVC did appear to display some abnormal behavior when tested under pressure in tension. After reaching the maximum load, it did not neck, rather it was found that numerous

circumferential cracks had developed. At first it was suspected that the oil was impregnating into microcracks thereby assisting in the opening up of these cracks. To investigate this, it was decided to coat a specimen with a very thin layer of silicon rubber (about 0.001-inch thick). On testing this rubber-coated specimen in tension it was found that no cracks developed, rather a neck formed and propagated. Additionally, it was found that the maximum loads attained for both rubber-coated specimens and noncoated specimens were identical. This led to the conclusion that the oil pressure does not initiate cracks but does assist in their propagation after they are formed. No such abnormal behavior was exhibited by either of the other polymers.

CHAPTER VI. CONCLUSIONS AND RECOMMENDATIONS FOR FURTHER WORK

VI.1 Conclusions

From the results presented earlier the following conclusions can be drawn from a macroscopic viewpoint:

1. From the yield locus plots of PC and PVC, the correlation between the experimental results and theoretical predictions based upon a pressure modified von Mises criterion is excellent. With HDPE there exists a modest disagreement between the theoretical and experimental results. This could be due to the anisotropy observed in all HDPE specimens; additionally, the fairly high creep rate of HDPE (compared with the other two polymers) relative to the test conditions can influence the type of results found here. On the whole, however, the three different HDPE rods gave results that fit inside a narrow band; this is bounded by two yield loci based upon the extremes of tensile and compressive yield stress values as measured. Thus, the proposed yield criterion predicts the yieldings of glassy amorphous as well as crystalline polymers reasonably well.

2. A comparison of equations (2.39) and (2.44a), which predict the effect of pressure on yield strength, has been made using results published in the literature. The proposed criterion appears to predict a more reasonable correlation, especially at higher pressures, than does the criterion suggested by others. In addition, the general shape of the curve based upon the proposed criterion appears to be in better agreement with experimental evidence.

3. Observation of the fracture modes indicated that for first quadrant loading, the failure of PC was shear while PVC exhibited a brittle failure mode. For fourth quadrant stress states, failure could be

attributed to a buckling effect which causes a type of bulge. No fracture was observed for any of the materials when they were subjected to such states of stress.

4. The two amorphous polymers, PC and PVC, were reasonably isotropic in the as received condition. Their tensile properties in both the axial and tangential directions were identical for all practical purposes. A similar comment is applicable in regard to compressive properties in the axial and radial directions. It was noted however, that the properties of PVC, obtained in two different batches, did not show equivalence between batches although said properties were practically identical within a given batch.

The HDPE did not exhibit isotropic behavior. In general, it was observed that the compressive yield strength in the radial direction was higher than in the axial direction. Regarding tensile behavior it was observed that the true stress-strain curves in the axial and tangential directions were somewhat similar for small values of strains, but showed distinct differences at higher values of strain.

5. As reported by many workers, the yield strength in compression was always observed to be higher than the tensile yield strength for all three polymers. The influence of hydrostatic pressure is to increase the yield strength in tension and compression.

6. It has been demonstrated that polymers as well as many other solids [see 64] obey this yield criterion (equation 2.26). It would appear that yielding of materials in general is influenced, to varying degrees, by pressure effects which could cause volume or morphological changes at yield. The need to incorporate such effects is apparently not significant with those materials that obey the regular von Mises criterion.

VI.2 Recommendations for Future Studies

1. It is believed [35]-[42] that mechanical properties are dependent upon free volume which in turn depends upon cooling rate (or "heat treatment"). Brady and Yeh [32] reported that yielding behavior of "well annealed" polymers was different from "ice quenched" polymers; in this context, this showed an influence of cooling rate.

From these observations the yielding behavior of a variety of amorphous and crystalline polymers, subjected to various heat treatments, should be studied using the yield criterion proposed in this thesis.

2. Further studies that involve third quadrant loading should be carried out to determine if the criterion as proposed is more reasonable than the one based upon the octahedral shear stress.

3. An investigation of yield behavior as a function of strain rate and temperature would be of interest to determine if a type of time-temperature relationship might exist.

4. Further studies of the influence of hydrostatic pressures, well in excess of those used in this study, on tensile and compressive yield strengths should be conducted. Of principal concern is the rate of variation of these two properties with increasing pressure.

5. It was shown that dilatation is proportional to the difference in tensile and compressive yield strength. Experiments are needed to measure the plastic volume change during both modes of deformation in order to test the ideas presented on this point in Chapter II.

6. An attempt should be made to see if the proposed criterion can be extended to include the yield behavior of anisotropic polymers. Initially, one might follow the approach suggested by Hill [70] where pressure effects were not included. In essence, such a criterion in principal stress space could be expressed as:

$$F(\sigma_2 - \sigma_3)^2 + H(\sigma_3 - \sigma_1)^2 + M(\sigma_1 - \sigma_2)^2 + N\sigma_1 + Q\sigma_2 + S\sigma_3 = 1 \ ,$$

if the principal axes coincide with the axes of anisotropy. Here, F, H, M, N, Q, and S represent constants that must be evaluated experimentally. Under special conditions one might need to evaluate only four of the above constants (i.e., N, Q and S are "combined" as one constant).

7. To be more convinced of the universality of the criterion proposed in this thesis, other isotropic polymers should be subjected to the approach used herein.

8. The effect of preorientation on the subsequent yield locus requires detailed study.

APPENDIX A

The full derivation leading to equation (2.30) under Section II.5, entitled Plane Strain Flow is given below.

From the flow rules, as expressed by equation (2.29) one has:

$$d\epsilon_{ij} = \beta \frac{\partial f}{\partial \sigma_{ij}} df \quad . \tag{A.1}$$

Expressing (2.10) as f there results

$$f = J_2^{1/2} + aI_1 - b \quad . \tag{A.2}$$

Now, using I_1 and J_2 as given by equations (2.4a) and (2.6b), inserting into (A.2) then into (A.1) where one differentiates with respect to σ_2, there results:

$$d\epsilon_2 = \beta \left[\left(\frac{1}{2} J_2^{-1/2} \right) \frac{1}{6} \left(4\sigma_2 - 2\sigma_1 - 2\sigma_3 \right) + a \right] \quad . \tag{A.3}$$

If there is no flow in direction 2,

$$d\epsilon_2 = 0$$

or

$$(2\sigma_2 - \sigma_1 - \sigma_3) = -6aJ_2^{1/2} \quad , \tag{A.4}$$

squaring equation (A.4),

$$(2\sigma_2 - \sigma_1 - \sigma_3)^2 = 36\, a^2 J_2 \tag{A.5}$$

$$(4\sigma_2^2 + \sigma_1^2 + \sigma_3^2 - 4\sigma_{12} + 2\sigma_{13} - 4\sigma_{23}) = 36\, a^2 J_2 \qquad (A.6)$$

But

$$J_2 = \frac{1}{6}\left\{(\sigma_1 - \sigma_2)^2 + (\sigma_2 - \sigma_3)^2 + (\sigma_3 - \sigma_1)^2\right\}$$

or

$$12J_2 = 2(2\sigma_1^2 + 2\sigma_2^2 + 2\sigma_3^2 - 2\sigma_{12} - 2\sigma_{23} - 2\sigma_{31})$$

Therefore

$$12J_2 = 4(\sigma_1^2 + \sigma_2^2 + \sigma_3^2 - \sigma_{12} - \sigma_{23} - \sigma_{31})$$

or

$$4\sigma_2^2 - 4\sigma_{12} - 4\sigma_{23} = 12J_2 - 4\sigma_1^2 - 4\sigma_3^2 + 4\sigma_{31} \qquad (A.7)$$

Substituting the left-hand side of equation (A.7) into equation (A.6) then results,

$$\sigma_1^2 + \sigma_3^2 + 2\sigma_{13} - 4\sigma_1^2 - 4\sigma_3^2 + 4\sigma_{31} + 12J_2 = 36\, a^2 J_2$$

or

$$12J_2 + 6\sigma_{13} - 3\sigma_1^2 - 3\sigma_3^2 = 36\, a^2 J_2$$

or

$$-3(\sigma_1 - \sigma_3)^2 = 36\, a^2 J_2 - 12\, J_2$$

or

$$-(\sigma_1 - \sigma_3)^2 = 4J_2(3a^2 - 1)$$

$$J_2 = -\frac{(\sigma_1 - \sigma_3)^2}{4(3a^2 - 1)} = \frac{(\sigma_1 - \sigma_3)^2}{4(1 - 3a^2)} \qquad (A.8)$$

Substituting (A.8) into equation (2.10)

$$\frac{(\sigma_1 - \sigma_3)}{2\sqrt{1 - 3a^2}} + a(\sigma_1 + \sigma_2 + \sigma_3) = b \qquad (A.9)$$

But from equation (A.4)

$$\sigma_2 = \frac{\sigma_1 + \sigma_3}{2} - 3aJ^{1/2}$$

Hence

$$\sigma_2 = \frac{\sigma_1 + \sigma_3}{2} - \frac{3a}{2} \frac{(\sigma_1 - \sigma_3)}{(1 - 3a^2)^{1/2}} \qquad (A.10)$$

Substituting (A.10) into (A.9) we get

$$\frac{(\sigma_1 - \sigma_3)}{2(1 - 3a^2)^{1/2}} + a \left[\sigma_1 + \sigma_3 + \frac{\sigma_1 + \sigma_3}{2} - \frac{3a}{2} \frac{(\sigma_1 - \sigma_3)}{(1 - 3a^2)^{1/2}} \right] = b$$

or

$$\frac{(\sigma_1 - \sigma_3)}{2(1 - 3a^2)^{1/2}} (1 - 3a^2) + \frac{3a}{2} (\sigma_1 + \sigma_3) = b$$

Hence

$$\frac{\sigma_1 - \sigma_3}{2} = -\frac{3a}{(1 - 3a^2)^{1/2}} \left(\frac{\sigma_1 + \sigma_3}{2} \right) + \frac{b}{(1 - 3a^2)^{1/2}} \qquad (A.11)$$

Equation (A.11) is equation (2.30) given under Section II.5. Now following an identical approach but using equation (2.26) as the function f (instead of (2.10) as was used above), one starts with:

$$f = (\sigma_1 - \sigma_2)^2 + (\sigma_2 - \sigma_3)^2 + (\sigma_3 - \sigma_1)^2$$

$$+ 2(C - T)(\sigma_1 + \sigma_2 + \sigma_3) - 2\,CT \qquad (A.12)$$

Substituting (A.12) into (A.1) and differentiating with respect to σ_2 there results for the case of plane strain ($d\epsilon_2 = 0$):

$$-2(\sigma_1 - \sigma_2) + 2\sigma_2 - 2\sigma_3 + 2(C - T) = 0$$

or

$$4\sigma_2 - 2\sigma_1 - 2\sigma_3 = 2(T - C)$$

thus,

$$\sigma_2 = \frac{T - C}{2} + \frac{(\sigma_1 + \sigma_3)}{2} \qquad (A.13)$$

Putting (A.13) into (2.26), one gets,

$$\left\{\sigma_1 - \frac{(T - C)}{2} - \frac{(\sigma_1 + \sigma_3)}{2}\right\}^2 + \left\{\frac{(T - C)}{2} + \frac{(\sigma_1 + \sigma_3)}{2} - \sigma_3\right\}^2 + (\sigma_3 - \sigma_1)^2$$

$$+ 2(C - T)\left\{\sigma_1 + \sigma_3 + \frac{(T - C)}{2} + \frac{(\sigma_1 + \sigma_3)}{2}\right\} = 2\,CT$$

or

$$\left\{ \frac{(\sigma_1 - \sigma_3)}{2} - \frac{(T - C)}{2} \right\}^2 + \left\{ \frac{(T - C)}{2} + \frac{(\sigma_1 - \sigma_3)}{2} \right\}^2 + (\sigma_3 - \sigma_1)^2$$

$$+ 2(C - T) \left\{ \frac{3}{2} (\sigma_1 + \sigma_3) + \frac{(T - C)}{2} \right\} = 2\,CT$$

Hence

$$2\left(\frac{\sigma_1 - \sigma_3}{2} \right)^2 + 2\left(\frac{T - C}{2} \right)^2 + (\sigma_3 - \sigma_1)^2 + 2(C - T) \left\{ \frac{3}{2} (\sigma_1 + \sigma_3) \right\}$$

$$- (C - T)^2 = 2CT$$

$$\frac{3}{2} (\sigma_1 - \sigma_3)^2 = \frac{1}{2} (C - T)^2 + 2CT + 3(T - C)(\sigma_1 + \sigma_3)$$

$$\frac{3}{2} (\sigma_1 - \sigma_3)^2 = \frac{1}{2} [C^2 + T^2 - 2CT + 4CT] - 3(C - T)(\sigma_1 + \sigma_3)$$

$$\frac{3}{2} (\sigma_1 - \sigma_3)^2 = \frac{(C + T)^2}{2} - 3(C - T)(\sigma_1 + \sigma_3)$$

$$\left(\frac{\sigma_1 - \sigma_3}{2} \right)^2 = \frac{(C + T)^2}{12} - (C - T) \left(\frac{\sigma_1 + \sigma_3}{2} \right) \qquad \text{(A.14)}$$

Thus (A.14) is identical to (2.31).

APPENDIX B. DERIVATION OF EQUATIONS FOR WALL THICKNESS AND DIAMETER OF TUBULAR SPECIMENS

The true strain in the direction of wall thickness t_i is [82,83]:

$$\epsilon_3 = \ell n \frac{t_i}{t} \tag{B.1}$$

Invoking volume constancy

$$\epsilon_3 = -(\epsilon_1 + \epsilon_2) \tag{B.2}$$

From equations (B.1) and B.2)

$$t_i = \frac{t}{\ell n^{-1}(-\epsilon_1 - \epsilon_2)} \tag{B.3}$$

The relations between the true strains ϵ_1 and ϵ_2 in the axial and lateral directions in terms of nominal strains e_1 and e_2 in these directions are:

$$\epsilon_1 = \ell n(1 + e_1) \tag{B.4}$$

$$\epsilon_2 = \ell n(1 + e_2) \tag{B.5}$$

By adding equations (B.4) and (B.5) and taking the antilogarithms of the resulting equation,

$$\ell n^{-1}(-\epsilon_1 - \epsilon_2) = \frac{1}{(1 + e_1)(1 + e_2)} \tag{B.6}$$

From equations (B.3) and (B.6),

$$t_i = \frac{t}{1 + e_1 + e_2 + e_1 e_2} \qquad (B.7)$$

Since $e_1 e_2$ is small compared with e_1 and e_2, equation (B.7) may be written

$$t_i = \frac{t}{1 + e_1 + e_2} \qquad (B.8)$$

Similarly instantaneous internal diameter

$$di = (d + 2t)(1 + e_2) - 2t_i \qquad (B.9)$$

APPENDIX C

Table C.1 Summary of Modifications of the Tresca and von Mises Yield Criteria

Criterion	Equation No. in Text	Reference No. in Text	Type of Test	Test Materials
I.* Modified von Mises criterion:				
a) $J_2^{1/2} + aI_1 = b$ or $\sqrt{1/6[(\sigma_1 - \sigma_2)^2 + (\sigma_2 - \sigma_3)^2 + (\sigma_3 - \sigma_1)^2]} + a(\sigma_1 + \sigma_2 + \sigma_3) = b$	2.10	Drucker et al. [19]	None	Suggested for soil
b) $\tau_{oct} = \tau_s - \mu\sigma_m$ or $1/3\ \sqrt{(\sigma_1 - \sigma_2)^2 + (\sigma_2 - \sigma_3)^2 + (\sigma_3 - \sigma_1)^2} = \tau_s - \mu(\sigma_1 + \sigma_2 + \sigma_3)/3$	2.11	Sternstein et al. [15]	Biaxial tension	PMMA

Table C.1 (cont.)

Criterion	Equation No. in Text	Reference No. in Text	Type of Test	Test Materials
c) $\sqrt{(\sigma_1 - \sigma_2)^2 + (\sigma_2 - \sigma_3)^2 + (\sigma_3 - \sigma_1)^2}$ $+ \frac{\sqrt{2}(C - T)}{(C + T)}(\sigma_1 + \sigma_2 + \sigma_3) = \frac{2\sqrt{2}\,CT}{(C + T)}$	2.21	Bauwens et al. [18]	Torsion accompanied by axial tension	PVC
d) $\sqrt{(\sigma_1 - \sigma_2)^2 + (\sigma_2 - \sigma_3)^2 + (\sigma_3 - \sigma_1)^2}$ $= \sqrt{6}\left[K + \mu_1 \frac{(\sigma_1 + \sigma_2 + \sigma_3)}{3}\right]$	2.23	Bowden et al. [17]	Plane strain compression accompanied by axial pull, "Ford"-type test	PMMA
II.** Modified Tresca Criterion				
a) $\frac{\sigma_1 - \sigma_3}{2} = \frac{T}{2} + \tan\Theta\,(\sigma_1 + \sigma_2 + \sigma_3)$	2.22	Whitney et al. [13]	Uniaxial tension and compression, plane strain compression	PS
b) $\frac{\sigma_1 - \sigma_3}{2} = K + \mu_2 \frac{(\sigma_1 + \sigma_3)}{2}$	2.24	Bowden et al. [16]	Plane strain compression accompanied by axial pull, "Ford"-type test	PMMA
c) $\frac{\sigma_1 - \sigma_3}{2} = K + \mu_3 \frac{(\sigma_1 + \sigma_2 + \sigma_3)}{3}$	2.25	Bowden et al. [17]		PS

Criterion	Equation No. in Text	Reference No. in Text	Type of Test	Test Materials
III. Proposed criterion in this study:				
$(\sigma_1 - \sigma_2)^2 + (\sigma_2 - \sigma_3)^2 + (\sigma_3 - \sigma_1)^2$ $+ 2(C - T)(\sigma_1 + \sigma_2 + \sigma_3) = 2CT$	2.26		Uniaxial tension and compression Biaxial tension and compression Plane strain compression	PV, PVC, HDPE
		Stassi-D'Alia [64]	Biaxial tension	Gray cast iron, sandy clay, marble, concrete

*Usual form of von Mises yield criterion:

$$(\sigma_1 - \sigma_2)^2 + (\sigma_2 - \sigma_3)^2 + (\sigma_3 - \sigma_1)^2 = T^2$$

**Usual form of Tresca criterion:

$$(\sigma_1 - \sigma_3) = 2T \quad \text{where } \sigma_1 > \sigma_2 > \sigma_3$$

LIST OF REFERENCES

1. P. W. Bridgman, Rev. Modern. Phys. 17, 3 (1945).
2. H. Tresca, Compt. Rend., Acad. Sci., Paris, 59 (1864).
3. R. von Mises, Gottinger Nachrichten, Math.-Phys., Klasse, 583 (1913).
4. J. J. Guest, Phil. Mag. V50, Ser. 5, 69 (1900).
5. J. J. Guest, Phys. Soc. London (Proc.) 51, 286, 652, (1939).
6. J. J. Guest, Inst. Auto. Engrs. Jour. V9, 33 (1940).
7. A. Nadai, Theory of Flow and Fracture of Solids, Vol. 9, McGraw-Hill Book Co., Inc., New York, 1950.
8. H. Hencky, Zeits, Ang. Math, Mech. 4, 323 (1924).
9. W. Lode, Zeitsch f. Physik, 36, 11, 12, 192, (1926).
10. G. I. Taylor and H. Quinney, Proc. Roy. Soc. London (A), 143 307 (1931).
11. F. D. Stockton and D. C. Drucker, J. Coll. Sci. (Rheology Issue) 5, 239 (1950).
12. J. M. Lessells and C. W. MacGregor, J. Frank. Inst. 230, 163 (1960).
13. W. Whitney and R. D. Andrews, J. Poly. Sci. C5, 16, 2981 (1967).
14. S. S. Sternstein, L. Ongchin and A. Silverman, Appl. Poly., Symposia 7, 175 (1968).
15. S. S. Sternstein, and L. Ongchin, AME Chem. Soc., Polymer Preprints 10, 2, 1117 (1969).
16. P. B. Bowden and J. A. Jukes, J. Mater. Sci., 3, 183 (1968).
17. P. B. Bowden and J. A. Jukes, J. Mater. Sci., 7, 52 (1972).
18. J. C. Bauwens, J. Poly. Sci. A-28, 893 (1970).
19. D. C. Drucker and W. Prager, Quart. Appl. Math, 8, 2, 157 (1952).

20. F. H. Müller, Rubb. Chem. Tech., 1027, 30, (1957).

21. K. Jackel, Kolloid Z. 137, 130 (1954).

22. R. E. Robertson, J. Appl. Poly Science, 7, 443 (1963).

23. T. Ree and H. Eyring, J. Appl. Phys., 26, 985 (1957).

24. J. S. Lazurkin, J. Poly. Sci., 30, 595 (1958).

25. C. Bauwens-Crowet, J. C. Bauwens, G. Homes, J. Poly. Sci. A2, 7, 735 (1969).

26. C. Bauwens-Crowet and G. A. Homes, Appl. Mater.-Res., 3, 1, (1964).

27. C. Bauwens-Crowet and G. A. Homes, Compt. Rend. Acad. Sci. (Paris) 259, 3434, (1964).

28. C. Bauwens-Crowet, J. C. Bauwens and G. Homes, Jour. Mater. Sci., 7, 176, (1972).

29. J. A. Roetling, Polymer, London, 6, 311 (1965).

30. J. A. Roetling, Polymer, London, 6, 315 (1965).

31. J. A. Roetling, Appl. Polymer Smp., (5), 161, (1967).

32. T. E. Brady and G.S.Y. Yeh, J. Appl. Phys., 42, 12, 4622 (1971).

33. R. E. Robertson, J. Chem. Phys., 44, 3950 (1966).

34. R. E. Robertson, App. Poly. Symp., 7, 201 (1967).

36. M. H. Litt, and A. V. Tobolsky, J. Macromal Sci., 587 (1967).

37. K. C. Rusch and R. H. Becker, J. Macromol. Sci., B3, 365 (1969).

38. K. C. Rusch and R. H. Beck, J. Macromol. Sci., B4, 621 (1970).

39. D. H. Ender, J. Appl. Phys., 39, 11, 4877 (1968).

40. A. T. Dibenedetto and K. L. Trachte, J. Appl. Sci., 14, 2249 (1970).

41. L. Nicolaus and A. T. Dibenedetto, J. Appl. Poly. Sci., 15, 1585, (1971).

42. A. K. Doolittle, J. Appl. Phys., 22, 1471 (1951).

43. R. G. Vadimsky, H. D. Keith, and F. J. Padden, Jr., J. Poly. Sci., A-2, 1367 (1969).

44. P. H. Geil, Polymer Single Crystals, Interscience, 1963.

45. A. Peterlin, J. Poly Sci., C9, 61 (1965).

46. L. Holliday, J. Mann, G. A. Pogany, Ll, D. Puch, and D. A. Gunn, Nature, London, 202, 381 (1964).

47. G. Biglione, E. Baer and S. V. Radcliffe, Proc. 2nd Int. Conf. on Fracture, Brighton, April 1969.

48. S. B. Ainbiner, M. G. Laka and I. Yu Maiors, Mekhanika Polimerov 1 (1) 65 (1965).

49. K. D. Pae and D. R. Mears, J. Poly. Sci. B-6, 269 (1968).

50. K. D. Pae, D. R. Mears and J. A. Sauer, Poly. Letters 6, 773 (1968).

51. D. R. Mears, K. D. Pae and J. A. Sauer, J. Appl. Phys., 40, 4229 (1969).

52. D. Sardar, S. B. Radcliffe and E. Bear, Poly. Eng. and Sci., 7, 4, 290 (1968).

53. W. I. Vroom and R. F. Westover, SPE-27th Annual Tech. Conf., Chicago, Ill., 15 May 5-8, 159 (1969).

54. M. G. Laka and A. A. Dzenis, Mekhanika Polimerov 3, 6, 1043 (1967).

55. S. Rabinowitz, I. M. Ward and J.S.C. Parry, J. Mater. Sci., 5, 29 (1970).

56. L. A. Davis and C. A. Pampillo, J. Appl. Phys., 42, 12, 4659 (1971).

57. L. W. Hu, Proc. Sec. Symp. Naval Structural Mechanics, (1960).

58. B. Crossland, Proc. Inst. Mech. Engrs. 18, 40, 935 (1954).

59. J. Marin, and L. W. Hu, Trans. ASME, August, 1181 (1955).

60. D. C. Drucker, "Stress-Strain Relations in the Plastic Range, A Survey of Theory and Experiment," Office of Naval Research, Contract No. N7 onr-358, NR-041-032 (1950).

61. W. F. Hosford, Jour. App. Mech. (Trans. ASME, 439, E, 2), 607 (1972).

62. B. Paul, Fracture, Vol. II, Edited by H. Liebowitz, Academic Press, Inc., New York and London, 446 (1968).

63. A. N. Schofield and C. P. Wroth, Crtical State Soil Mechanics (McGraw-Hill Maidenhead) (1968).

64. F. Stassi-D'Alia "Meccanica" No. 3 (Vol. II, 1967) Jour. of Italian Assoc. of Theoretical and Applied Mechanics.

65. A. Meldahl, Brown Boveri Rev., 31, 260 (1926).

66. F. Schleicher, Z. Agnew. Math. Mech. 6, 199 (1926).

67. N. W. Tschogel, J. Poly Sci. C32, 239 (1971).

68. L. F. Coffin, Jr., Jour. of Appl. Mech. Sept. (1950).

69. R. Hill, The Mathematical Theory of Plasticity, Clarendon Press, (1967).

70. D. C. Drucker, Quat. Appl. Math. 7, (1950).

71. L. A. Davis and C. A. Pampillo, Jour. Appl. Phys., 42, 12, 4674 (1971).

72. J. G. Williams and H. Ford, Jour. Mech. Eng. Sci., 6, 4, 405 (1964).

73. P. W. Bridgman, Large Plastic Flow and Fracture, McGraw-Hill Book Co., Inc., New York (1952).

74. H. Ll. D. Pugh and D. Green, Inst. Mech. Engrs. Proc. 179, 415 (1964-1965).

75. R. S. Raghava, R. M. Caddell, L. Buege, A. G. Atkins, J. Macromol., Sci. Phys. B6 (4), 655 (1972).

76. A. S. Argon, R. D. Andrews, J. A. Godrick and W. Whitney, J. Appl. Phys., 39, 1899 (1968).

77. F. F. Rawson and J. G. Rider, J. Poly Sci., Part C, 33, 87 (1971).

78. A. W. Christiansen, E. Baer and S. V. Radcliffe, Phil. Mag. London., 24, 451 (1971).

79. E. G. Thomsen, C. T. Yang and S. Kobayashi, Mechanics of Plastic Deformation in Metal Processing. The Macmillan Co., New York 152 (1965).

80. E. A. Davis, Trans. ASME, J. Appl. Mech. A-13, A-24 (1945).

81. Private communication with E. Baer (1970).

82. J. Marin, B. H. Ulrich and W. P. Hughes, NACA Technical Notes No. 24, 25 (1951).

83. J. Marin, J. H. Raupel, V. L. Dutton and M. W. Brossman, NACA Technical Notes No. 1536 (1948).